Studies on the influences of trees and understory vegetation on the soil nitrogen dynamics in a cool-temperate mixed forest

(冷温帯混交林における土壌窒素動態に対する樹木と下層植生の影響に関する研究)

北海道大学大学院環境科学院

井上　貴央

Contents

Chapter1. General introduction

1.1 Forest ecosystem as a provider of ecosystem services

Forests cover approximately four billion hectares globally, approximately 30% of global land area (FAO 2016) and forests account for 48% of terrestrial gross primary production (Beer et al. 2010). The ability of forest to sequester carbon is an important aspect of forests under climate change (McKinley et al. 2011). In addition, forests support the biodiversity on Earth and provide valuable ecosystem services to humanity, including food, fuel wood, timber, medicine, water supply, and aesthetic and spiritual values (Chapin et al. 2011).

It is considered that natural disturbances are fundamental factors that drive the development and maintenance of the structure and function of forest ecosystems (Attiwill 1994), which supports the provision ecosystem services (Collins et al. 2011). Hence, understanding how complex forest structure affects ecosystem processes not only advance our understanding of the functioning of forest ecosystem but also contributes to prediction of the impacts of future environmental change on ecosystem services.

1.2 Nitrogen cycle and soil processes

Nitrogen (N) is an essential nutrient for organisms and is a limiting nutrient for the plant growth in many forest ecosystems, especially boreal and temperate forests (Vitousek and Howarth 1991). Nitrogen is supplied to forests via atmospheric deposition and biological N fixation by N-fixing plants. Plants absorb available nitrogen in the soil and return it to the soil as dead organic matter. The organic matter in the soil is also derived from animals and microbes. The main form of nitrogen absorbed by plants is inorganic nitrogen, namely ammonium (NH_4^+) and nitrate (NO_3^-), and the inorganic nitrogen is produced through the microbial decomposition of organic matter. Some of the nitrogen produced by microbes is lost by leaching and by gaseous loss from forest ecosystems. In natural ecosystems, the flux of internal cycling of nitrogen is larger than fluxes of nitrogen input and output.

Soil microbes produce dissolved organic nitrogen (DON) from soil organic matter and absorb DON to obtain nitrogen and carbon to support their growth. When their nitrogen requirement is met, they excrete excess nitrogen as NH_4^+ (N mineralization). The NH_4^+ is further transformed to NO_3^- (nitrification) when the

availability of NH_4^+ is high for nitrifying microorganisms (nitrifier). When DON is insufficient to meet the microbial nitrogen requirement, they absorb additional inorganic nitrogen (Vitousek and Matson 1988; Fenn et al. 1988). Therefore, the soil N dynamics (i.e. decomposition of organic matter, competition for available nitrogen among plants, decomposer microbes, and nitrfiers accompanied by transformation of nitrogen), and the fate of the different forms of nitrogen are important processes for the ecosystem functions and services of forest ecosystems.

1.3 Relationship between vegetation and soil N dynamics

Vegetation is a major factor that controls soil N dynamics through the supply of litterfall and absorption of N. Vegetation in mature forests exhibit complex structure and plant distribution as a result of small-scale natural disturbances such as windfall and subsequent succession which forms patches of vegetation at different successional stages. Influences of large scale disturbance such as clear-cutting on soil N dynamics and leaching of nitrogen to streams have been relatively well studied. For example, Bormann and Likens (1979) studied the biogeochemistry of watershed for 15 years at the Hubbard Brook Experimental Forest located in northeastern America and found that the stream NO_3^- concentration largely increased after the clear-cutting of secondary forest and it decreased as vegetation recovered. This temporal change in the stream water NO_3^- concentration was attributed to the rapid decomposition of organic matter and loss of vegetation N uptake after clear-cutting. From their study and other studies, it is generally considered that loss of vegetation causes an increase in N leaching and the recovery of vegetation reduces the leaching. However, effects of small-scale disturbance and subsequent succession in mature forests on soil N dynamics has not been extensively examined.

It is well known that tree species influences soil N dynamics (Binkley and Giardina 1998; Augusto et al. 2015). Generally, evergreen coniferous species shows lower rates of N mineralization and nitrification in the soil compared to deciduous broadleaved species although several exceptions have been reported (Binkley and Giardina 1998; Augusto et al. 2015). The differences in soil N dynamics is attributed to the differences in litter chemistry (Scott and Binkley 1997), nutrient uptake by roots (Hobbie 1992), mycorrhizal type (Chapman et al. 2006), and throughfall and stemflow chemistry (Knops et al. 2002). However, our understanding of plant species effects on soil N dynamics is still incomplete. The effects of tree species are often examined by comparing the differences in soil N dynamics and other properties between

monospecific stands of different tree species, and whether the findings from monospecific stands are applicable to natural mixed forests has not been examined extensively (Binkley and Giardina 1998; Lovett et al. 2004).

Stability of plant distribution in forests may also be important to understand the plant-soil relationship. Hobbie (1992) has suggested that plants grown on high-nutrient site produce high-quality litter, thereby creating fast nutrient cycling in the soil, while plants grown on nutrient-poor site produce low-quality litter that decompose slowly and retards nutrient cycling. This suggest that different plant-soil relationship often observed between tree species may be a result of long-term positive feedback. Hence, whether the dynamic plant distribution in mature forest, which is caused by natural disturbance and succession, is related to spatial variation of soil N dynamics is not clear.

Understory species has large impact on the regeneration of canopy species in canopy gaps and under closed canopy in many forest ecosystems (Royo and Carson 2006). However, influence of understory vegetation on ecosystem processes have been less studied compared to that of canopy tree species. Nilsson and Wardle (2005) reviewed studies carried out in the Swedish boreal forest and concluded that understory vegetation affects decomposition, availability of soil N, and ultimately aboveground tree and shrub productivity in the long time scale. Their study suggest that understory vegetation needs to be taken into account if we are to understand how forest structure and plant distribution are related to soil N dynamics in mature forest.

1.4 Mechanism behind the relationship between plant species and inorganic N production in soil

Relationships between leaf litter quality such as lignin/N ratio and C/N ratio and net N mineralization rates in soil is well known, and low lignin/N ratio or C/N ratio of litterfall, which decompose relatively faster, is usually associated with high rates of net N mineralization and/or net nitrification (Scott and Binkley 1997; Ferrari 1999). However, the mechanism behind the relationship is not clearly understood (Knops et al. 2002; Prescott 2005).

Dissolved organic matter (DOM), which includes DON and dissolved organic carbon (DOC), is an important source of both N substrate and energy for microbes (Chapin et al. 2011). Hence, differences in the properties of DOM between plant species may be a factor that connects litter decomposition and production of inorganic N in soils. DOM is a substance that leaches from plant tissues and is produced during decomposition of dead organic matter in forest floor and of soil organic matter in

mineral soil. Throughfall and leaching from forest floor (litter leachate) are the main source of DOM to mineral soil (Qualls et al. 1991; Froberg et al. 2007). DOM is constituted of various fractions with different chemical properties, such as recalcitrant humin, carbohydrates, microbially released compounds (Guggenberger et al. 1994). The majority of DOM leaching from forest floor has been suggested to be adsorbed rapidly in the mineral soil and later, the adsorbed DOM would be decomposed slowly by soil microbes (Qualls and Haines 1992). Therefore, it can be suggested that chemical properties of DOM supplied from throughfall and forest floor affect the mineralization rates of N in the soil. However, significance of DOM in soil N dynamics is less studied compared to that in C dynamics (McDowell 2003).

Effects of tree species on DOM dynamics are less understood. Michalzik et al. (2001) synthesized studies conducted in temperate forests, and did not find consistent differences in the concentrations and fluxes of DON and DOC percolating from forest canopy to mineral soil horizon between coniferous and broadleaved forests. A few studies have indicated that the DOM quality in decomposing leaf litter was different among different tree species (Nishimura et al. 2012; Kiikkila et al. 2013). Influence of DOM quantity and quality on inorganic N production is hardly studied probably because most of the labile fraction of DOM is rapidly utilized by microbes and large proportion of DOM from forest floor and mineral soil is refractory (Qualls et al. 1991). However, the new organic matter supplied to the mineral soil is generally more decomposable for soil microbes compared with old humic substances already present in the soil (Zech et al. 1997). Hence, DOM supplied from forest floor to mineral soil can be considered as an important N source for soil microbes.

1.5 Cool-temperate mixed forest in Hokkaido

Cool-temperate mixed conifer-broadleaved forest is a major forest type in Hokkaido. Dwarf bamboo usually forms dense understory; it occupies about 95 % of the total forested area in Hokkaido (Toyooka 1983). Dwarf bamboo quickly dominate the forest floor once canopy gap is formed after disturbance, and its continuous densely packed foliage canopy reduces light availability on the forest floor, thereby preventing the tree regeneration (Nakashizuka 1982; Hiura et al. 1996; Yoshida et al. 2006). Tree regeneration in such canopy gaps is restricted to microsites, such as fallen logs and tip-up mounds, and dense coniferous canopy supports the saplings of tree species by reducing the biomass of dwarf bamboo (Hiura et al. 1996; Yoshida et al. 2006). Although our understanding of the demography of major tree species and the influence

of dwarf bamboo on it in the cool-temperate mixed conifer-broadleaved forest has been advanced, how the dynamics of vegetation is related to biogeochemical cycle is less understood. Several studies have examined the characteristics of dwarf bamboo in terms of nutrient cycling. For example, the decomposition rate of fresh dwarf bamboo litter was found to be slower than those of tree species (Tripathi et al. 2006; Watanabe et al. 2013). Another study has suggested that dwarf bamboo plays an important role in N retention after clear-cutting of trees by increasing its fine root biomass, hence N uptake (Fukuzawa et al. 2006). However, it is still not clear whether general differences in the impact on soil N dynamics between coniferous and broadleaved trees exist in natural mixed forest, whether understory dwarf bamboo affect soil N dynamics differently from canopy species, and whether the distribution of the canopy and understory species are related to the spatial pattern of soil N dynamics in these dynamic natural mixed forests where natural disturbances continuously change the plant distribution. Understanding the influence of plant species on soil N dynamics in such forests would contribute to evaluate and predict the impacts of small-scale disturbance such as windfall and selection cutting on ecosystem processes.

1.6 Research question

Our understanding of the effects of canopy tree species and understory species on soil N dynamics in natural mixed forests, where natural disturbance and succession create complex forest structure and heterogeneous plant distribution, is limited. In addition, the mechanism behind the general relationship between litter decomposition and production of inorganic N in soils is still not clear, and the differences in DOM properties among plant species could be a possible link between these processes. Therefore, the overarching research question of this dissertation is:

How do trees and understory vegetation grown in a natural mixed forest influence soil N dynamics?

In order to answer this question, the two following specific questions were developed:

1. *What is the spatial pattern of soil nitrogen availability and is it related to the plant distribution?*
2. *How do the DOM and dissolved inorganic N (DIN) dynamics differ among plant species, and does DOM property affect leaching DIN?*

To address these questions, this study was conducted in a cool-temperate natural conifer-broadleaved forest in the Uryu Experimental Forest of Hokkaido University, located in northern Hokkaido, Japan. In Chapter 2, I examined the spatial pattern of litterfall, soil moisture, accumulation of organic matter in the forest floor, and soil N availability (soil inorganic N pools and net transformation rates), and analyzed the spatial relationships with the plant distribution.

In Chapter 3, I collected throughfall, litter leachate, and soil water under oak, spruce, and dwarf bamboo grown in canopy gaps. Then, DOM properties (concentrations and fluxes of DON and DOC, optical properties of DOM) and concentrations and fluxes of DIN, as well as natural stable isotopic composition of NO_3^- were analyzed. Differences in the measured variables among the vegetation types, and the influence of DOM properties on leaching NO_3^- were discussed.

In Chapter 4, a synthesis of the findings from Chapter 2 and 3 is presented, followed by the discussion regarding to the overarching question. Limitation of this study and emerging questions are described. Finally, general conclusion of this study is stated.

Chapter 2. Spatial pattern of soil nitrogen availability and its relationship to stand structure

2.1 Introduction

Natural disturbances are fundamental factors that drive the development and maintenance of the structure and function of forest ecosystems (Attiwill 1994). To maintain biodiversity and ecosystem functions, forest management is shifting toward approaches that are based on understanding natural disturbance regimes (Franklin 1993; Attiwill 1994). Treefall, which creates canopy gaps, is a consequence of the disturbance regime, and it leads to the creation of a complex forest structure in many forest ecosystems (Attiwill 1994). In Hokkaido, northern Japan, occasional strong typhoons and windstorms are major natural disturbance regimes, and they create various sizes of canopy gaps in the forests (Yoshida and Noguchi 2009). The creation of a canopy gap alters the supply of light, water, and litterfall to the ground, which then alter various ecosystem processes, such as litter decomposition, soil microbial activity, soil nutrient and organic matter dynamics, and water and nutrient uptake by vegetation. These changes in ecosystem processes then feedback to the productivity of the ecosystem and the vegetation composition; therefore, understanding the impact of the change in vegetation structure on the ecosystem processes would aid the design of sustainable forest management treatments that aim to balance timber production and ecosystem processes. However, how a complex forest structure, which consists of both overstory and understory vegetation, is related to these ecosystem processes is not well understood.

Plants synthesize organic matter, and then litterfall supplies the organic matter, which is a source of energy, carbon (C) and nutrients (e.g., nitrogen (N), phosphorous, and potassium) to soil biota (Wardle et al. 2004). Nitrogen is a limiting nutrient for the growth of organisms in boreal and temperate forests (Vitousek and Howarth 1991), and its dynamics in soil not only affects plant growth, but also influences various ecosystem functions and services. For example, soil N availability affects carbon sequestration by influencing CO_2 balances between the forest and atmosphere via gross photosynthesis by vegetation, as well as organic matter decomposition (Compton et al. 2011). Additionally, nitrification affects water quality via NO_3^- leaching from soil to streams (Vitousek et al. 1997; Compton et al. 2011). Plant species affect soil N dynamics via their litter traits (Binkley and Giardina 1998), nutrient uptake by roots (Hobbie 1992), mycorrhizal type (Chapman et al. 2006), and throughfall and stemflow chemistry

(Knops et al. 2002). Therefore, in forests with a complex forest structure, the plant community composition and configuration will regulate the distribution of soil nutrients, which in turn affects plant community and ecosystem dynamics (John et al. 2007; Boyden et al. 2012).

Litter traits are some of the major factors that control litter decomposition, which is related to soil N dynamics (Chapin et al. 2011). Plant litter with high C/N (Enriquez et al. 1993) or lignin/N ratios (Melillo et al. 1982) generally decomposes slowly, and net N transformation rates in soils under slow-decomposing litter are often lower than those under fast-decomposing litter (Scott and Binkley 1997). Differences in litter decomposition rates often lead to differences in the C/N ratios of soil organic matter (Finzi et al. 1998), which affects N transformation rates (Booth et al. 2005). Additionally, the cations and aluminum (Al) contained in plant litter can modify soil pH, which can in turn influence soil N cycling (Tietema et al. 1992; Reich et al. 2005).

Soil moisture affects soil N dynamics through microbial biomass and its activities (Bengtson et al. 2005; Baldrian et al. 2010). Soil moisture conditions are influenced by the interception of precipitation by the canopy (Barbier 2009), the reduction in evaporative losses from soil by canopy shade (Muscolo 2007), transpiration by vegetation (Oren et al. 1998), and the redistribution of soil moisture via water uptake by roots (Burgess et al. 1998) according to the spatial structure of the vegetation. The creation of water repellency by the production of hydrophobic compounds by living or decomposing plants (Doerr et al. 2000) also affects water infiltration and storage, which influence soil moisture.

Our understanding of the effects of plants on soil N dynamics has largely been advanced by studies that compared the soil N dynamics among monospecific stands or beneath individual trees of different species (Scott and Binkley 1997; Finzi et al. 1998; Reich et al. 2005). However, most natural forests consist of multiple plant species, and their spatial structures are complex because of natural disturbances and succession. In mixed-species forests, the supplies of light, rainfall, and litterfall to the ground are spatially heterogeneous, which creates spatial variations in the available soil N that influence the growth of both existing plants and newly established seedlings. Soil N dynamics are spatially heterogeneous at various spatial scales, and apart from plant species composition, spatial patterns of topography, bedrock geology, and hydrology, it is known to affect the heterogeneity of soil N dynamics at local scales, such as watersheds. In the forested watersheds in most parts of Japan, where the topography is usually steep, spatial patterns in soil N transformation have been observed along slopes because of the variation in the soil water content that affects the vegetation pattern and

the soil C/N ratio (Hirobe et al. 1998; Isobe et al. 2015). Plant distribution caused by natural disturbances and succession creates highly diverse patterns of litterfall and soil moisture even in small spatial scales with flat topographies, consequently resulting in diverse soil N dynamics patterns. However, how the complex forest structure of natural forests is related to the spatial pattern of soil N dynamics in relatively small and flat areas is not well understood.

Understory vegetation plays an important role in forest dynamics. The density and cover of understory species largely increase after the creation of canopy gaps (by natural disturbances, etc.), and in many cases they prevent or inhibit the regeneration of canopy species, thereby leading to their domination of canopy gaps (Royo and Carson 2006). Despite the importance of understory vegetation in forest dynamics, its effects on belowground processes have usually been overlooked in biogeochemical studies. Nilsson and Wardle (2005) found that the dominant understory species in boreal forests affect soil microbial activity and soil N availability through the effect of their litter traits, thereby demonstrating that understory vegetation should be taken into account if we are to understand the forest structure–soil N dynamics relationship in natural forests. Many of the natural forests in Hokkaido, northern Japan, are cool-temperate conifer-broadleaved mixed forests with dense undergrowth of dwarf bamboo (*Sasa* species) (Hiura et al. 1996; Yoshida et al. 2006; Yoshida and Noguchi 2009). After treefall, *Sasa* dwarf bamboos tend to dominate in canopy gaps and inhibit the regeneration of other plant species (Hiura et al. 1996). *Sasa* dwarf bamboo leaf litter has been reported to decompose more slowly than the litter of overstory species (Tripathi et al. 2006; Watanabe et al. 2013). Hence, it can be expected that the influence of *Sasa* dwarf bamboo on soil N dynamics differs from that of canopy species in these forest ecosystems.

In this study, we examined the spatial relationship between the distributions of coniferous and broadleaved species, and understory *Sasa* dwarf bamboo and soil N dynamics in a natural mixed stand with relatively flat topography in northern Japan that contains canopy gaps that are covered with dense undergrowth. We hypothesized that the spatial pattern of soil N dynamics would be controlled largely by the spatial pattern of canopy trees and understory *Sasa* dwarf bamboo through the interacting effects of soil moisture and litter chemical properties on litter decomposability.

2.2 Materials and methods

2.2.1 Study site

This study was conducted in the Uryu Experimental Forest (UREF) of Hokkaido University (44°21′N, 142°16′E), a core site of the Japan Long-Term Ecological Research Network that is located in northern Hokkaido, Japan. According to the meteorological data recorded in the UREF from 2000 to 2009, the mean annual temperature is approximately 4 °C, and the mean annual precipitation is approximately 1,150 mm. The forest floor is usually covered by snow from November to May, with a maximum snow depth of approximately 200 cm. The soil is a Cambisol (IUSS Working Group 2006) that is situated on Pleistocene sedimentary rock. The organic horizon mainly consists of an Oe/Oa horizon with a relatively thin Oi horizon. The annual wet N deposition is approximately 7 kg N ha^{-1} yr^{-1} (Ogawa et al. 2006). Coniferous-broadleaved mixed forest is a major forest type of the UREF, with the dominant coniferous species being *Abies sachalinensis* and *Picea glehnii*, and the dominant deciduous broadleaved species being *Quercus crispula*, *Acer mono*, and *Betula ermanii* (Noguchi and Yoshida 2004). Dense *Sasa* dwarf bamboo covers the forest floor in areas where tree densities are low. We established a study site (approximately 800 m^2 in area) in a primary coniferous-broadleaved mixed stand in the UREF. The study site has no record of human disturbances (i.e., timber production) during the past 100 years. Occasional strong typhoons are a primary disturbance regime in this region, and they play an important role in creating the complex forest structure and various sizes of canopy gaps, which are covered with *Sasa* dwarf bamboo (Yoshida and Noguchi 2009). The site is located on relatively flat topography, and the elevation is approximately 340 m a.s.l. The total basal area of evergreen coniferous species is greater than that of deciduous broadleaved species in the site (Table 2.1). The coniferous species consist of *A. sachalinensis* and *P. glehnii*, while the dominant deciduous broadleaved species are *B. ermanii* and *Q. crispula* (Table 2.1). The forest floor is mainly covered by the dwarf bamboo *Sasa senanensis* (hereafter referred to as *Sasa*). The site contains a canopy gap that has existed for at least 7 years according to 2004 tree census data obtained by the research group of the UREF. The size of the canopy gap is approximately 190 m^2. We used intensive grid and quadrat samplings to examine the spatial relationships among the plant community composition and configuration (including trees and understory vegetation), and litterfall, the organic horizon, and mineral soil properties.

2.2.2 Intensive grid sampling

A 4 × 4 m grid system was established in a 768-m^2 area within the site (Fig. 2.1). The number of sampling grids was 48. We measured a number of properties at each grid in September 2012, which comprises the latter part of the growing season, and in June 2014, which constitutes the beginning of the growing season after the snowmelt. The *Sasa* biomass, the thickness of the Oe/Oa horizon (hereafter referred to as the O horizon), the soil inorganic N content, and the soil water content were measured in each grid. A sampling point was selected approximately 1 m from the northwest corner of each grid for the September sampling, and approximately 1 m from the southeast corner of each grid for the June sampling. The sampling points for the two sampling periods were approximately 2 m from each other. At each sampling point, one soil core was taken using a 4.2-cm diameter auger, and the top 10 cm of the mineral soil was collected after the thickness of O horizon was measured. The soil samples were transported to the laboratory for further analysis. The *Sasa* biomass was calculated by multiplying the total culm number by the average height of standing *Sasa* within a 1-m radius from each sampling point. To assess soil acidity, the exchangeable calcium (Ca) and Al concentrations in the soil, as well as soil pH, were measured for the soils that were collected in September.

2.2.3 Sampling at quadrats

We categorized the forest structure into three types in terms of the dominant vegetation: 1) canopy gaps with dense *Sasa* cover on the forest floor (*Sasa* quadrats), 2) canopy trees with *Sasa* understory (*Sasa*/tree quadrats), and 3) canopy trees without *Sasa* understory (tree quadrats). We established five quadrats (1 × 1 m) in each category (Fig. 2.1). Their locations were selected so that they were not clumped in a particular part of the site (Fig. 2.1).

At one point within each quadrat, the thickness of the O horizon was measured, and approximately 200 g of surface mineral soil (0–10-cm depth) was collected to analyze the soil physicochemical properties (inorganic N contents, potential net N mineralization and nitrification rates, concentrations of exchangeable Ca and Al, total C and N concentrations, pH, and the water content). *Sasa* biomass was obtained by harvesting all the aboveground parts of each *Sasa* within each quadrat, and their oven-dried (70 °C, 48 h) weight was measured. All samplings were conducted in early

September 2011. Leaf litterfall was collected at a location adjacent to each quadrat using litter traps constructed of a plastic basket (collecting area: 0.18 m^2) covered with a 1-mm mesh net. The litter traps were fixed at a 30-cm height. Litterfall was collected monthly in August and September 2012, and biweekly during October 2012. The leaf litters were air dried, separated into four types (coniferous canopy species, broadleaved canopy species, *Sasa*, and others), oven-dried at 70 °C for 48 h, and weighed. The dried litter samples were analyzed for total C and N, Ca, and Al concentrations.

2.2.4 Analysis of litter and soil chemical properties

Total C and N concentrations in the litter were analyzed using a CHNS/O analyzer (PE2400II; PerkinElmer, Waltham, MA, USA) after the dried subsample was ground using a ball mill. Ground litter (0.5 g) was digested with 5 ml of nitric acid (60 %) and 2 ml of hydrogen peroxide (30 %) in an automatic microwave digester (Microwave Digestion System; O.I. Analytical, Tokyo, Japan). The Ca and Al concentrations in the digested solution were analyzed by inductively coupled plasma–atomic emission spectrometry (IRIS Advantage, Nippon Jarrell Ash Co., Kyoto, Japan).

The fresh soil samples were passed through a 4-mm sieve to remove rocks and coarse roots prior to further analysis. Total C and N concentrations in the soil were analyzed using a CHNS/O analyzer after the subsample was air-dried and ground. Ten grams of fresh soil was extracted with 100 ml of 2 M potassium chloride, and the extract was analyzed for ammonium (NH_4^+) and nitrate (NO_3^-) concentrations by a colorimetric method using an auto analyzer (AACS-4, BL-TEC Inc., Osaka, Japan). Another 10-g subsample was extracted with 100 ml of 1 M ammonium acetate (pH 7) to analyze the exchangeable Ca and Al concentrations by inductively coupled plasma–atomic emission spectrometry. The gravimetric soil water content was measured by drying the soil at 105 °C for 24 h. Soil pH was measured using a glass electrode (1:2.5 soil:water ratio).

2.2.5 Potential net N mineralization and net nitrification rates

Potential N mineralization and nitrification rates were measured by laboratory incubation for 7 d. Thirty grams of sieved, fresh soil was placed in a glass jar and covered with aluminum foil with ventilation holes. The temperature was maintained at 25 °C, and the soil moisture was kept at 60 % of the field capacity. The net N mineralization rate is the net difference in the $NH_4^+ + NO_3^-$ contents, and the net

nitrification rate is the net difference in NO_3^- contents during the incubation period.

2.2.6 Mapping the spatial pattern of soil and vegetation properties

The locations of canopy trees (stem diameter at breast height > 10 cm) were mapped using ArcGIS (Arc Desktop version 10, Esri Japan, Tokyo, Japan). We used the data from a tree census that was conducted at the site in 2007, and we assumed that the tree distributions in the data are similar to those in 2011–2014. The *Sasa* biomass was measured only for the September sampling, and we assumed that its spatial variation did not change significantly between the two samplings.

2.2.7 Data processing and statistical analysis

Properties of the forest floor and soil at each sampling point are influenced by adjacent trees through canopy cover, litterfall, root, and mycorrhiza. The spatial range of the influence of trees varies among studies. Hence, to understand the range of influence of the trees, we calculated the number and total basal area of coniferous and broadleaved trees within 5-, 10-, and 15-m radii buffers around each sampling point and sampling quadrat. We then compared the number of significant correlations between the canopy trees and the other variables, as well as the fitting of the models obtained by a stepwise multiple regression analysis.

We analyzed the spatial relationships between the response and explanatory variables obtained in the intensive grid samplings using a stepwise multiple regression analysis. The variance inflation factor was assessed to ensure that multicollinearity among the explanatory variables did not significantly affect the model results. Spatial autocorrelation in the data could lead to incorrect assessments of hypotheses (i.e., a high tendency to reject the null hypothesis) and biased coefficients in the prediction model (Legendre 1993; Dormann 2007). When model residuals exhibit spatial autocorrelation, the spatial autocorrelation needs to be incorporated into regression models (Legendre 1993). Therefore, we first assessed the spatial structure of the observations using Moran's I statistics (Plant 2012). Some of the variables in our data, such as the soil NO_3^- content and the soil water content, were spatially autocorrelated (Table 2.2). For these variables, we assessed the spatial structure of the model residuals using Moran's I test for regression residuals for the selected model with the highest degree-of-freedom adjusted R^2 (Plant 2012). In our analysis, the selected models did not have spatially autocorrelated residuals; thus, the results of ordinary least square models were used for

further analysis and discussion. Spearman's rank correlation coefficient was used to examine the relationships between the variables measured in the quadrats and in the grids. Comparisons of measured variables across litter types and sampling quadrats were conducted using a single factor analysis of variance with a post-hoc Tukey's honestly significant difference test. Prior to the analyses, all data were transformed (log(x+1)) to achieve a normal distribution. All statistical analyses were performed using R software (version 3.1.1, The R Foundation).

2.3 Results

2.3.1 Spatial patterns of plants, soil properties, and soil N availability

Coniferous trees predominated in the closed canopy, while small-to-medium sized broadleaved trees were mainly found near the canopy gap (Fig. 2.1). *Sasa* biomass tended to be high in the canopy gap that is located in the western part of the study site, and it tended to be low under groups of medium-to-large coniferous trees in the middle and eastern parts of the study site (Fig. 2.1).

The mean soil NH_4^+ contents were 11.7 and 11.1 mg N kg soil^{-1} in September and June, respectively (Table 2.2). The mean soil NO_3^- contents were 1.17 and 1.62 mg N kg^{-1} soil in September and June, respectively (Table 2.2). The mean soil water content was significantly higher in June than in September (Table 2.2). Moran's I values indicated that the soil NO_3^- content and the soil water content exhibited a positive spatial autocorrelation at both sampling dates (Table 2.2).

The soil NO_3^- contents were higher in the canopy gap and near the southeastern corner of the site where a few broadleaved trees grew, compared with those under the dense coniferous canopies in both sampling dates (Figs. 2.2a and b). The soil water contents were higher under the canopy gap than under the dense coniferous canopy on both sampling dates (Figs. 2.2d and e). The thicknesses of the O horizons tended to be high around coniferous trees and low in the canopy gap and around broadleaved trees on both sampling dates (Figs. 2.2g and h). The spatial patterns of the soil NO_3^- content, the soil water content, and the thickness of O horizon were similar between the two samplings dates (Fig. 2.2c, f, and i), although the ranges and coefficients of variation for the soil NO_3^- contents and soil water contents were larger in June than in September (Table 2.2).

2.3.2 Spatial relationships among plants, soil properties, and soil N availability

The number of broadleaved trees within the 10- and 15-m radii buffers exhibited more significant correlations with the measured variables (11 and nine variables, respectively, for $P< 0.01$; 14 and 14 variables, respectively, for $P< 0.05$) than that within the 5-m radius buffer (two variables for $P< 0.01$; seven variables for $P< 0.05$), while the number of coniferous trees within the 5-m radius buffer exhibited more correlations with the variables (11 variables for $P< 0.01$; 16 variables for $P< 0.05$) than those within the 10- and 15-m radii buffers (10 and eight variables, respectively, for $P< 0.01$; 13 and 13 variables, respectively, for $P< 0.05$) (Table 2.3). The total basal area of trees showed a similar trend in the correlation analysis, but the number of significantly correlated pairs was less than that in the analysis using the number of trees (data not shown).

The *Sasa* biomass showed positive correlations with the number of broadleaved trees within the 10- and 15-m radii buffers, while it showed stronger negative correlations with the number of coniferous trees within the 5-m radius buffer, compared with those within the other radii (Table 2.3).

The proportions of broadleaved litter to the total litterfall were significantly and positively correlated with the numbers of broadleaved trees within the 10- and 15-m radii buffers, and the proportion of coniferous litter was significantly and positively correlated with the number of coniferous trees within any of the three buffers (Table 2.3). The proportion of *Sasa* litter was significantly and negatively correlated with the number of coniferous trees, especially within the 5-m radius buffer (Table 2.3).

The proportion of *Sasa* litter was significantly and positively correlated with the *Sasa* biomass (Table 2.4). The thickness of the O horizon was significantly and positively correlated with the proportion of coniferous litter, and it was significantly negatively correlated with the proportions of broadleaved litter and *Sasa* litter (Table 2.4).

The spatial variation in the soil NO_3^- content was best explained by the spatial variation in the soil water content, the number of broadleaved trees within the 5-m radius buffer, and the thickness of O horizon on both sampling dates (Table 2.5). The spatial variation in the soil water content was explained by the spatial variation in the thickness of the O horizon, as well as the number of coniferous trees within the 5-m radius buffer, on both sampling dates; these variables had significantly negative effects (Table 2.5). The spatial variation in the number of coniferous trees within the 5-m radius buffer had a positive impact on the spatial variation of the O horizon thickness on both sampling dates (Table 2.5).

2.3.3 Plant, litter, and soil properties in different forest structures

In the *Sasa* quadrats, the numbers of broadleaved trees and coniferous trees were significantly higher and lower, respectively, than those in the other two types of quadrats, except for the number of broadleaved trees within the 5-m radius buffer (Table 2.6). The proportion of broadleaved litter in the total litterfall was significantly higher in the *Sasa* quadrats than in the *Sasa*/tree quadrats (Table 2.6). The proportion of coniferous litter was lowest in the *Sasa* quadrats (Table 2.6). In the *Sasa* quadrats, broadleaved litter was the dominant litter type; on average, broadleaved litter accounted for 68 % of the total litter, while *Sasa* litter accounted for 20 % (Table 2.6). The O horizon thickness was significantly lower in the *Sasa* quadrats than in the other quadrats (Table 2.6).

The coniferous litter had a significantly higher C/N ratio and Al concentration than the broadleaved and *Sasa* litters, while the coniferous litter contained significantly less N than the broadleaved litter (Table 2.7). The *Sasa* litter had a significantly lower Ca concentration than the broadleaved and coniferous litters (Table 2.7).

The soil NO_3^- content and net nitrification rate were significantly higher in the *Sasa* quadrats than in *Sasa*/tree and tree quadrats, while there were no significant differences in the soil NH_4^+ content and soil pH among the quadrats (Table 2.6). The soil in the *Sasa* quadrats had the highest concentration of exchangeable Ca, while the soil in the tree quadrats had the highest exchangeable Al concentration (Table 2.6). There was a significantly positive correlation between the soil NO_3^- content measured at the quadrats and the net nitrification potential measured in the laboratory (Table 2.8). Neither the soil C/N ratio nor the net N mineralization rate in the soil explained the net nitrification rate (Table 2.8).

2.4 Discussion

2.4.1 Relationships between forest structure and dynamics and the spatial pattern of soil properties

Current spatial forest structure is shaped not only by species competition for resources (light, water, nutrients, etc.), but also by past disturbances and the following forest succession. Occasional windstorms and typhoons are major natural disturbance regimes in Hokkaido (Yoshida and Noguchi 2009), and they create spatially

heterogeneous canopy structures. The spatial pattern of light availability, which is regulated by the canopy structure, is a major determinant of the distribution of *Sasa* undergrowth, and it results in high biomass in canopy gaps and low biomass under coniferous trees (Noguchi and Yoshida 2005). The distribution of *Sasa* biomass in our study site was consistent with this common pattern (Fig. 2.1). The positive correlation between the *Sasa* biomass and the broadleaved tree abundance, and the negative correlation between the *Sasa* biomass and the coniferous tree abundance indicate that the distribution of the two functional types of trees creates a spatial variation of *Sasa* growth even under the tree canopy (Table 2.3). In general, *Sasa* quickly covers the forest floor under a canopy gap once the gap is formed, and it exclusively dominates the area and inhibits the regeneration of canopy species; hence, canopy gaps with dense *Sasa* coverage tend to be sustained for a long time (Noguchi and Yoshida 2004). Tree regeneration under canopy gaps is usually restricted to occasionally disturbed microsites such as tip-up mounds (Hiura et al. 1996; Yoshida et al. 2006; Vodde et al. 2011). Shade-intolerant broadleaved species (e.g., *B. ermanii*, *B. platyphylla*, and *Kalopanax septemlobus*) are usually the first tree species (pioneer species) to become established on these microsites, and they grow faster than shade-tolerant coniferous species (Hiura et al. 1996; Yoshida et al. 2006; Vodde et al. 2011). In contrast, the seedling and sapling densities of tree species tend to be higher under conifer canopies because of the lower inhibition by *Sasa* cover (Noguchi and Yoshida 2004). In our site, some shade-intolerant broadleaved trees (*Phellodendron amurense*) grew around the canopy gap (Fig. 2.1), implying that these trees were established after the forest floor of the canopy gap had been covered by *Sasa*. However, the timing of the establishment of *Sasa* and shade-intolerant broadleaved species varies depending on canopy-gap conditions such as gap size, the species composition of adjacent vegetation, and light availability.

The spatial range of influence of broadleaved trees on *Sasa* biomass, litter composition, and soil properties was relatively large (10- to 15-m radii), while the influence of coniferous trees was strongest within the 5-m radius, although the 10- and 15-m radii buffers also showed significant relationships with these variables (Table 2.3). This could be explained partly by the fact that the lower density of broadleaved trees made the variation of the number of broadleaved trees within the 5-m radius buffer insufficient to capture the variation of the *Sasa* biomass and other variables, compared with the more abundant coniferous tree in this study site. However, our result showing that the *Sasa* biomass was positively correlated with the abundance of broadleaved trees within the 10- and 15-m radii buffers and negatively correlated with the abundance of coniferous trees within the 5-m radius buffer could reflect the generally brighter forest

floor under the deciduous broadleaved canopy, compared with that under the evergreen coniferous canopy. The negative influence of conifer abundance was also found on the proportion of *Sasa* litterfall (Table 2.3). These radii of tree influence could also reflect the wider range of leaf litterfall by the broadleaved species, compared with that of the coniferous species (Ferrari and Sugita 1996), because the number of broadleaved trees within the 10- and 15-m radii buffers was positively correlated with the proportion of broadleaved litter, and the number of coniferous trees within the 5-m radius buffer was positively correlated with the proportion of coniferous litter (Table 2.3).

We observed that the litter composition was determined largely by the surrounding plant community composition (Table 2.3). Locations where coniferous litter was dominant exhibited a relatively thick O horizon, while those where broadleaved and *Sasa* litters were dominant exhibited a relatively thin O horizon (Table 2.4). The coniferous litter had a lower N content and a higher C/N ratio than the broadleaved and *Sasa* litter (Table 2.7). These results indicate that the dominance of recalcitrant coniferous litter in the litterfall leads to the accumulation of organic matter on the forest floor, suggesting that the spatial pattern of the O horizon thickness is regulated by the spatial distribution of trees. An increase in O horizon thickness because of the recalcitrant litter quality was also reported in previous studies (Rothe et al. 2002b; Guckland et al. 2009).

In the canopy gap, the O horizon was relatively thin (Figs. 2.2 g and h, Table 2.6). The thin O horizon appeared to have resulted from the small contribution of recalcitrant coniferous litter to the total litterfall, as well as the dominance of fast-decomposing broadleaved litter in the total litterfall in the canopy gap (Table 2.6). The observed litter composition is probably caused by the narrow dispersal range of coniferous litter, compared with that of broadleaved litter (Ferrari and Sugita 1996), as well as the concentration of broadleaved trees around the canopy gap (Table 2.1). In addition to the litter composition, the wet condition of the forest floor in the canopy gap may have enhanced litter decomposition, as moisture is one of the major factors that controls litter decomposition (Prescott 2010). The forest floor under the canopy gap is likely to have received more precipitation than that under the canopy, as coniferous and broadleaved canopies intercept 23–33 % of total precipitation (Barbier et al. 2009). Additionally, understory vegetation cover prevents an increase in soil temperature by attenuating the input of radiant energy to the ground (Balisky and Burton 1993), which consequently reduces evaporation (Muscolo et al. 2007). Previous studies indicated that the decomposition rate of *Sasa* litter is slower than that of overstory species (Tripathi et al. 2006; Watanabe et al. 2013), suggesting that the dense *Sasa* in the canopy gap area

increases the thickness of the O horizon. However, our results indicate the opposite pattern (i.e., a thin O horizon in the gap area), implying that the positive effects of the absence of coniferous litter, the dispersed input of deciduous litter, and the wet conditions outweigh the negative impact of *Sasa* litter on litter decomposition in the canopy gap. We also observed that there were large spatial and temporal variations in the thickness of O horizon within the study site (Fig. 2.2i), possibly caused by large spatial differences in litterfall amount, litter storage (e.g., the degree of physical fragmentation and compaction), and litter decomposition. Further investigations of the temporal and fine-scale spatial variations of the O horizon thickness are needed.

The soil water content tended to be low near coniferous trees (Table 2.5). Differences in water uptake by roots are often attributed to be a factor that contributes to soil moisture heterogeneity (Asbjornsen et al. 2011; Naithani et al. 2013). Canopy interception of precipitation is another factor. Coniferous trees tend to intercept more precipitation than broadleaved species owing to their larger leaf area index and bundled needle arrangement (Barbier et al. 2009). In addition, spatial variation in snowpack depth is suggested to cause spatial variation in the soil water content during the growing season because of soil moisture recharge by snowmelt water (Maurer and Bowling 2014), and the snowpack amount is usually lower under coniferous canopies, compared with that in canopy gaps (Harpold et al. 2015).

The thick O horizon had a negative influence on the soil water content (Table 2.5). The negative effect of the thick forest floor on the soil water content might be attributed to the presence of hydrophobic compounds. Hydrophobic compounds derived from plants can induce soil water repellency, which can impede water infiltration; severe soil water repellency is usually found under slow-decomposing litter layers under evergreen coniferous species (Doerr et al. 2000). Therefore, the spatial variations in soil moisture observed in September 2012 and June 2014 could be the result of the interacting effects of canopy interception of rainfall and snow (especially for the soil moisture condition in spring), and of soil water repellency under slow-decomposing litter in this snow-dominated forest ecosystem.

2.4.2 Controlling factor of the spatial pattern of soil N dynamics in a forest with a complex structure

The selected regression model for the spatial pattern of the soil NO_3^- content showed that the soil water content has a positive influence on the soil NO_3^- content (Table 2.5). Additionally, the soil NO_3^- content in the field was strongly related to the

net nitrification rate that was measured in the laboratory, and it was used as an index of nitrifier activity (Table 2.8). These results suggest that differences in nitrifier activity (i.e., nitrification) strongly affect the spatial pattern in the soil NO_3^- content. They also suggest that the nitrification potential differs under various soil moisture conditions. Thus, our results suggest that the spatial pattern of the soil water content, which was created by the plant distribution, influences the spatial pattern of soil microbial activity, which is related to NO_3^- production in the soil. However, there was no significant difference in the soil moisture among the quadrats, although the nitrification rate in the *Sasa* quadrat was significantly higher than that of the other quadrats (Table 2.6). These might be caused by the large spatial variation of the soil moisture in the study sites. A further study with finer spatial resolution will be necessary to analyze these relationships.

The spatial influence of the soil water content on net nitrification rates, microbial biomass, and enzyme activities was also observed in previous studies (Robertson et al. 1988; Baldrian et al. 2010). A positive influence of soil moisture on nitrifier abundance and gross nitrification was found along a hillslope of another broadleaved forest in Japan (Isobe et al. 2015). Additionally, Bustamante et al. (2012) found that the addition of water to semiarid soil microcosms increased the net nitrification rate by changing the nitrifier composition. These findings suggest that the spatial pattern of the soil water content creates spatial patterns of nitrifier abundance and composition, which might be responsible for the spatial pattern of the soil NO_3^- content at the study site, but further investigations of the microbial community are necessary to confirm this.

The regression model for the soil NO_3^- content also showed a positive influence of the abundance of broadleaved trees within the 5-m radius buffer on the soil NO_3^- content, suggesting that the soil NO_3^- content is high near groups of broadleaved trees and low where broadleaved trees are scarce (Table 2.5). This reflects the plant distribution of our site: most of the broadleaved trees are found in and around the canopy gap, while coniferous trees are abundant where broadleaved trees are scarce (Fig. 2.1). Locations near the broadleaved trees in the canopy gap receive fast-decomposing broadleaved litter, while the contribution of slow-decomposing conifer litter is small in the canopy gap because of the narrow dispersal range of conifer litter (Table 2.6). This leads to the thinner O horizon and higher soil moisture near the broadleaved trees in the canopy gap as discussed earlier. Therefore, our results suggest that the characteristics of forest dynamics in a cool-temperate mixed forest with a dense understory, in which canopy gaps are created by occasional natural disturbances, subsequently leading to the subsequent dominance of *Sasa* understory and the establishment of broadleaved pioneer

species on limited locations, determines the spatial pattern of soil N dynamics, especially the soil NO_3^- content. As we examined only one representative forest stand that contains a single canopy gap, our results can serve as an important case study, as few studies have investigated how soil N dynamics are controlled in complex, disturbed, and mixed forests in detail.

Among the variables measured in our study, the O horizon thickness, the soil NO_3^- content, and the soil water content obtained from the intensive grid sampling were spatially dependent. Statistical analyses of spatially autocorrelated data could lead to incorrect assessments of hypotheses (Legendre 1993; Dormann 2007). Therefore, when the relationships between these variables and controlling factors were modeled, an ordinary linear regression analysis was used after confirming that the model residuals were not spatially structured. In contrast, we used a correlation analysis and a single factor analysis of variance to test for significant relationships and differences among data obtained across the sampling quadrats. We believe that these methods are valid because previous studies dealing with the spatial patterns of soil variables used these statistical analyses (Gross et al. 1995; Hirobe et al. 2003; Bengtson et al. 2006). However, it is still possible that the assumption of mutually independent data may have been violated. Therefore, the incorporation of spatial autocorrelation into the analysis of data obtained from the quadrats will be required to better understand the spatial relationship between the forest structure and soil N dynamics.

Nevertheless, our results suggest that canopy gap creation and subsequent plant succession create high soil moisture conditions via biological and hydrological processes that are influenced by plants growing in and around the canopy gap in cool-temperate conifer-broadleaved mixed forests with dense undergrowth (Figs. 2.2d and e), and that the high soil water content may be responsible for the relatively high nitrification potential, which explains the high soil NO_3^- content in the canopy gap (Figs. 2.2a and b). Our findings suggest that even in a relatively small and flat area within the watershed, the complex forest structure caused by occasional gap creation, and long-term maintenance of the gaps by the dense *Sasa* understory affect the spatial patterns of litterfall and hydrology, which create the spatial variation of soil N dynamics. Furthermore, our results imply that natural disturbances that create patchy canopy gaps will result in the long-term presence of locations with relatively high nitrification rates and soil NO_3^- contents in this forest. Further studies of soil N dynamics in other forest stands with canopy gaps are necessary because nitrification and the soil NO_3^- content affect plant N uptake, NO_3^- leaching to deeper soil, and N_2O emissions in forest ecosystems; additionally, the frequency of strong typhoons, which is a major factor that

creates canopy gaps, is predicted to increase because of global warming (Emanuel 2005; Webster et al. 2005).

2.5 Conclusions

Figure 2.3 shows a summary of our findings. We found that the distributions of overstory and understory vegetation, which reflect the current species competition for resources and the legacy of past disturbances, create spatial patterns of nitrification potential and soil NO_3^- content in a conifer-broadleaved mixed forest with a dense *Sasa* undergrowth. Coniferous trees, which were dominant in the closed canopy, and broadleaved trees, which grew mainly around the canopy gap, largely determined the spatial pattern of the O horizon thickness via differences in litter decomposition. The dominance of recalcitrant coniferous litter resulted in a thick O horizon, while the dominance of fast-decomposing broadleaved and *Sasa* litters led to a thin O horizon. Differences in the canopy interception of precipitation between the conifer-dominated area and the canopy gap could also contribute to the spatial pattern of O horizon thickness through its influence on the moisture conditions of the forest floor. Locations around coniferous trees where the O horizon is thick had dry soils, whereas locations beneath broadleaved trees and in the canopy gap where the O horizon was thin exhibited high soil water contents. High soil water content was related to high nitrification rates and, hence, high soil NO_3^- contents. Our results suggest that the distribution of plant species affects the spatial patterns of litterfall and hydrology, which create the spatial variation of soil N dynamics even in a relatively small and flat area within the watershed. Additionally, our results suggest that the high level of nitrification and the high soil NO_3^- content in the canopy gap may last for decades, given that canopy species have difficulty in naturally regenerating once the canopy gap is dominated by *Sasa*.

Table 2.1 Density, diameter at breast height, and total basal area of overstory vegetation and the abundance of understory vegetation at the study site

Vegetation	Plant species	Tree density (tree ha^{-1})	Mean DBH (cm)	Basal area (m^2 ha^{-1})
Coniferous	*Abies sachalinensis*	691.2	22.46 (9.42)	32.1
	Picea glehnii	46.1	67.33 (37.47)	20.2
	not identified	80.6	14.79 (13.42)	2.4
	Total	818.0	24.23 (16.38)	54.7
Broadleaved	*Betula ermanii*	57.6	36.44 (25.79)	8.4
	Quercus crispula	57.6	33.98 (27.65)	8.0
	Betula platyphylla	57.6	22.38 (9.33)	2.6
	Phellodendron amurense	80.6	18.20 (4.69)	2.2
	Aria alnifolia	69.1	14.97 (2.1)	1.2
	Kalopanax septemlobus	34.6	15.47 (2.16)	0.7
	Tilia japonica	11.5	16.40	0.2
	not identified	69.1	8.44 (2.68)	0.4
	Total	437.8	20.91 (16.14)	23.8
Understory	*Sasa senanensis* *		0.69 (0.75)	

Note: DBH: diameter at breast height. Data for overstory species are derived from the tree census data of the Uryu Experimental Forest.

*The value for *Sasa senanensis* is mean biomass (kg DW m^{-2}). Data was obtained in this study. Standard deviations are given in parentheses.

Table 2.2 Spatial variation of soil properties measured in the intensive grid sampling

		2012 September				2014 June			
		Mean	Range	CV	Moran's I	Mean	Range	CV	Moran's I
O horizon thickness	(cm)	3.3 *a*	1.0 – 7.0	0.43	0.11	3.6 *a*	0.5 – 8.0	0.55	0.27 **
Soil NH_4^+	(mgN kg $soil^{-1}$)	11.70 *a*	6.56 – 23.72	0.30	0.07	11.10 *a*	6.72 – 22.13	0.26	0.08
Soil NO_3^-	(mgN kg $soil^{-1}$)	1.17 *a*	0.31 – 4.03	0.74	0.23 **	1.62 *a*	0.12 – 6.40	0.93	0.33 **
Soil water content	(%)	31.8 *b*	26.4 – 40.0	0.11	0.40 **	34.2 *a*	27.7 – 47.6	0.14	0.29 **
Soil pH		4.6	4.2 – 5.4	0.05	0.03	–			
Soil exchangeable Ca	(mg kg $soil^{-1}$)	165.2	25.0 – 553.8	0.79	0.22 **	–			
Soil exchangeable Al	(mg kg $soil^{-1}$)	26.9	5.8 – 64.7	0.41	−0.01	–			

Note: Different letters indicate significant differences ($P < 0.05$) between sampling dates. Asterisks indicate significant autocorrelation in the variable. ** $P < 0.01$, * $P < 0.05$

Table 2.3 Spearman's rank correlation coefficients between the number of trees and the measured variables

		Number of broadleaved tree			Number of coniferous tree		
	Sampling	5-m radius	10-m radius	15-m radius	5-m radius	10-m radius	15-m radius
Number of Brd tree (5 m)		1.00	0.36	0.46 **	-0.20	-0.40 **	-0.37 **
(10 m)		0.36	1.00	0.77 **	-0.55 **	-0.70 **	-0.65 **
(15 m)		0.46 **	0.77 **	1.00	-0.62 **	-0.77 **	-0.67 **
Number of Cnf tree (5 m)		-0.20	-0.55 **	-0.62 **	1.00	0.77 **	0.77 **
(10 m)		-0.40 **	-0.70 **	-0.77 **	0.77 **	1.00	0.90 **
(15 m)		-0.37 **	-0.65 **	-0.67 **	0.77 **	0.90 **	1.00
Sasa biomass	Grid I	0.16	0.39 **	0.39 **	-0.52 **	-0.37	-0.32
	Quadrat	-0.14	0.51	0.62 *	-0.90 **	-0.62 *	-0.79 **
Litterfall (mass)							
Total litter	Quadrat	0.59 *	-0.02	0.03	0.31	0.31	0.21
Broadleaf litter	Quadrat	0.64 *	0.37	0.46	0.02	-0.04	-0.07
Conifer litter	Quadrat	0.11	-0.81 **	-0.80 **	0.63 *	0.77 **	0.52 *
Sasa litter	Quadrat	-0.33	0.35	0.42	-0.69 **	-0.48	-0.62 *
Litterfall (proportion)							
Broadleaf litter	Quadrat	0.46	0.66 **	0.73 **	-0.38	-0.40	-0.37
Conifer litter	Quadrat	-0.18	-0.88 **	-0.88 **	0.60 *	0.68 **	0.53 *
Sasa litter	Quadrat	-0.35	0.45	0.48	-0.76 **	-0.58 *	-0.65 **
O horizon thickness	Grid I	-0.17	-0.22	-0.11	0.33 *	0.27	0.30
	Grid II	-0.12	-0.38 **	-0.38 **	0.56 **	0.50 **	0.57 **
	Quadrat	0.24	-0.69 **	-0.59 *	0.65 **	0.81 **	0.66 **
Soil water content	Grid I	0.26	0.37 **	0.37 *	-0.56 **	-0.53 **	-0.52 **
	Grid II	0.25	0.40 **	0.39 **	-0.55 **	-0.53 **	-0.60 **
	Quadrat	-0.63 *	0.08	-0.05	-0.23	-0.44	-0.30
Exchangeable Ca	Grid I	0.33 **	0.42 **	0.60 **	-0.41 **	-0.48 **	-0.47 **
	Quadrat	0.18	0.56 *	0.57 *	-0.68 **	-0.54 *	-0.51
Exchangeable Al	Grid I	-0.32 *	-0.22	-0.32 *	0.18	0.21	0.18
	Quadrat	0.05	-0.03	-0.05	0.59 *	-0.14	0.15
Soil NO_3^-	Grid I	0.42 **	0.43 **	0.47 **	-0.44 **	-0.40 **	-0.43 *
	Grid II	0.34 *	0.40 **	0.41 **	-0.28	-0.24	-0.25
	Quadrat	-0.07	0.60 *	0.46	-0.50	-0.62 *	-0.57 *
Net nitrification	Quadrat	-0.08	0.64 *	0.50	-0.53 *	-0.68 **	-0.59 *
Correlated pairs (P < 0.05)		7	14	14	16	13	13
Correlated pairs (P < 0.01)		2	11	9	11	9	7

Note: Only the variables that showed significant correlation with the number of trees are shown. Brd: Broadleaved; Cnf: Coniferous, Grid I: Grid sampling in September 2012; Grid II: Grid sampling in June 2014. Correlated pairs (P < 0.05/0.01): the number of pairs between the number of trees and other variables that showed significant (P < 0.05/0.01) correlation; Asterisks indicate significant correlation in the variable. ** P < 0.01, * P < 0.05

Table 2.4 Spearman's rank correlation coefficients among the *Sasa* biomass, the litterfall, and the thickness of O horizon

			Litterfall (mass)				Litterfall (proportion)			
		Sasa biomass	Total litter	Broadleaf	Conifer	*Sasa*	Broadleaf	Conifer	Sasa	O horizon
	Sasa biomass	1.00								
Litterfall										
Mass	Total litter	-0.39	1.00							
	Broadleaf litter	-0.09	0.81 **	1.00						
	Conifer litter	-0.57 *	0.27	-0.21	1.00					
	Sasa litter	0.86 **	-0.24	-0.09	-0.49	1.00				
Proportion	Broadleaf litter	0.24	0.34	0.81 **	-0.62 *	0.09	1.00			
	Conifer litter	-0.51	-0.11	-0.53 *	0.89 **	-0.43	-0.78 **	1.00		
	Sasa litter	0.90 **	-0.37	-0.15	-0.61 *	0.96 **	0.12	-0.50	1.00	
	O horizon thickness	-0.53 *	0.18	-0.17	0.77 **	-0.48	-0.52 *	0.72 **	-0.55 *	1.00

Asterisks indicate significant correlations among variables. ** $P < 0.01$, * $P < 0.05$.

Table 2.5 Summary of stepwise multiple regression analysis for soil nitrate concentration, soil water content, and O horizon thickness

Response variable	Sampling date	Independent variable	Coefficients	*P* value	Model R^2	Moran's I error
Soil NO_3^-	September 2012	Intercept	-2.3E-16	1.000	0.40	NS
		Soil water content	0.36	0.011		
		Number of Brd (5 m)	0.32	0.010		
		O horizon thickness	−0.21	0.120		
	June 2014	Intercept	1.4E-16	1.000	0.37	NS
		O horizon thickness	-0.33	0.019		
		Soil water content	0.30	0.034		
		Number of Brd (5 m)	0.24	0.044		
Soil water content	September 2012	Intercept	1.1E-15	1.000	0.41	NS
		Number of Cnf (5 m)	−0.44	0.001		
		O horizon thickness	−0.39	0.002		
	June 2014	Intercept	1.7E-17	1.000	0.39	NS
		Number of Cnf (5 m)	−0.40	0.004		
		O horizon thickness	−0.33	0.018		
O horizon thickness	September 2012	Intercept	1.6E-16	1.000	0.09	NS
		Number of Cnf (5 m)	0.31	0.031		
	June 2014	Intercept	7.8E-17	1.000	0.26	NS
		Number of Cnf	0.52	< 0.001		

Coefficients: standard partial regression coefficients. Model R^2: degree of freedom adjusted R^2. Number of Brd, number of broadleaved trees; Number of Cnf, number of coniferous trees. All models are significant at $P < 0.05$; Moran's I error: *P* value of the Moran's I test for regression residuals. NS: not significant

Table 2.6 Properties of vegetation, total litterfall mass, and the proportion of each litter type in total litterfall in three types of quadrats (*Sasa*, *Sasa*/tree, and tree)

			Sasa		*Sasa*/tree		tree	
			Mean	Range	Mean	Range	Mean	Range
Vegetation	Number of Brd tree (5 m)	(tree buffer^{-1})	0.8 a	0 - 1	0.6 a	0 - 2	1.4 a	0 - 3
	(10 m)	(tree buffer^{-1})	7.6 a	5 - 10	3.0 b	1 - 4	4.2 b	3 - 5
	(15 m)	(tree buffer^{-1})	17.4 a	15 - 19	8.0 b	5 - 13	9.2 b	6 - 10
	Number of Cnf tree (5 m)	(tree buffer^{-1})	0.0 c	0 - 0	3.8 b	2 - 5	5.2 a	5 - 6
	(10 m)	(tree buffer^{-1})	8.0 b	7 - 10	14.2 a	13 - 16	13.0 a	10 - 16
	(15 m)	(tree buffer^{-1})	19.8 b	18 - 21	28.2 a	25 - 35	28.4 a	25 - 31
	Sasa biomass	(kg m^{-2})	1.6 a	1.1 – 2.4	0.5 b	0.4 – 0.5	0.0 b	0.0
Litterfall	Total amount	(g m^{-2})	18.4	9.5 – 34.9	19.6	17.3 – 23.4	24.4	19.5 – 32.6
	Broadleaved	(%)	67.9 a	36.7 – 81.3	37.2 b	18.7 – 50.9	56.3 ab	29.2 – 71.2
	Coniferous	(%)	10.3 b	5.6 – 15.5	58.0 a	48.4 – 76.8	43.6 a	28.5 – 70.8
	Sasa	(%)	19.7 a	7.0 – 54.6	4.8 ab	0.6 – 10.1	0.1 b	0.0 – 0.4
	Others	(%)	2.1	0.0 – 10.5	0.0	0.0	0.0	0.0
Forest floor	O horizon thickness	(cm)	1.8 b	1.5 – 2.0	3.5 a	2.5 – 5.0	3.0 a	2.3 – 4.0
Soil	Soil water content	(%)	32.3	29.4 – 34.8	32.4	26.4 – 39.5	28.7	23.9 – 32.9
	Soil pH		4.6	4.4 – 4.9	4.5	4.4 – 4.7	4.4	4.3 – 4.5
	NH_4^+	(mgN kg soil^{-1})	6.04	3.02 – 11.37	7.67	3.21 – 11.24	5.38	4.16 – 7.37
	NO_3^-	(mgN kg soil^{-1})	1.97 a	0.48 – 2.94	0.39 b	0.06 – 0.70	0.55 b	0.06 – 1.40
	Net N mineralization	(mgN kg soil^{-1} day^{-1})	4.58	2.84 – 5.85	8.03	3.01 – 14.13	2.75	1.00 – 4.26
	Net nitrification	(mgN kg soil^{-1} day^{-1})	2.28 a	0.36 – 3.69	0.24 b	0.08 – 0.53	0.41 b	0.03 – 1.20
	Exchangeable Ca	(mg g soil^{-1})	0.24 a	0.08 – 0.32	0.08 b	0.02 – 0.12	0.08 b	0.03 – 0.15
	Exchangeable Al	(mg g soil^{-1})	0.04 b	0.02 – 0.05	0.03 b	0.02 – 0.05	0.07 a	0.05 – 0.10

Note: Different letters indicate significant differences ($P < 0.05$) among quadrat types. Number of Brd: number of broadleaved trees; Number of Cnf: number of coniferous trees

Table 2.7 Chemical properties of leaf litter

		Broadleaved			Coniferous			*Sasa*		
		Mean		Range	Mean		Range	Mean		Range
Carbon	(mg g^{-1} litter)	527.4 *b*	(n=15)	499.8 – 556.2	552.8 *a*	(n=15)	530.1 – 587.3	423.3 *c*	(n=11)	378.4 – 479.9
Nitrogen	(mg g^{-1} litter)	17.4 *a*	(n=15)	13.7 – 28.3	8.3 *b*	(n=15)	7.5 – 9.1	13.0 *b*	(n=11)	10.4 – 17.3
C/N ratio		31.3 *b*	(n=15)	17.7 – 39.0	66.8 *a*	(n=15)	61.7 – 72.5	33.4 *b*	(n=11)	22.7 – 43.8
Calcium	(mg g^{-1} litter)	7.68 *a*	(n=15)	5.87 – 10.46	8.07 *a*	(n=15)	6.86 – 9.72	3.08 *b*	(n=9)	1.46 – 3.90
Aluminum	(mg g^{-1} litter)	0.064 *c*	(n=15)	0.043 – 0.097	0.322 *a*	(n=15)	0.237 – 0.420	0.137 *b*	(n=9)	0.073 – 0.187

Note: Different letters indicate significant differences ($P < 0.05$) among litter types

Table 2.8 Spearman's rank correlation coefficients between net N transformation rates and soil properties in the quadrat survey

	Net N mineralization	Net nitrification	Soil C/N	Soil pH	Soil NH_4^+	Soil NO_3^-
Net N mineralization	1.00					
Net nitrification	0.13	1.00				
Soil C/N	-0.04	-0.42	1.00			
Soil pH	-0.29	-0.31	-0.41	1.00		
Soil NH_4^+	-0.25	-0.26	-0.51	0.73 **	1.00	
Soil NO_3^-	0.08	0.99 **	-0.40	-0.31	-0.29	1.00

Note: Asterisks indicate significant correlation among variables. ** $P < 0.01$, * $P < 0.05$

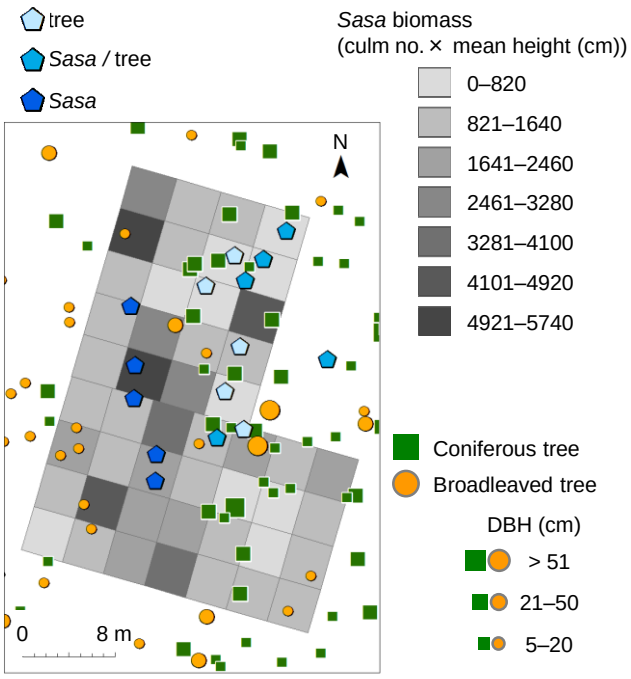

Fig. 2.1 Spatial pattern of canopy trees, *Sasa* biomass, the sampling grid and the locations of sampling quadrats (*Sasa*, *Sasa*/tree, tree). Locations and diameter at breast height of overstory vegetation are indicated for filled circle (broadleaf trees) and filled square (coniferous trees). *Sasa* biomass was calculated by multiplying the total number of culms by the average height of standing *Sasa* within a 1-m radius from each sampling point. The sampling grids (4×4 m) are indicated by gray lines. DBH: diameter at breast height

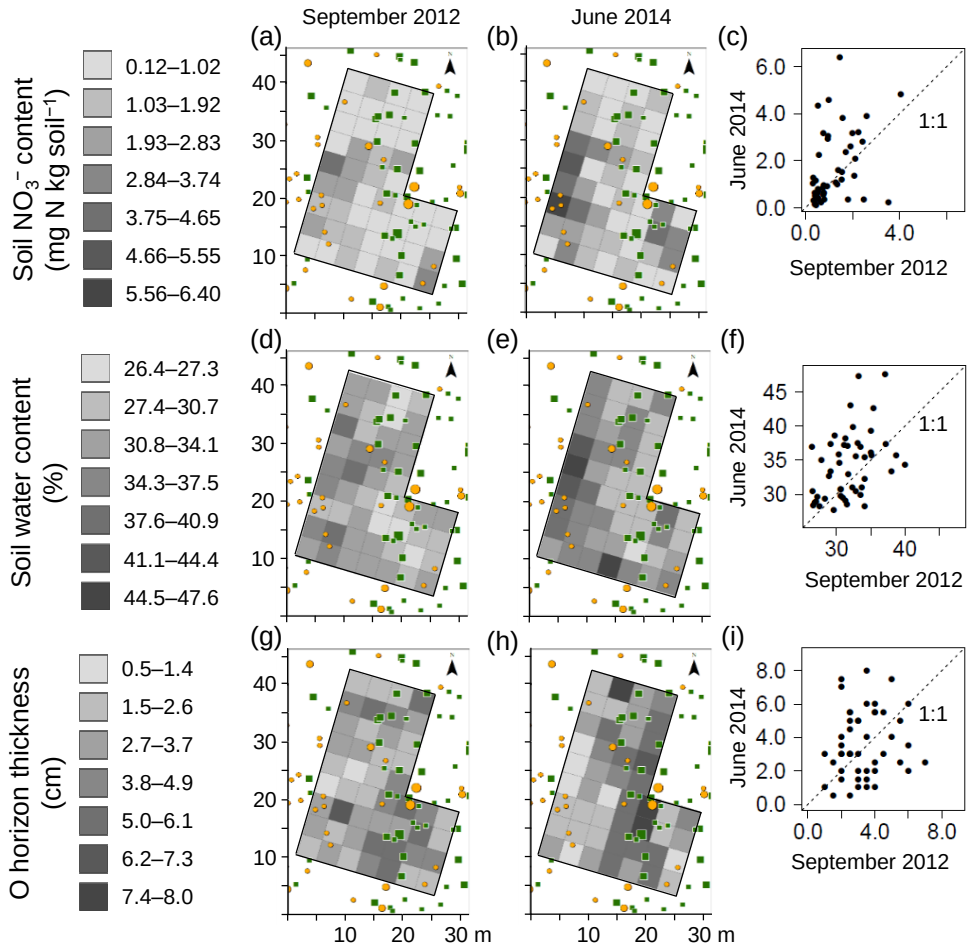

Fig. 2.2 Spatial patterns of the measured variables and the distribution of overstory vegetation. (a) soil NO_3^- content (mg N kg $soil^{-1}$), (d) soil water content (%), and (g) thickness of the O horizon (cm) in 2012 September. (b) soil NO_3^- content (mg N kg $soil^{-1}$), (e) soil water content (%), and (h) thickness of the O horizon (cm) in 2014 June. The relationships between the observed values in 2012 September and those in 2014 June for (c) soil NO_3^- content (mg N kg $soil^{-1}$), (f) soil water content (%), and (i) thickness of the O horizon (cm). The dashed line shows that the ratio of the value in September to that in June is 1. Locations and DBHs of overstory vegetation are indicated for filled circle (broadleaf trees) and filled square (coniferous trees). The symbol sizes of overstory vegetation are the same as those in Fig. 2.1

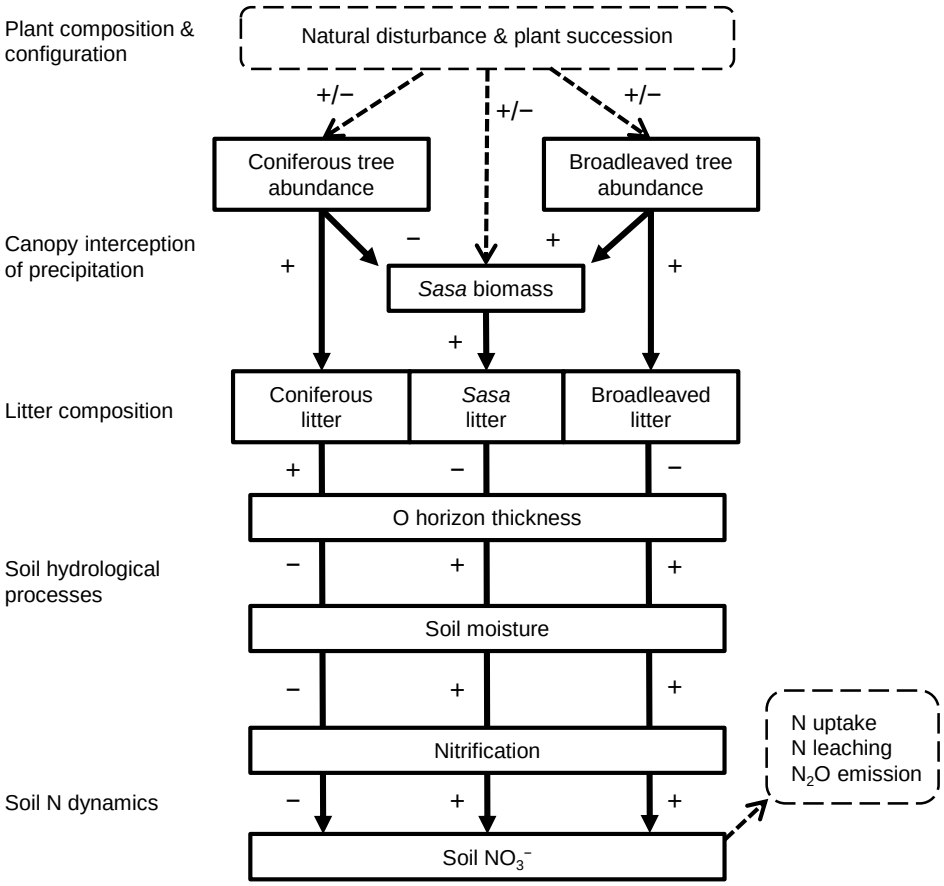

Fig. 2.3 Schematic diagram describing how plants affect the spatial pattern of soil NO_3^- contents in the coniferous-broadleaved mixed forest stand with dense *Sasa* undergrowth. The detailed explanations of each process and relationship are found in the Discussion and Conclusion sections. The boxes and arrows with solid lines indicate the observed variables and influences, and those with dashed line indicate unmeasured variables and influences. + and − signs indicate positive and negative influences, respectively

Chapter 3. Differences in the dynamics of dissolved organic matter among vegetation types and its effects on nitrate leaching from soil

3.1 Introduction

The chapter 2 demonstrated that soil NO_3^- contents around broadleaved trees and in the canopy gap dominated by *Sasa* were higher than those around coniferous trees. The spatial pattern of the soil NO_3^- content was related to the spatial pattern of litterfall that supply organic matter to the soil and that of soil moisture which affect microbial activity.

Litterfall is a major source of N for soil organic matter. It is well known that faster litter decomposition is related to higher net rates of N mineralization and nitrification in soils (Scott and Binkley 1997; Binkley and Giardina 1998; Ferrari 1999), although the mechanisms behind the relationship is not fully understood (Knops et al. 2002; Prescott 2005). Some studies have found a significant negative relationship between soil C/N ratio and net N mineralization rates in the soil when soils under different tree species were examined, and attributed the difference in the soil organic matter quality to the differences in litter decomposition rates (Finzi et al. 1998). In contrast, other studies did not find such a clear relationship between soil C/N ratio and net N mineralization rates (Lovett et al. 2004). These contrasting results suggest that examination of soil quality by its bulk C and N contents may not be sufficient to understand how plants affect soil N dynamics via differences in litter decomposition and subsequent soil organic matter formation.

Knops et al. (2002) have proposed a model in which litter quality differences among plant species control the decomposition rate of a part of soil organic matter pool (active soil organic matter), and the difference in the decomposition rate of the active soil organic matter affects N mineralization rate. Leaching of organic matter from canopy and forest floor is a major pathway that the organic matter is incorporated into mineral soils (Qualls et al. 1991; Froberg et al. 2007), and the new organic matter, such as plant residues and microbial products, is generally more decomposable for soil microbes compared with old humic substances already present in the soil (Zech et al. 1997). DOM is an important source of energy for microbes and substrate of nitrogen for microbial mineralization and nitrification. Therefore, the properties of DOM that is supplied from plants to soils, and their differences among coniferous and broadleaved trees and *Sasa* grown in canopy gaps may be an important factor that create the spatial variation in soil NO_3^- contents.

A number of studies have advanced the understandings of DOM dynamics. Throughfall and leaching from forest floor are major sources of DOM in forest ecosystems (Qualls et al. 1991; Froberg et al. 2007). DOM is constituted of various fractions with different chemical properties, such as recalcitrant humin, carbohydrates, microbially released compounds (Guggenberger et al. 1994). The chemical properties of DOM reflect the biodegradability of DOM (Kalbitz et al. 2003), and the biodegradability of DOM is higher in throughfall and is lower in DOM from forest floor and surface mineral soil (Qualls and Haines 1992).

Influence of tree species on DOM dynamics are less understood. The concentrations and fluxes of DOC and DON percolating from forest canopy to mineral soil horizons is well studied, however, whether there is consistent difference in DOC and DON concentrations and fluxes is not clear (Michalzik et al. 2001). This could be partly due to the complex dynamics of DOM. Don and Kalbitz (2005) examined the DOC release from fresh litter and decomposing litter, and found that DOC release from fresh litter was larger for broadleaved leaf litter than for coniferous needle litter, while the DOC release at the later stages of decomposition became similar between the two types of litter as the DOC release from coniferous litter increased at these stages. Biodegradability of DOM from fresh coniferous litter has also been found to be higher than that from fresh deciduous litter (Don and Kalbitz 2005; Kiikkila et al. 2013). However, the source of DOM supplied to mineral soil has been suggested to be more decomposed organic layer in the forest floor rather than fresh litter (Kalbitz et al. 2007), and the DOM properties of organic layer, such as composition of hydrophobic and hydrophilic fractions and molecular weight, have been found to be similar between broadleaved and coniferous specie (Don and Kalbitz 2005; Kiikkila et al. 2006, 2011). Although results of these studies have advanced our understanding of DOM properties among tree species, majority of the studies focused on DOC dynamics in relation to C accumulation in soil. Therefore, whether differences in DOM properties among plant species affect microbial N transformation in soils is not clear.

Characterization of DOM properties using techniques such as fractionation or ^{13}C NMR spectroscopy requires large sample volumes and many analytical stages (Guggenberger et al. 1994). The recent availability of spectrofluorometric tools such as ultra violet (UV–visible) absorbance and fluorescence of DOM allows for rapid characterization of DOM properties with small sample volumes (Stedmon et al. 2003). The optical properties obtained from these techniques provide indices such as specific ultra-violet absorbance (SUVA, Weishaar et al. 2003), spectral slope ratio (S_R, Helms et al. 2008), and humification index (HIX) (Zsolnay et al. 1999; Ohno 2002), and they

provide important insights into DOM dynamics, which may affect N mineralization process.

NO_3^- in soils consists of NO_3^- directly derived from the atmosphere and those produced by microbial nitrification. Thus, it is important to understand the contribution of microbially produced NO_3^- in the total NO_3^- to understand the influence of DOM on inorganic N production in soils. Although the relationship between atmospheric N deposition and NO_3^- output in soil water and stream water have been examined in many studies, the relative contributions of atmospheric NO_3^- and microbially produced NO_3^- in the total NO_3^- in soil water and the effects of plant species on the contributions are not well understood (Rose et al. 2015).

Recent advance in stable isotopic composition of NO_3^- made possible to understand the dynamics of atmospheric NO_3^- in soil water, ground water, and stream water. Studies that examined $\delta^{15}N$ and $\delta^{18}O$ of NO_3^- have found that atmospheric NO_3^- is rapidly replaced by microbial NO_3^- after entering forest floor and surface mineral soil in forest ecosystems (Osaka et al. 2010). Although studies that examined $\delta^{15}N$ and $\delta^{18}O$ of NO_3^- have advanced our understanding of the N dynamics of leaching water in soil horizons, several challenges remain in the quantitative differentiation of atmospheric and microbial NO_3^-using the dual isotope approaches. The fraction of atmospheric NO_3^- has been estimated using a two end-member mixing model that bases on the fact that $\delta^{18}O$ value of atmospheric and microbial NO_3^- is distinct (Kendall et al. 2007). However, the relatively wide ranges of $\delta^{18}O$ values in both atmospheric and microbial NO_3^- and the mass-dependent fractionation of $\delta^{18}O$ value during denitrification and assimilation of NO_3^- produce some uncertainties in the estimated fraction of atmospheric NO_3^- (Rose et al. 2015). Methods using $\Delta^{17}O$ of NO_3^- has been recognized as a more precise method of tracing atmospheric NO_3^- in terrestrial ecosystem because $\Delta^{17}O$ of NO_3^- is not affected by denitrification and assimilation of NO_3^-, and it enables us to calculate the relative contribution of atmospheric NO_3^- in the total NO_3^- (Michalski et al. 2004).

The objective of this chapter is to understand 1) the difference in the dynamics of DOM from forest canopy to surface soil among vegetation types, and 2) whether DOM properties influence NO_3^- leaching. The concentrations and fluxes of DON, DOC, NH_4^+ and NO_3^-, the spectrofluorometric indices of DOM, and stable isotopic composition of NO_3^- in throughfall, litter leachate, and soil water were examined beneath oak, spruce, and *Sasa* grown in canopy gaps. Then, the influence of DOM properties in the litter leachate on NO_3^- in the soil water was analyzed. The working hypotheses are that 1) DOM in litter leachate will be more degradable beneath oak and

Sasa than spruce, thereby producing more NO_3^- in the soil beneath oak and *Sasa* than spruce. 2) The higher production of NO_3^- in the soil beneath oak and *Sasa* will also result in lower proportion of atmospheric NO_3^- in the leaching NO_3^-.

3.2 Material and methods

3.2.1 Study site

Within the forested watershed (ca. 3 ha) where the study site for Chapter 2 was established, we selected four mature individuals of *Q. crispula* (hereafter Oak) and *P. glehnii* (hereafter Spruce), and four canopy gaps with dense *Sasa senanensis* (hereafter *Sasa*) to collect throughfall, litter leachate, and soil water (Fig. 3.1). The diameter at breast height of the trees ranges from 39 to 105 cm, and the area of canopy gap ranges from 113 to 1019 m^2. The age of the canopy gaps is at least 9 years. The forest floor beneath the oak trees is covered by dense *Sasa* although its biomass is usually smaller compared with *Sasa* in the canopy gaps. *Sasa* is sparse beneath the spruce trees. The organic horizon mainly consists of an Oe/Oa horizon with a relatively thin Oi horizon. The A horizon is about 10 cm, AB horizon is about 15 cm, followed by B horizon (Ozawa et al. 2001).

3.2.2 Sample collection

Rainfall was collected at one location in a large canopy gap next to the study watershed, using a polyethylene funnel (diameter: 30 cm) attached to a polyethylene plastic bottle (Fig. 3.2). I assumed that the quality of rainfall would be same within the relatively small spatial scale. Throughfall was collected using a PVC rain gutter (10×180 cm) attached to a polyethylene plastic bottle (Fig. 3.2). The collector was set at the height below understory *Sasa*. Both rainfall and throughfall collector were covered with 1 mm-mesh screen to prevent litterfall and insects going into the plastic bottle. Tension-free lysimeters made of half-cut PVC column (5×20 cm) attached to a polyethylene plastic bottle were installed at the bottom of Oa layer and 10 cm depth of mineral soil to collect litter leachate and soil water, respectively (Fig. 3.2). One throughfall collector, three lysimeters for litter lechate, and three lysimeters for soil water were installed beneath each of the tree canopy and beneath the *Sasa* canopies in each canopy gap. In total, 1 rainfall collector, 12 throughfall collectors, 36 tension-free lysimeters for each of the litter leachate, and another 36 tension-free lysimeters for the

soil water were set in this study.

The throughfall collectors and the tension-free lysimeters were installed between late August and early September 2013 and left for about one month before we started the sample collection in October 2013. The rainfall collector was set in May 2014. I collected water samples in October 2013, June, September, and October 2014. For the sampling of October 2013, water samples were collected every two weeks. From June 2014, the water samples were collected within three days after one to several rain event, depending on the rainfall amount, to reduce the change of water quality in the plastic bottles installed in the field. The sample collection was conducted once in June, September, and October in 2014. The samples were kept on ice, returned to the laboratory, filtered through GF/F filters within 24 hours after collection and stored in the freezer at −15°C until analysis. The sampling bottles were pre-washed by soaking 0.5 M HCl and rinsed with pure water. A selected subset of the water samples (n=106 in total) were transported to Nagoya University to analyze the stable isotopic composition of NO_3^-.

To measure gravimetric moisture contents, the Oe/Oa horizon (O horizon) and top 10 cm of mineral soil were sampled near each of the point of water collection (n= 12 for each vegetation). O horizon was sampled from 10×10 cm area and the thickness was also recorded. The mineral soil was sampled using an auger with a 4.2-cm diameter.

3.2.3 Analysis of dissolved inorganic and organic nitrogen and dissolved organic carbon concentration

The concentrations of NH_4^+, NO_3^-, and total N in the water samples were analyzed by colorimetric method using a continuous flow injection analyzer (AACS-4, BL-Tech Co. Ltd., Osaka, Japan). The DON concentration was calculated by subtracting NH_4^+ and NO_3^- from total dissolved N. The DOC concentration was analyzed by a TOC analyzer (TOC-V CPH, Shimadzu Co Ltd., Kyoto).

3.2.4 Soil water content

The gravimetric water content of the O horizon was measured by drying the sample at 70°C for 48 hours after roots were removed. The gravimetric soil water content was measured by drying the sieved sample (4 mm-mesh) at 105°C for 24 hours.

3.2.5 Characterization of DOM quality using spectrofluorometric indices

Optical indices used to characterize DOM quality are given in Table 3.1. After the frozen water sample was thawed and reached room temperature, the absorbance of the sample was measured from λ = 200 nm to 800 nm at 0.5 nm intervals using a 1 cm quartz-windowed cell with a spectrophotometer (UV-1800, Shimadzu). Absorbance spectra of a blank (Milli-Q) and samples were obtained against air, and a blank spectrum was subtracted from each sample spectrum. Samples with high absorbance value were diluted and re-analyzed until the absorbance at 254 nm lowered 0.3 cm^{-1} to correct the fluorescence inner-filtering effects (Ohno 2002). The specific UV absorbance ($SUVA_{254}$), an indicator of the DOM aromaticity, was determined by dividing the UV absorbance measured at 254 nm by the DOC concentration (Weishaar et al. 2003) (Table 3.1). The spectral slope ratio (S_R), which is inversely related to the molecular weight of DOM, was calculated as the ratio of the spectoral slope of the shorter UV wavelength region (275–295 nm) to that of the longer UV wavelength region (350–400 nm) (Helms et al. 2008) (Table 3.1). Each spectral slope was obtained using linear regression on the log-transformed spectral ranges (Helms et al. 2008).

Excitation-emission matrix (EEM) fluorescence was measured using a fluorometer (Fluoromax-4, Horiba) with a quartz cell. The inner filter effect was corrected using the absorbance spectrum, according to McKnight et al. (2001). Then, a blank spectrum (Milli-Q) was subtracted from each sample spectrum. Fluorescence intensities were corrected for the area under the water Raman peak (excitation = 350 nm), analyzed daily, and were converted to Raman units (Lawaetz and Stedmon 2009). The fluorescence index (FI) was calculated as the ratio of fluorescence emission intensities at 470 and 520 nm at an excitation wavelength of 370 nm (Cory and McKnight 2005). FI can serve as an index of the relative contribution of microbial versus higher plant organic matter (McKnight et al. 2001) (Table 3.1). The humification index (HIX), an indicator of the extent of humification of DOM, was calculated by dividing the sum of the fluorescence intensity in the longer emission wavelength region (434–480 nm) by the sum of those in the shorter emission wavelength region (300–346 nm) at excitation wavelength of 255 nm (Zsolnay et al. 1999; Ohno 2002) (Table 3.1).

Parallel factor analysis (PARAFAC) was performed in MATLAB (Mathworks, Natick, MA) with the DOMFluor toolbox (version 1.7) (Stedmon and Bro 2008). PARAFAC statistically decomposes the complex mixture of DOM fluorophores into components (Stedmon and Bro 2008). The data set for PARAFAC modelling was composed of 257 water samples (rain, throughfall, litter leachate, and soil water). The

EEMs of the excitation wavelengths from 250 nm to 400 nm and emission wavelengths from 290 nm to 540 nm were used for PARAFAC modeling, and the four-component model was validated by split half validation and random initialization (Stedmon and Bro 2008) (Fig 3.6). The spectral characteristics of the four fluorescent components (C1, C2, C3, and C4) were assigned based on those of DOM in previous studies (Table 3.2), using the open fluorescence data base, OpenFluor (Murphy et al. 2014). The relative abundance of each of the four fluorescent components was calculated by dividing the fluorescence intensity of individual components by the sum of those of all components, then multiplied by 100 (i.e., %Ci = Ci / (C1 + C2 + C3 + C4) × 100). In this study, the relative abundance of each of the four components was expressed as %C1, %C2, %C3, and %C4.

3.2.6 The stable isotopic compositions of NO_3^-

The stable isotopic compositions of NO_3^- were determined using the method that chemically convert NO_3^- into N_2O, according to Tsunogai et al. (2016). Approximately 10mL of each sample solution was pipetted into a vial with a septum cap. Then, 0.5 g of spongy cadmium was added, followed by 150 μL of a 1M $NaHCO_3$ solution. The sample was then shaken for 18–24 h at a rate of 2 cycles s^{-1}. Then, the sample solution was decanted into a different vial with a septum cap. After purging the solution using high purity helium, 0.4mL of the azide/acetic acid buffer was added. After 45 min, the solution was made basic by adding 0.2mL of 6M NaOH.

Then, the stable isotopic compositions ($\delta^{15}N$, $\delta^{18}O$, and $\delta^{17}O$) of N_2O in each vial were determined by using a continuous-flow isotope ratio mass spectrometry (CF-IRMS) system at Nagoya University. The isotopic ratio of N and O of NO_3^- in the sample are expressed as,

$$\delta^{15}\mathrm{N}\ (\text{or } \delta^{18}\mathrm{O} \text{ or } \delta^{17}\mathrm{O})\ (‰) = \left(\frac{R_{\mathrm{SAMPLE}}}{R_{\mathrm{standard}}} - 1\right) \times 1000$$

where R is the $^{15}N/^{14}N$ (or $^{18}O/^{16}O$ or $^{17}O/^{16}O$) ratio of a sample or standard material. Then, $\Delta^{17}O$ value of NO_3^- in the sample was calculated by the following equation:

$$\Delta^{17}\mathrm{O} = \frac{1 + \delta^{17}\mathrm{O}}{(1 + \delta^{18}\mathrm{O})^{\beta}} - 1$$

where the constant β is 0.5279 (Miller 2002; Kaiser et al. 2007).

The obtained values of $\delta^{15}N$, $\delta^{18}O$, and $\Delta^{17}O$ for N_2O derived from the NO_3^- in each sample were compared with those derived from the local laboratory NO_3^- standards that had been calibrated using the internationally distributed isotope reference

materials to calibrate the values of the sample NO_3^- to an international scale and to correct for both the isotope fractionation during the chemical conversion to N_2O and the progress of oxygen isotope exchange between the NO_3^--derived reaction intermediate and water (ca. 20 %). In this study, the internal standard method (Nakagawa et al., 2013; Tsunogai et al., 2014) was adopted for the calibrations of sample NO_3^-. All values in this study are expressed relative to air (for nitrogen) and VSMOW (for oxygen).

To determine whether samples were deteriorated or contaminated during storage and whether the conversion rate from NO_3^- to N_2O was sufficient, concentrations of NO_3^- in the samples were determined each time we analyzed isotopic compositions using CF-IRMS based on the N_2O^+ or O_2^+ outputs. The $d^{15}N$, $d^{18}O$, or $\Delta^{17}O$ values were adopted only when concentrations measured by CF-IRMS correlated with those measured by ion chromatography just after the sampling within a difference of 10 %. About 10% of the whole isotope analyses showed conversion efficiencies lower than his criterion. NO_3^- in these samples was converted to N_2O again and re-analyzed for the stable isotopic compositions. None of the samples showed significant NO_3^- deterioration or NO_3^- contamination during storage.

The analyses of the $d^{15}N$, $d^{18}O$, and $\Delta^{17}O$ values of NO_3^- for each sample were repeated at least three times to attain high precision. All isotopic data presented in this study have an error (standard error of the mean) within ±0.2‰ for $d^{15}N$, ±0.3‰ for $d^{18}O$, and ±0.1‰ for $\Delta^{17}O$.

The proportion of unprocessed atmospheric NO_3^- was estimated by the following equation:

$$\frac{NO_{3\,atm}^-}{NO_{3\,total}^-}(\%) = \frac{\Delta^{17}O_{sample}}{\Delta^{17}O_{atm}} \times 100$$

where $NO_3^-{}_{atm}$ is atmospheric NO_3^-, $NO_3^-{}_{total}$ is total NO_3^-, $\Delta^{17}O_{sample}$ is $\Delta^{17}O$ value of sample, and $\Delta^{17}O_{atm}$ is $\Delta^{17}O$ value of rain sample. Only for the samples collected in October 2013, when rainfall collection had not been started, the average $\Delta^{17}O$ value of throughfall collected in the canopy gaps were used as $\Delta^{17}O_{atm}$, assuming that the value would not differ significantly from that of rainfall.

3.2.7 Statistical analysis

Before statistical analysis, concentrations and optical indices of DOM quality were averaged over the four sampling period. Fluxes of each nitrogen form and DOC per rain day were calculated as follows:

$$\text{Flux} = \frac{\Sigma(\text{concentration} \times \text{water volume in each sampling})}{\text{total number of rain days}}$$

Differences in the variables among vegetation type was analyzed using nested one-way ANOVA with the replication under individual tree or *Sasa* sampling plot being treated as an error. Tukey's honestly significant difference test was used as a post-hoc test. Vertical change in the variables was analyzed using pair-wise t-test.

The influence of DOM properties in the litter leachate on the NO_3^- concentration and the proportion of NO_3^- to DIN(NO_3^-/DIN) in the soil water was analyzed using step-wise multiple regression analysis combined with principal component analysis (PCA). Because DOM properties were highly correlated each other, PCA was performed to obtain the principal component scores. The first to third principal component scores were used as explanatory variables in the regression analysis. Spearman's rank correlation was used to examine correlation between variables. Where necessary, variables were log (X+1) transformed to obtain normal distribution before statistical analysis.

3.3. Results

3.3.1 Properties of O horizon and mineral soil

The thickness of O horizon beneath spruce was significantly higher than beneath oak and *Sasa* (Table 3.3). The gravimetric water content of O horizon was lowest beneath spruce, and that of mineral soil was lower beneath spruce than beneath oak (Table 3.3).

3.3.2 Concentrations and fluxes of DON, DOC, and DIN

Water flux was significantly lower under spruce canopy than under oak and *Sasa* (Fig. 3.3). The major N form in the throughfall was DON; the proportions of DON to the total dissolved N (DON/TN) were 85%, 94%, and 62% for oak, spruce, and *Sasa*, respectively (Appendix table 1). The DON concentration of throughfall was significantly higher under the canopy of oak and spruce than under *Sasa* canopy (Fig. 3.4). The DOC concentration of throughfall was highest under spruce canopy and lowest under *Sasa* canopy (Fig. 3.4). The DOC/DON ratio of throughfall was significantly higher under spruce canopy than under oak and *Sasa* canopy (Fig. 3.4). The DOC flux of throughfall under spruce canopy was significantly higher than under

Sasa (Fig. 3.4). The concentrations of NH_4^+, NO_3^- of throughfall did not significantly differ among plant species, while NO_3^- flux was significantly higher under *Sasa* canopy than under oak and spruce (Fig. 3.5).

From throughfall to litter leachate, the concentrations of DON and DOC increased (Fig. 3.4) and the DON/TN decreased (Appendix table 1), while the fluxes of DON and DOC did not increase except beneath *Sasa* (Fig. 3.4). The DOC/DON ratio decreased beneath spruce while it increased beneath oak (Fig. 3.4). In litter leachate, the DON and DOC concentrations were highest beneath spruce, and DOC/DON ratio was highest beneath spruce and lowest beneath *Sasa* (Fig. 3.4). Both the concentrations and the fluxes of NH_4^+ and NO_3^- also significantly increased from throughfall to litter leachate (Fig. 3.5). The concentrations of NH_4^+, NO_3^-, and DIN of litter leachate did not significantly differ among plant species, but the NO_3^-/DIN was significantly higher beneath *Sasa* than beneath spruce (Fig. 3.5; Appendix table 1). In the litter leachate, the NO_3^- flux was highest beneath *Sasa* and the DIN flux was significantly higher beneath *Sasa* than beneath spruce (Fig. 3.5; Appendix table 2).

From litter leachate to soil water, the concentrations of DON and DOC significantly decreased, and only beneath *Sasa*, the fluxes of DON and DOC significantly decreased (Fig. 3.4). In the soil water, the DON and DOC concentrations were highest beneath spruce, and the DOC/DON ratio was highest beneath spruce and lowest beneath *Sasa* (Fig. 3.4). DOC flux of soil water was significantly higher beneath spruce than beneath *Sasa* (Fig. 3.4). The NH_4^+ concentration beneath oak and *Sasa* significantly decreased, and the NH_4^+ fluxes significantly decreased beneath oak from litter leachate to soil water (Fig. 3.5). In the soil water, the NO_3^- concentration of soil water was marginally higher, and the NO_3^-/DIN and the NO_3^- flux were significantly higher beneath *Sasa* than beneath spruce (Fig. 3.5).

3.3.3 Fluorescent components

Four fluorescent components were validated by the PARAFAC modelling (Fig. 3.6), and the characteristics of the four components are described in Table 3.2. Spectral characteristics of the components identified from rain, throughfall, litter leachate, and soil water in the present study were similar to those of DOM that previous studies identified in aquatic environments. Component 1 (C1) (excitation maximum at <250 and 340 nm with emission maximum at 480 nm) corresponds to a terrestrial humic-like DOM (Table 3.2). Component 2 (C2) (excitation maximum at 250 nm with emission maximum at 402 nm) was assigned as ubiquitous humic-like DOM in the present study

as the characterization of the components in the previous studies includes both terrestrial humic-like and microbial humic-like DOM (Table 3.2). Component 3 (C3) (excitation maximum at 275 nm with emission maximum at 304 nm) is characterized as protein-like component, specifically, tyrosine-like component (Table 3.2). Component 4 (C4) (excitation maximum at 255 and 345 nm with emission maximum at 408 nm) is similar to a reported microbially derived fulvic acid (Table 3.2). The proportion of C1 (%C1) was significantly positively correlated to $SUVA_{254}$ ($r = 0.88$, $P < 0.001$, Fig. 3.7A). The proportion of C4 (%C4) was significantly positively correlated to FI ($r = 0.77$, $P < 0.001$, Fig. 3.7B)

3.3.4 DOM quality metrics

Throughfall under spruce canopy showed significantly higher fluorescence intensity of C1, C2, C3, and C4 than throughfall under *Sasa* canopy (Fig. 3.8). The relative abundance of C1 (%C1) in the *Sasa* throughfall was lowest among the three vegetation types (Fig. 3.8). HIX of oak throughfall was significantly higher than *Sasa* throughfall (Fig. 3.9). $SUVA_{254}$ was highest in oak throughfall and lowest in *Sasa* throughfall (Fig. 3.9).

After percolating through the forest floor, the fluorescence intensity of C1, C2, and C4 significantly increased beneath all vegetation types, while C3 significantly decreased beneath spruce and oak (Fig. 3.8). HIX and $SUVA_{254}$ significantly increased and S_R significantly decreased (Fig. 3.9). In litter leachate, C3 was of minor component in the total fluorescent DOM, accounting for less than 10 % on average, and the majority of DOM was constituted of C1, C2, and C4 (Fig. 3.8). However, there was a significant difference in %C3 among the vegetation types with *Sasa* litter leachate showing higher value than oak and spruce (Fig. 3.8). *Sasa* litter leachate also showed significantly lower %C1 and HIX values than oak and spruce (Figs. 3.8 and 3.9).

From litter leachate to soil water, C1, C2, and C4 significantly decreased beneath all vegetation types, while C3 significantly decreased only beneath *Sasa* (Fig. 3.8). %C4 significantly increased beneath spruce and *Sasa* (Fig. 3.8), and FI value also significantly increased beneath all vegetation types (Fig. 3.9). In soil water, %C4 and FI was significantly higher beneath *Sasa* than spruce, while %C1 was lowest beneath *Sasa* (Figs. 3.8 and 3.9).

3.3.5 Isotopic composition of NO_3^-

The average $\Delta^{17}O$ value and $\delta^{18}O$ of rain was 24.7±1.1‰ and $\delta^{18}O$ was 76.5± 3.5‰, respectively. The proportion of atmospheric NO_3^- ($NO_3^-{}_{atm}$) to the total NO_3^- in throughfall was significantly higher under *Sasa* (97.3±1.3%) than under oak (78.8±12.1%) and spruce (81.9±7.6%) (Table 3.4). The proportion of $NO_3^-{}_{atm}$ decreased to 14.4±16.1% on average in litter leachate, and 7.0±6.1% on average in soil water (Table 3.4). The proportion of $NO_3^-{}_{atm}$ in the litter leachate and soil water was not statistically different among the vegetation types.

3.3.6 Principal component analysis, multiple regression analysis

The first, second, and third principal component scores (PC1, PC2, and PC3) explained 96%, 78%, and 84% of the variation of DOM properties in throughfall, litter leachate, and soil water, respectively (Table 3.5).

The thickness of O horizon and the first principal component score of DOM quality metrics in litter leachate were significantly positively correlated (Fig. 3.10A). The PC1 of DOM quality metrics in the litter leachate explained 44% of the variability (Table 3.5). The PC1 was positively related to %C1 and HIX, and was negatively related to %C3 (Fig. 3.10B)

The regression models to explain the variation of NO_3^-/DIN of soil water were obtained by the stepwise multiple regression analysis (Table 3.6). The PC3 and PC1 of DOM quality metrics in the litter leachate explained the variation of NO_3^-/DIN of soil water, and the PC3 and PC1 had positive and negative influence on the NO_3^-/DIN of soil water, respectively (Table 3.6). The property-property plot between the first and third principal factor loadings of PCA shows that DOM in litter leachate with positive PC3 value and negative PC1 value is characterized as high value of tyrosine-like DOM (%C3) and microbially derived DOM (%C4) and low degree of humification (HIX) and DOC/DON ratio (Fig. 3.10B). Therefore, the regression model indicates that DOM in litter leachate with high proportion of tyrosine-like DOM (%C3) and microbially derived DOM (%C4) and low degree of humification (HIX) and DOC/DON ratio is related to high NO_3^-/DIN of soil water.

3.4. Discussion

3.4.1 Contribution of atmospheric NO_3^- to the leaching NO_3^-

The proportion of $NO_3^-_{atm}$ to the total NO_3^- in the litter leachate was about 14 %, indicating that the contribution of atmospheric NO_3^- to the total NO_3^- is small, and the NO_3^- production in the forest floor is the major source of leaching NO_3^- from the forest floor (Table 3.4). The proportion of $NO_3^-_{atm}$ to the total NO_3^- further decreased to about 7 % in the soil water, suggesting further mixing of $NO_3^-_{atm}$ with NO_3^- produced in the soil and/or consumption of $NO_3^-_{atm}$ by soil microbes (Table 3.4). The proportions of $NO_3^-_{atm}$ in the litter leachate and soil water were similar to the reported values of other study. Costa et al. (2011) measured the proportion of $NO_3^-_{atm}$ to the total NO_3^- in the extracts of forest floor and soil (0–30 cm) using $\Delta^{17}O$ in a temperate forest in northern Lower Michigan, and found that forest floor NO_3^- and soil NO_3^- contained about 15% and 9% of $NO_3^-_{atm}$, respectively. Our results suggest that not the direct deposition of atmospheric NO_3^- to the soil, but the N mineralization and nitrification in forest floor and soil are the major factors that influence the variation of NO_3^- concentration and flux in this forest ecosystems with relatively low atmospheric deposition.

3.4.2 PARAFAC components

Among the four DOM components identified by PARAFAC, the spectral characteristics of C1 was similar to those of terrestrial humic-like DOM identified in previous studies (Table 3.2). The significant positive correlation between %C1 and $SUVA_{254}$ (Fig. 3.7A) indicates C1 is rich in aromatic carbon (Weishaar et al. 2003). The high content of aromatic carbon reflects the contribution of lignin degradation to their formation (McKnight et al. 2001). Hence, C1 identified in this study can be considered as plant-derived humic-like DOM produced during the decomposition of organic matter. The spectral characteristics of C4 was similar to that of microbially derived fulvic acid identified by Cory and McKnight (2005) (Table 3.2). The significant positive correlation between %C4 and FI, which indicates DOM is microbial origin when the value is high, supports the assignment of C4 as microbially derived DOM (Fig. 3.7B). Although C1, C2, and C4 are characterized as humic-like DOM, the emission peaks of C1 appeared at longer wavelength compared with that of C2 and C4 (Table 3.2 and Fig. 3.6), suggesting a high degree of aromatic substitution and polycondensation and higher levels of conjugated chromophores (Yamashita et al. 2011).

3.4.3 Differences in the dynamics of DOM and DIN among vegetation types

DON and DOC concentrations and DOC flux of throughfall under *Sasa* were lower than those under the canopies of oak and spruce (Fig. 3.4). DOM in throughfall originates from both external inputs (i.e., atmospheric deposition) and internally originating compounds (e.g. leaching from leaf tissues and compounds produced by the microbial activities in the canopy), which are difficult to separate each other. Besides, various factors such as water flux, temperature, microbial activity in the canopy, and canopy structures interactively affect DON and DOC concentrations and fluxes in throughfall (Le Mellec et al. 2010), making it difficult to understand the effects of plant species on the concentrations and fluxes of DOM. Among these factors, coniferous canopies are known to be more effective in capturing atmospheric deposition than broadleaved canopies because the leaf area index is larger in coniferous canopies and the shape of coniferous needle leaves are more efficient to accumulate atmospheric compounds (Rothe et al. 2002a; De Schrijver et al. 2007). In fact, Le Mellec et al. (2010) observed higher DOC and DON concentrations in throughfall in spruce stands than in beech stands in Germany. Canopy species such as oak and spruce may be more effective in capturing airborne compounds and accumulate them on their leaves during dry period than understory *Sasa* in the canopy gaps because of the differences in height, and this could result in the differences in DON and DOC concentrations and fluxes observed in this study, but further investigations are necessary.

DOM quality of *Sasa* throughfall was also different from the canopy trees. The values of indices for recalcitrant DOM (%C1, HIX, $SUVA_{254}$) was lower under *Sasa* than oak and spruce (Figs. 3.8 and 3.9). DOC/DON ratio was also lower under *Sasa* than under spruce (Fig. 3.4). This indicates that forest canopy plays an important role in characterizing DOM quality that reaches to the forest floor as DOM in throughfall has been suggested to act as substrate for microbial activity and to promote decomposition process of organic matter in the forest floor (Michalzik et al. 2001).

Increases in the concentrations and fluxes of NH_4^+ and NO_3^- from throughfall to litter leachate indicate that net microbial N mineralization and nitrification are significant in the forest floor and that forest floor act as a source of DIN to mineral soils (Fig. 3.5). The significant decrease in the proportion of $NO_3^-{}_{atm}$ from throughfall to the litter leachate supports the idea (Table 3.4). In contrast, it was only beneath *Sasa* that showed significant increases in both concentrations and fluxes of DOC and DON (Fig. 3.4). This indicates that tree canopy is an important source of DOC and DON beneath

oak and spruce, while forest floor is the major source of DOC and DON in litter leachate beneath *Sasa* grown in the canopy gap. As DOC and DON concentrations increased from throughfall to litter leachate (Fig. 3.4), C1, C2, C4, HIX, and $SUVA_{254}$ also increased in all vegetation types (Figs. 3.8 and 3.9), suggesting that the increases in DOC and DON concentrations is mainly caused by the production of plant-derived humic-like DOM and microbially-derived DOM during the decomposition of organic matter in the forest floor. In contrast, fluorescence intensity of C3 (tyrosine-like DOM) decreased before leaching from the forest floor, but only beneath oak and spruce (Fig. 3.8). Tyrosine-like component has been classified as highly labile DOM in stream water (Cory and Kaplan 2012). Therefore, the result indicates that a large portion of the biodegradable component (i.e., C3) of throughfall DOM was consumed by microorganisms and possibly by plant uptake. In the *Sasa* forest floor, consumption of C3 supplied from throughfall and production of C3 from decomposing litter may have been balanced.

The chromophoric DOM in litter leachate was mainly constituted of humic-like C1, C2, and C4 (Fig. 3.8). Qualls et al. (1991) also found that DOM leaching from forest floor was mainly humic substances in a deciduous forest in North Carolina, USA. However, we found that the DOM quality of litter leachate was different among oak, spruce, and *Sasa* (Figs. 3.8 and 3.9). The litter leachate of *Sasa* contained more C3 and less plant-derived humic-like components indicated by %C1 and HIX, and showed lower DOC/DON ratio than those beneath oak and spruce. These difference in DOM quality of litter leachate was explained by the difference in the degree of organic matter decomposition (Fig. 3.10). The positive correlation between the thickness of O horizon and the PC1 score indicates that DOM leaching from thick O horizon is characterized with high proportion of plant-derived humic-like DOM (C1) and high degree of humification (HIX), while DOM leaching from thin O horizon is characterized with high proportion of tyrosine-like DOM (C3). Previous study has suggested that the major source of DOM leaching from forest floor is decomposed organic material stored in Oe/Oa horizons (Kalbitz et al. 2007), supporting the significant relationship between the thickness of O horizon and DOM quality observed in this study. Despite the similar thickness of the O horizon between oak and *Sasa*, the DOM of oak litter leachate showed more recalcitrant characteristics than *Sasa* (Fig. 3.10). The DOM of throughfall under oak showed higher values of HIX, %C1, and $SUVA_{254}$ than under *Sasa* (Figs. 3.8 and 3.9), indicating that the throughfall DOM under oak is more recalcitrant. As recalcitrant DOM is less likely utilized by microorganisms in the forest floor, most of this DOM fraction would be directly leached to the mineral soil. This would make the

DOM of oak litter leachate more recalcitrant characteristics than that of *Sasa* litter leachate. These results suggest that both throughfall DOM properties and forest floor properties (i.e., degree of litter decomposition) are important factors that determine the properties of DOM leaching into the mineral soil.

The concentrations of DOC and DON and the fluorescence intensity of humic-like C1, C2, and C4 decreased after percolating through the soil, probably due to the adsorption to the mineral soil (Figs. 3.4 and 3.8). Adsorption to soil, rather than biodegradation, is considered to be the reason for the decrease in the concentration of leaching DOC in the mineral soil (Qualls et al. 1992).

3.4.4 Influence of DOM properties on NO_3^- leaching from the surface mineral soil

In the litter leachate, the NO_3^- flux beneath *Sasa* was significantly higher than beneath other trees (Fig. 3.5). The proportion of NO_3^- to DIN, which can be considered as degree of nitrification, was also higher beneath *Sasa* than spruce (Fig. 3.5). These results indicate that net NO_3^- production in the forest floor beneath *Sasa* is relatively high compared to adjacent spruce and oak tree.

In the soil water, the mean NO_3^- concentration beneath *Sasa* was higher than oak and spruce although statistically not significant, and the NO_3^- flux beneath *Sasa* was significantly higher than beneath other trees (Fig. 3.5). NO_3^-/DIN was also higher beneath *Sasa* than beneath oak and spruce (Fig. 3.5). The decrease in the fluorescence intensity of C3 beneath *Sasa* from the litter leachate to the soil water could suggest that the highly biodegradable fraction was consumed (Fig. 3.8). The result of the regression analysis showed that the variation of NO_3^-/DIN in the soil water was explained by the properties of DOM that is supplied from canopy and forest floor to the soil (Table 3.6). Specifically, litter leachate DOM with higher proportion of C3 and C4, and lower values in HIX and DOC/DON was related to higher NO_3^-/DIN in the soil water (Table 3.6 and Fig. 3.10B). The characteristics of such DOM can be regarded as relatively biodegradable and N-rich DOM. Therefore, these results suggest that supply of biodegradable and N-rich DOM from forest floor promotes N mineralization and nitrification in the soil, which leads to high proportion of NO_3^- in the soil water. DON concentration in litter leachate was not significantly related to either NO_3^- concentration or NO_3^-/DIN in soil water (Data not shown). The results of this chapter suggest that bulk concentration of DON supplied to soil is not a good indicator of the variation in nitrification in soil, and that the biodegradability and C/N balance of DOM are important factors that link plants and inorganic N production in soils.

3.5 Conclusion

This study examined the dynamics of DOM and dissolved N from throughfall to the leaching water in the surface mineral soil beneath oak, spruce, and *Sasa* grown in canopy gaps, to understand the influence of DOM properties on soil N dynamics in natural mixed forest. Stable natural isotopic composition of NO_3^- revealed that majority of NO_3^- in litter leachate and soil water originates from microbially produced NO_3^-. The protein-like DOM in throughfall was rapidly consumed in the forest floor and DOM in the litter leachate was mainly constituted of recalcitrant DOM. However, there was significant difference in DOM quality between vegetation types; litter leachate beneath *Sasa* in the canopy gaps showed higher proportion of labile DOM, lower proportion of humic-like DOM, and lower DOC/DON ratio compared with that beneath spruce. DOM in the litter leachate beneath oak showed intermediate characteristics in terms of biodegradability. The NO_3^- flux and the proportion of NO_3^- to DIN in the soil water beneath *Sasa* was higher than those beneath spruce, and these differences were related to the quality of DOM in the litter leachate. DOM with high proportion of tyrosine-like and microbially-derived DOM, and low degree of humification and low DOC/DON ratio was related to high NO_3^-/DIN in the soil water.

Overall, this study found that *Sasa* in the canopy gaps supplies relatively labile and N-rich DOM to the mineral soil and the NO_3^- leaching is relatively high, while spruce supplies more recalcitrant and N-poor DOM to the mineral soil and the NO_3^- leaching is relatively low. These results suggest that differences in DOM quality among vegetation strongly influence nitrification in the soil and NO_3^- leaching.

Table 3.1 Definition and significance of the suite of DOM optical indices used in this study

DOM quality index	Definition and significance
UV absorbance	
Specific UV absorbance ($SUVA_{254}$)	UV absorbance at 254 nm divided by DOC concentration; A measure of aromaticity of DOM; high values indicate more aromatic material. (Weishaar et al.2003)
Slope ratio (S_R)	Ratio of the slope of the shorter UV wavelength region (275–295 nm) to that of the longer UV wavelength region (350–400 nm); A proxy for molecular weight (MW); S_R decreases with increasing MW (Helms et al. 2008)
Fluorescence	
Humification index (HIX)	The sum of the fluorescence intensity in the longer emission wavelength region (434–480 nm) divided by the sum of those in the shorter emission wavelength region (300–346 nm) at excitation wavelength of 255 nm; Humification status of DOM; ranges from 0 to 1 and increases with increasing degree of humification (Zsolnay et al. 1999; Ohno 2002)
Fluorescence index (FI)	Ratio of fluorescence intensities at 470 and 520 nm at excitation of 370 nm; Used to distinguish sources of DOM; FI = 1.3–1.4: higher terrestrial plant origin; FI = 1.7–1.9: microbial origin (McKnight et al. 2001)

Table 3.2 Characteristics of the four PARAFAC components compared with previously identified

Component (present study)	Excitation maximum	Emission maximum	Reference	Component	Description and possible sources assigned in the reference
C1	<250 (340)	480	Shutova et al. (2014)	C1	Terrestrial humic-like
			Tanaka et al. (2014)	C1	Terrestrial humic-like
			Yamashita et al. (2010)	C1	Ubiquitous humic-like
C2	250	402	Sondergaard et al. (2003)	C2	Humic M peak; C2 in Stedmon et al. 2003; High values found in algal DOM
			Osburn et al. (2012)	C2	Novel to this study; possible (photo)degradation product
			Lapierre et al. (2014)	C1	Terrestrial humic-like
			Murphy et al. (2011)	C2	Microbial humic-like
C3	275	304	Murphy et al. (2011)	C7	Tyrosine-like
			Yamashita et al. (2011)	C4	Tyrosine-like
C4	(255) 345	408	Cory & McKnight(2005)	SQ3	Microbially derived fulvic acid

Note: Secondary excitation maxima are shown in brackets

Table 3.3 Thickness of O horizon and soil water content of O horizon and mineral soil

	Thickness (cm)			Soil water content (%)					
Vegetation	O horizon	sd	n	O horizon	sd	n	Mineral soil	sd	n
Oak	3.6 b	1.4	12	72.1 b	4.0	12	40.3 a	3.7	12
Spruce	9.0 a	2.6	12	63.3 a	6.4	12	35.1 b	6.5	12
Sasa	2.5 b	1.4	12	75.8 b	2.8	12	39.2 ab	4.1	12

Note: Different letters indicate significant differences ($P < 0.05$) among vegetation types. sd: standard deviation

Table 3.4 The relative proportion of atmospheric NO_3^- in total NO_3^- ($NO_3^-_{atm}$) in throughfall, litter leachate, and soil water

Sample	Vegetation	$NO_3^-_{atm}$ (%)	sd	n
Throughfall	Oak	78.8 b	12.1	4
	Spruce	81.9 ab	7.6	3
	Sasa	97.3 a	1.3	4
	Average	86.4	11.5	11
Litter leachate	Oak	16.3	17.8	7
	Spruce	11.8	19.6	8
	Sasa	15.2	13.4	11
	Average	14.4	16.1	26
Soil water	Oak	6.9	7.9	8
	Spruce	7.5	6.4	3
	Sasa	7.0	4.7	8
	Average	7.0	6.1	19

Note: Different letters indicate significant differences ($P < 0.05$) among vegetation types. sd: standard deviation

Table 3.5 The first, second, and third principal component factor loadings of PCA using DOM quality metrics in throughfall, litter leachate, and soil water

	Throughfall			Litter leachate			Soil water		
DOM quality	PC1	PC2	PC3	PC1	PC2	PC3	PC1	PC2	PC3
DOC/DON	0.03	-0.50	0.23	0.33	0.10	-0.49	0.28	0.06	0.35
S_R	0.36	-0.29	-0.34	0.30	0.05	-0.04	0.08	-0.33	0.56
FI	0.23	0.42	-0.40	-0.22	-0.59	-0.07	-0.44	0.26	0.29
HIX	-0.48	-0.05	-0.13	0.44	-0.29	-0.10	0.27	0.52	0.14
%C1	-0.45	-0.19	-0.02	0.49	-0.04	0.02	0.49	0.24	0.10
%C2	-0.11	0.37	0.66	-0.27	-0.37	-0.51	-0.26	0.27	-0.50
%C3	0.45	-0.18	0.07	-0.36	0.48	0.06	-0.13	-0.59	0.00
%C4	-0.06	0.51	-0.25	-0.09	-0.43	0.57	-0.37	0.26	0.40
$SUVA_{254}$	-0.41	-0.17	-0.40	0.32	0.02	0.40	0.43	-0.09	-0.20
Proportion of Variance	0.47	0.39	0.10	0.44	0.19	0.15	0.37	0.29	0.18
Cumulative proportion	0.47	0.86	0.96	0.44	0.63	0.78	0.37	0.66	0.84

Note: S_R: spectoral slope ratio; FI: fluorescence index; HIX: humification index; $SUVA_{254}$: specific UV absorbance at 254 nm; %C1~%C4: the relative abundance of component C1~C4

Table 3.6 Summary of stepwise multiple regression analysis for NO_3^-/DIN ratio in soil water

Response variable	Independent variable	Coefficients	*P* value	Model R^2
NO_3^-/DIN(SW)	Intercept	1.03E-16	1.000	0.42
	PC3(LL)	0.65	0.021	
	PC1(LL)	−0.33	0.192	

Note: Coefficients: standardized partial regression coefficients; Model R^2: degree of freedom adjusted coefficient of determination; SW: soil water; LL: litter leachate; PC: principal component score

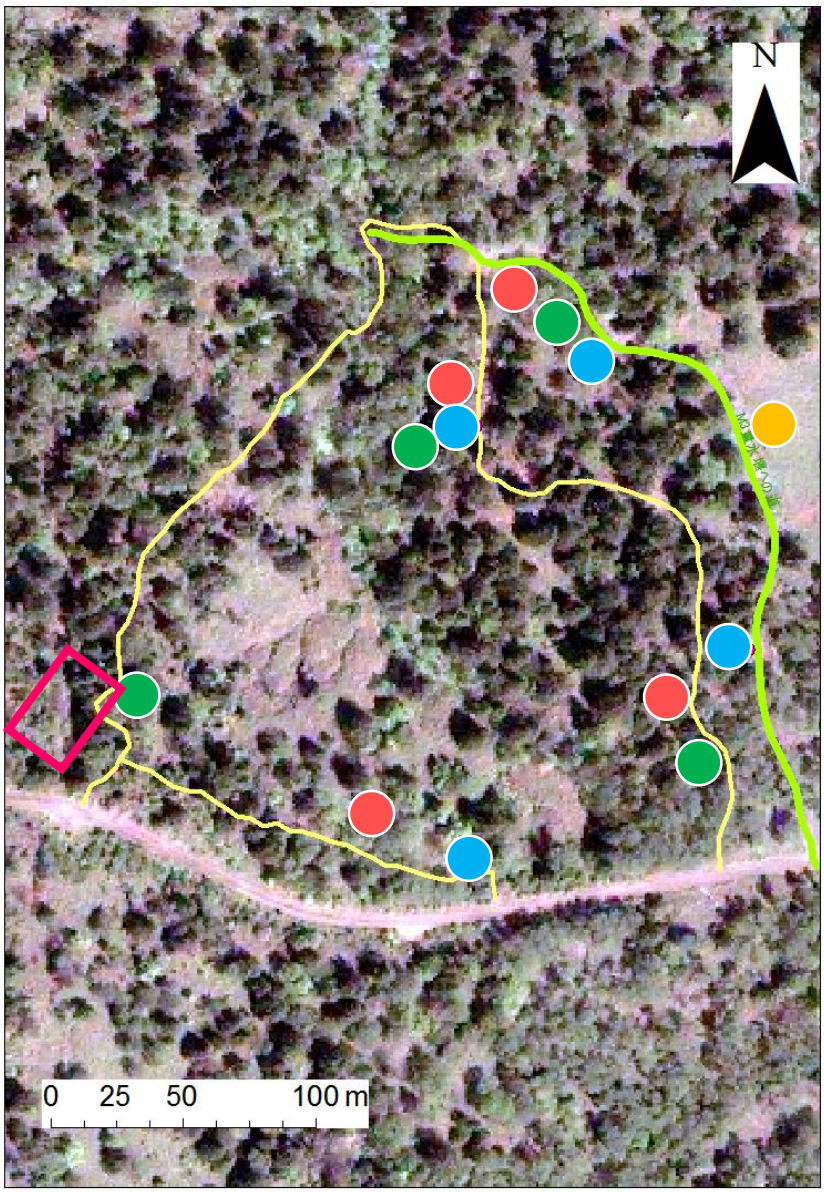

（© JAPAN SPACE IMAGING CORPORATION）

Fig.3.1 The location of oak and spruce trees and canopy gaps for water sampling, and that of rain collector; red circle: oak, green circle: spruce, blue circle: *Sasa* (canopy gap), yellow circle: rain collector. The red rectanble is the study site in chapter 2

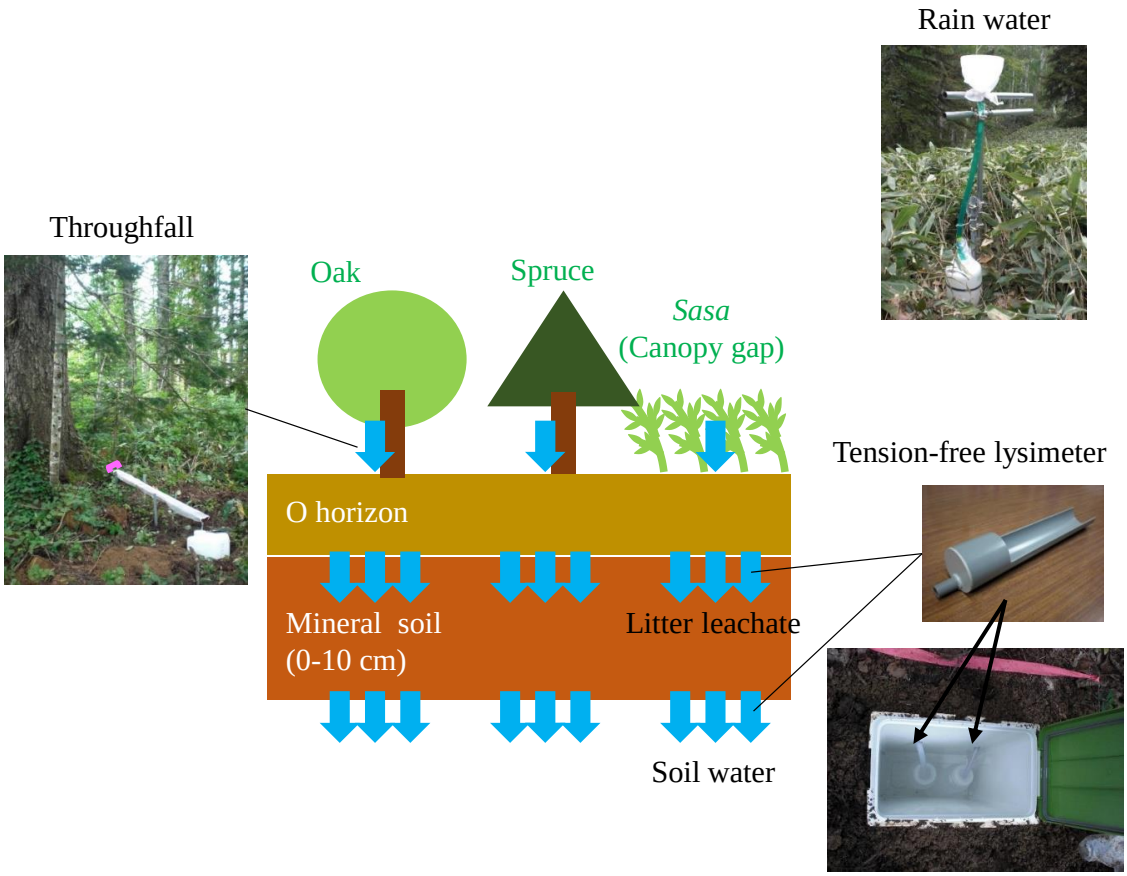

Fig. 3.2 Diagram of water collection. One throughfall collector and three tension-free lysimeters were installed at each vegetation replicate. One rainfall collector was installed in a large canopy gap locating next to the studied stand

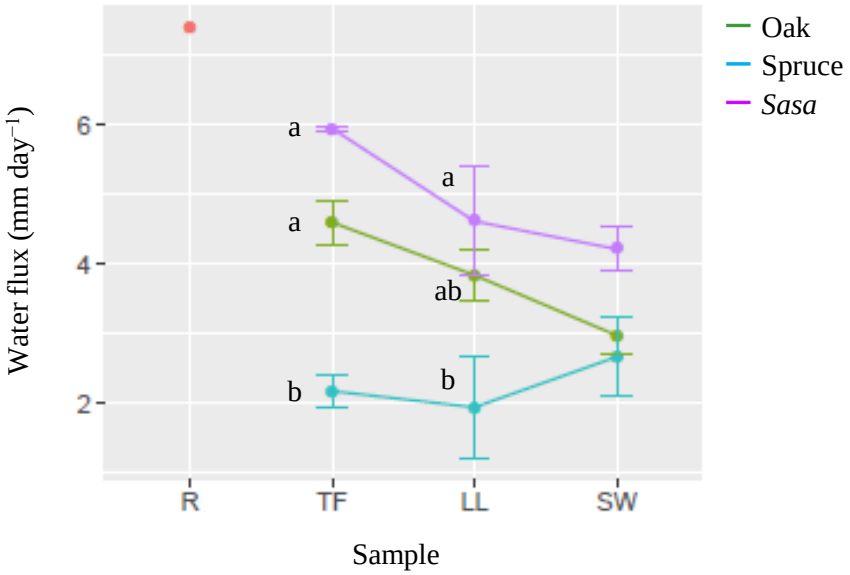

Fig. 3.3 The vertical trend of the water flux from rain to soil water at different vegetation type.

R: Rain; TF: Throughfall; LL: Litter leachate; SW: Soil water; Different letters indicate significant differences ($P < 0.05$) among vegetation types; Error bars indicate standard error

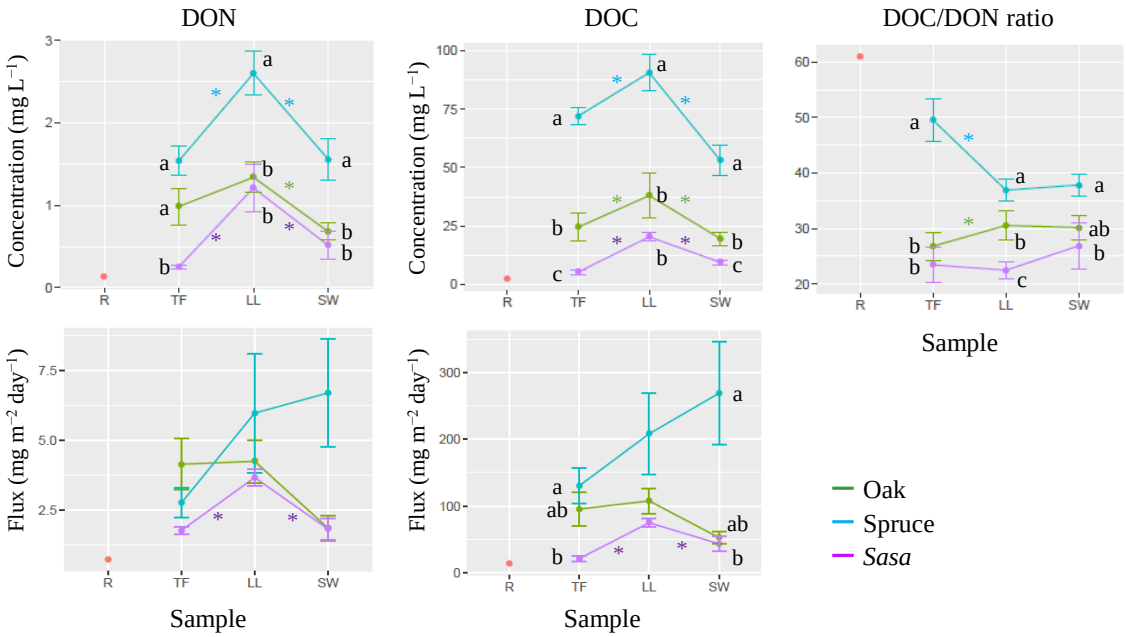

Fig. 3.4 The vertical trend of the concentrations and fluxes of DON and DOC, and DOC/DON ratio from rain to soil water.

R: Rain; TF: Throughfall; LL: Litter leachate; SW: Soil water; Different letters indicate significant differences ($P < 0.05$) among vegetation types; Error bars indicate standard error; Asterisks indicate significant difference ($P < 0.05$) between horizons

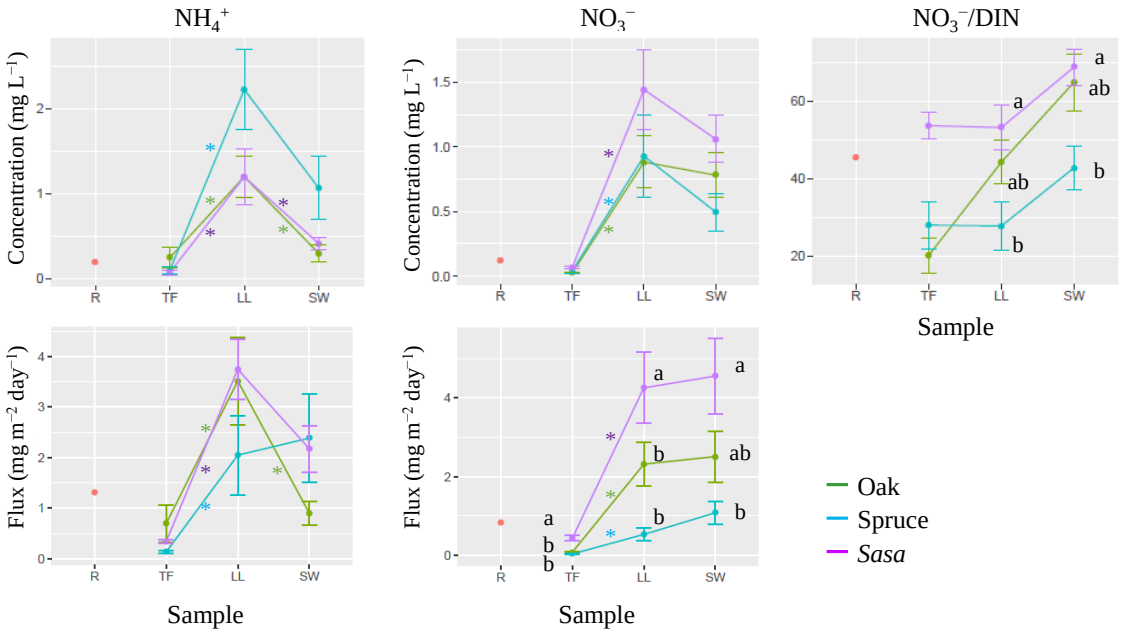

Fig. 3.5 The vertical trend of the concentrations and fluxes of DIN from rain to soil water.

R: Rain; TF: Throughfall; LL: Litter leachate; SW: Soil water; Different letters indicate significant differences (P< 0.05) among vegetation types; Error bars indicate standard error; Asterisks indicate significant difference (P < 0.05) between horizons

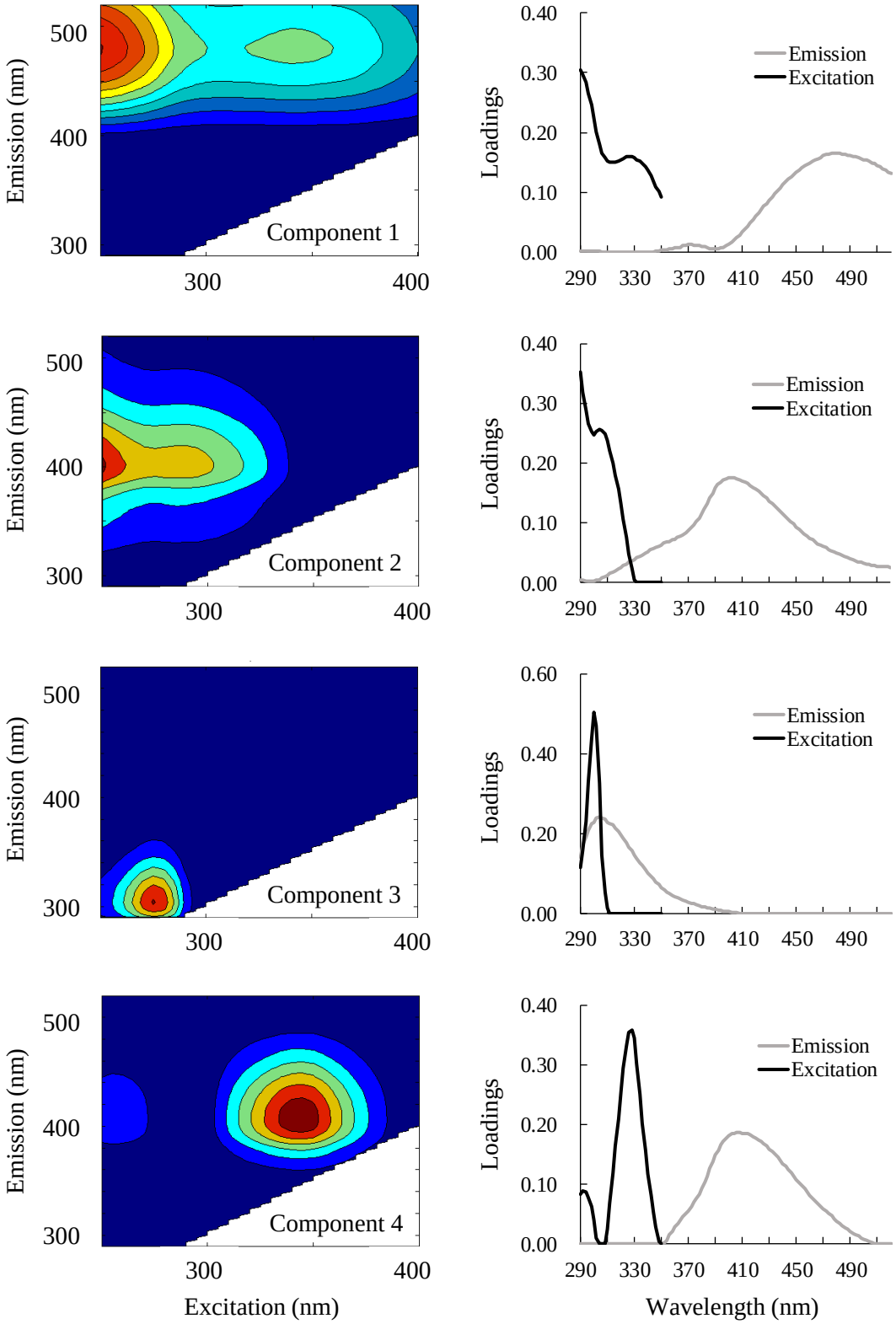

Fig. 3.6 Contour plots (left panel) and excitation and emission curves (right panel) for the four fluorescent components obtained by PARAFAC

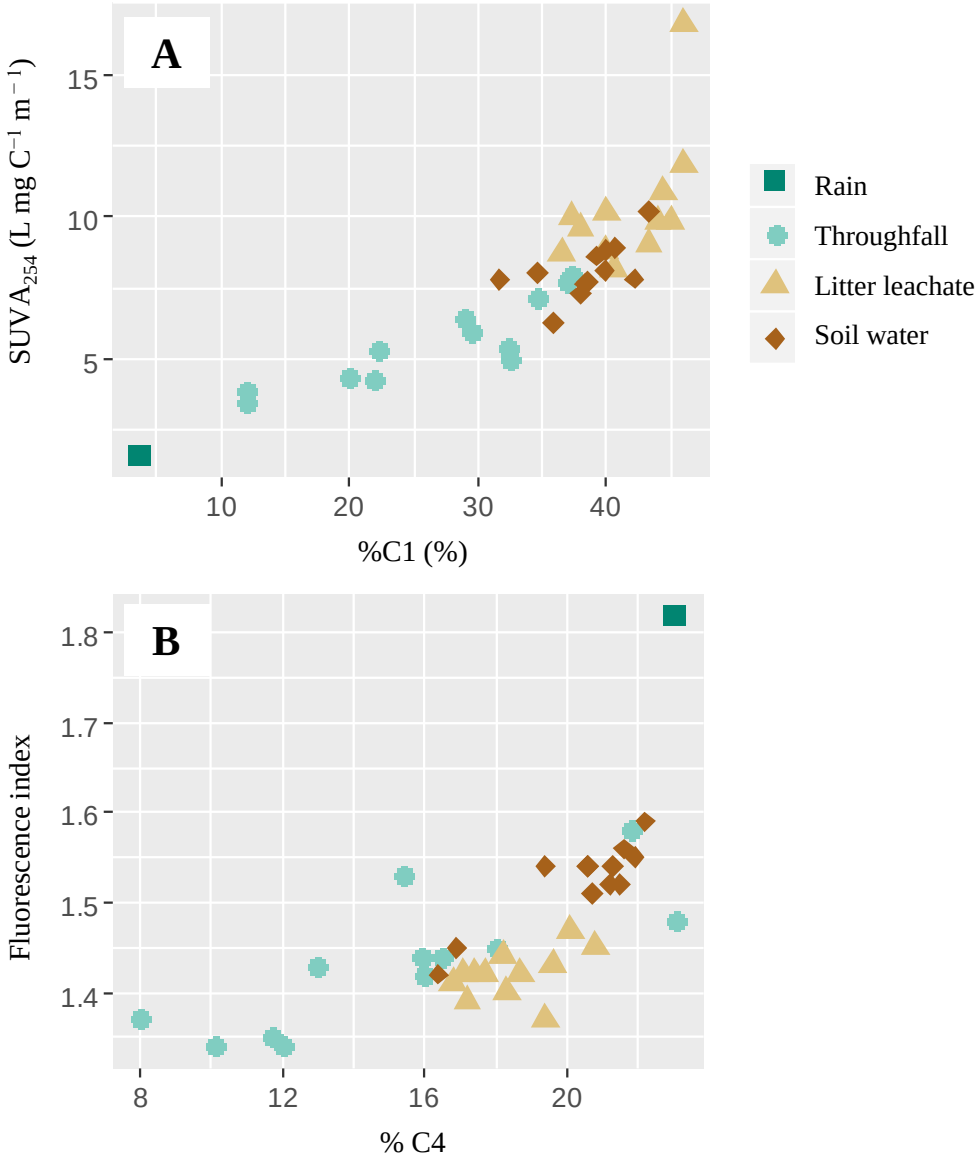

Fig. 3.7 (A) Relationship between the proportion of component 1(%C1) and $SUVA_{254}$, and (B) Relationship between the proportion of component 4(%C4) and fluorescence index, in rain, throughfall, litter leachate, and soil water. Each point represents the mean of measurements beneath a single canopy or within a single canopy gap

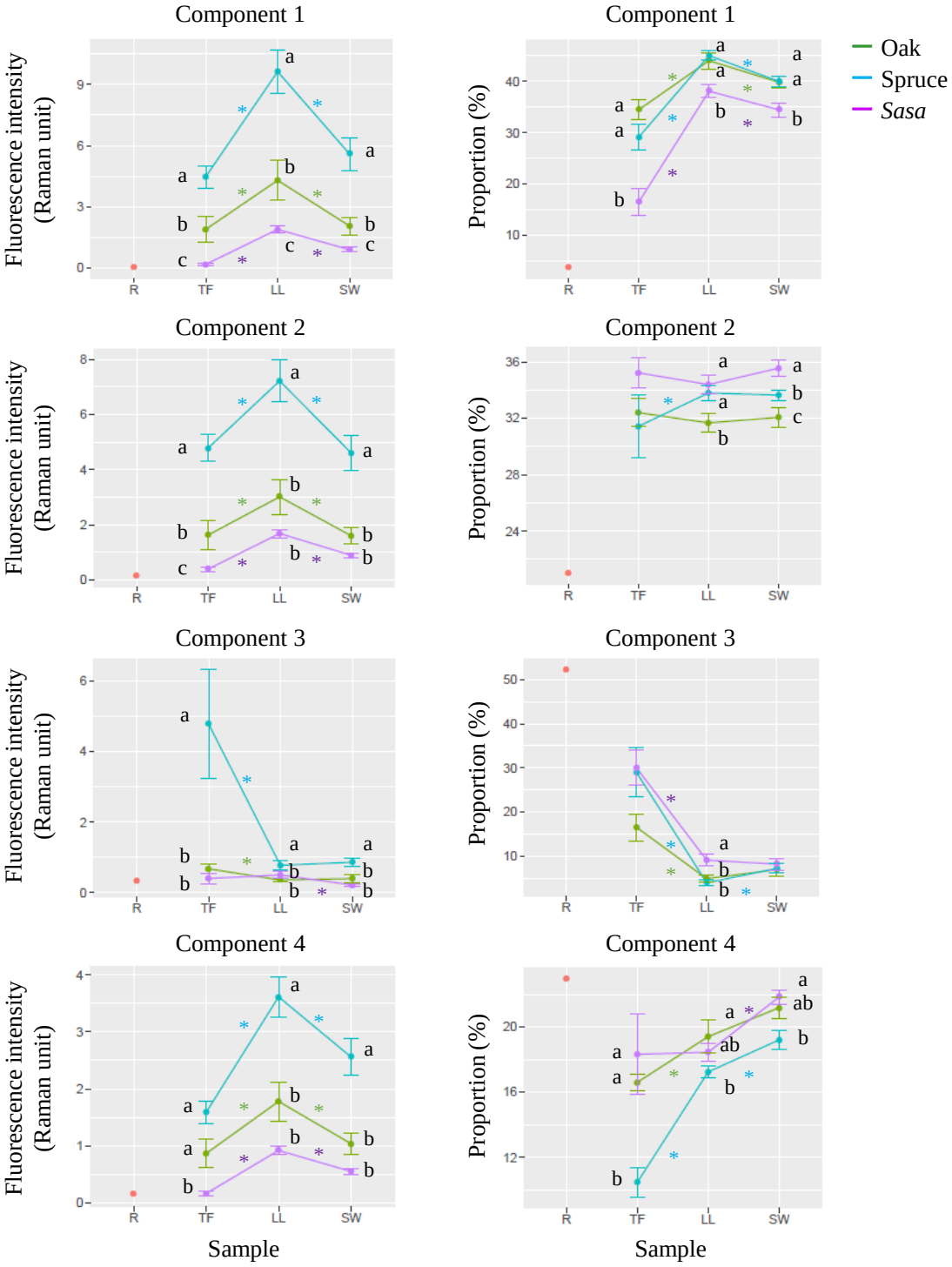

Fig. 3.8 The vertical trends of the fluorescence intensity and the proportion of the four components identified by PARAFAC from rain to soil water.

R: Rain; TF: Throughfall; LL: Litter leachate; SW: Soil water; Different letters indicate significant differences ($P < 0.05$) among vegetation types; Error bars indicate standard error; Asterisks indicate significant difference ($P < 0.05$) between horizons

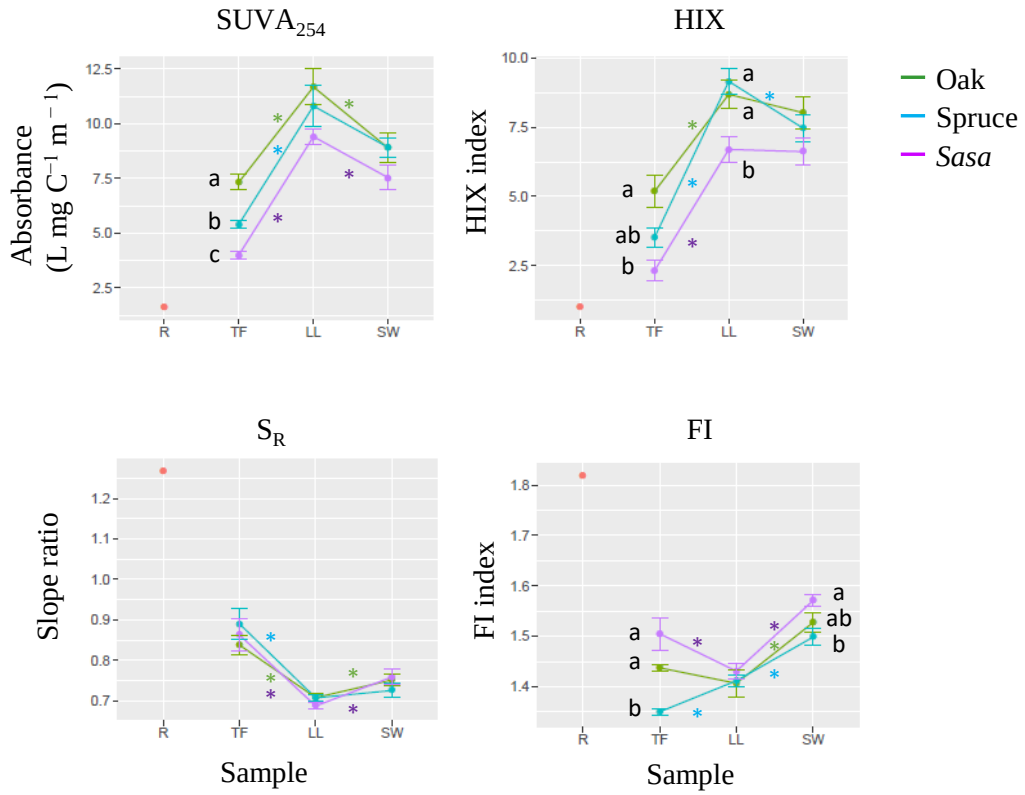

Fig. 3.9 The vertical trend of the optical indices of DOM from rain to soil water. $SUVA_{254}$: specific UV absorbance at 254 nm; HIX: humification index: S_R: spectoral slope ratio; FI: fluorescence index;
R: Rain; TF: Throughfall; LL: Litter leachate; SW: Soil water; Different letters indicate significant differences ($P < 0.05$) among vegetation types; Error bars indicate standard error; Asterisks indicate significant difference ($P < 0.05$) between horizons

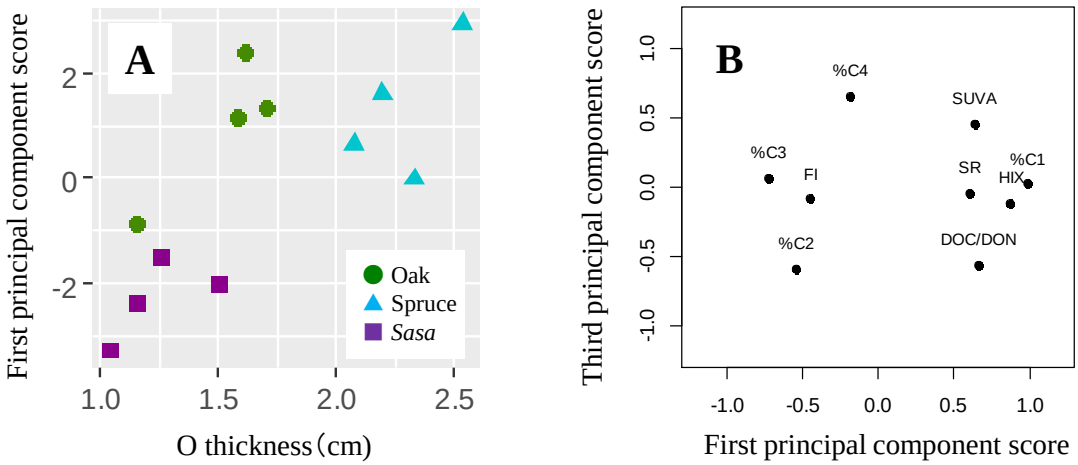

Fig. 3.10 (A) Relationship between the thickness of O horizon and the first principal component score of DOM quality metrics in the litter leachate. Each point represents the mean of measurements beneath a single canopy or within a single canopy gap; (B) property-property plot between the first and third principal factor loadings of PCA of DOM in the litter leachate ; SUVA: specific UV absorbance at 254 nm; HIX: humification index: S_R: spectoral slope ratio; FI: fluorescence index; %C1~%C4: the relative abundance of component C1~C4

Appendix table 1. Concentrations of dissolved nitrogen and dissolved organic carbon, and DOM quality metrics in rain, throughfall(TF), litter leachate(LL), and soil water(SW)

Variable	Sample	Vegetation	Mean		sd	n	Variable	Sample	Vegetation	Mean		sd	n
NH_4^+	Rain		0.20		–	1	TN	Rain		0.49		–	1
(mg/L)	TF	Oak	0.25	a	0.24	4	(mg/L)	TF	Oak	1.26	a	0.63	4
		Spruce	0.10	a	0.08	4			Spruce	1.68	a	0.45	4
		Sasa	0.08	a	0.05	4			*Sasa*	0.40	b	0.07	4
	LL	Oak	1.20	a	0.80	11		LL	Oak	3.44	a	1.22	11
		Spruce	2.23	a	1.62	12			Spruce	5.75	a	2.51	12
		Sasa	1.20	a	1.15	12			*Sasa*	3.88	a	2.72	12
	SW	Oak	0.30	a	0.34	11		SW	Oak	1.76	a	0.89	11
		Spruce	1.07	a	1.28	12			Spruce	3.17	a	1.97	12
		Sasa	0.42	a	0.26	12			*Sasa*	2.00	a	1.07	12
NO_3^-	Rain		0.13		–	1	DON/TN	Rain		20.3		–	1
(mg/L)	TF	Oak	0.02	a	0.01	4	(%)	TF	Oak	85.0	a	3.3	4
		Spruce	0.04	a	0.04	4			Spruce	93.7	a	3.7	4
		Sasa	0.07	a	0.02	4			*Sasa*	62.1	b	5.8	4
	LL	Oak	0.88	a	0.67	11		LL	Oak	43.5	ab	11.9	11
		Spruce	0.93	a	1.09	12			Spruce	56.9	a	15.5	12
		Sasa	1.44	a	1.08	12			*Sasa*	37.4	b	12.0	12
	SW	Oak	0.78	a	0.58	11		SW	Oak	49.3	ab	23.2	11
		Spruce	0.50	a	0.51	12			Spruce	57.2	a	20.2	12
		Sasa	1.06	a	0.64	12			*Sasa*	37.4	b	16.1	12
DIN	Rain		0.36		–	1	NO_3^-/DIN	Rain		45.5		–	1
(mg/L)	TF	Oak	0.27	a	0.23	4	(%)	TF	Oak	20.1	b	9.2	4
		Spruce	0.14	a	0.10	4			Spruce	28.1	b	12.2	4
		Sasa	0.14	a	0.03	4			*Sasa*	53.8	a	6.9	4
	LL	Oak	2.10	a	0.88	11		LL	Oak	44.3	ab	18.8	11
		Spruce	3.17	a	1.72	12			Spruce	27.8	b	21.7	12
		Sasa	2.67	a	2.03	12			*Sasa*	53.3	a	20.2	12
	SW	Oak	1.09	a	0.75	11		SW	Oak	65.0	ab	24.4	11
		Spruce	1.61	a	1.43	12			Spruce	42.9	b	19.8	12
		Sasa	1.49	a	0.74	12			*Sasa*	68.9	a	16.1	12
DON	Rain		0.13		–	1	DOC/DON	Rain		61.0		–	1
(mg/L)	TF	Oak	0.99	a	0.44	4		TF	Oak	26.8	b	5.1	4
		Spruce	1.54	a	0.36	4			Spruce	49.5	a	7.8	4
		Sasa	0.25	b	0.05	4			*Sasa*	23.4	b	6.2	4
	LL	Oak	1.34	b	0.60	11		LL	Oak	30.6	b	9.0	11
		Spruce	2.60	a	0.92	12			Spruce	36.9	a	6.8	12
		Sasa	1.21	b	0.98	12			*Sasa*	22.5	c	5.2	12
	SW	Oak	0.68	b	0.33	11		SW	Oak	30.2	ab	7.0	11
		Spruce	1.56	a	0.86	12			Spruce	37.9	a	6.8	12
		Sasa	0.52	b	0.58	12			*Sasa*	26.9	b	14.3	12
DOC	Rain		2.2		–	1							
(mg/L)	TF	Oak	24.5	b	12.1	4							
		Spruce	72.0	a	7.6	4							
		Sasa	5.2	c	2.3	4							
	LL	Oak	38.0	b	32.6	12							
		Spruce	90.6	a	26.7	12							
		Sasa	20.3	b	5.9	12							
	SW	Oak	19.6	b	9.3	11							
		Spruce	53.1	a	22.3	12							
		Sasa	9.4	c	3.5	12							

Note: S_R: spectoral slope ratio; FI: fluorescence index; HIX: humification index; $SUVA_{254}$: specific UV absorbance at 254 nm; %C1~%C4: the relative abundance of component C1~C4; Different letters indicate significant differences ($P < 0.05$) among vegetation types within each sample type

Appendix table 1. (Continued)

Variable	Sample	Vegetation	Mean		sd	n	Variable	Sample	Vegetation	Mean		sd	n
$SUVA_{254}$	Rain		1.6		–	1	C1	Rain		0.02		–	1
($L\ mg\ C^{-1}\ m^{-1}$)	TF	Oak	7.3	a	0.7	4	(Raman unit)	TF	Oak	1.89	b	1.23	4
		Spruce	5.4	b	0.4	4			Spruce	4.47	a	1.09	4
		Sasa	4.0	c	0.4	4			*Sasa*	0.18	c	0.08	4
	LL	Oak	11.7	a	2.7	11		LL	Oak	4.30	b	3.41	12
		Spruce	10.8	a	3.3	12			Spruce	9.62	a	3.60	12
		Sasa	9.4	a	1.2	12			*Sasa*	1.89	c	0.66	12
	SW	Oak	8.9	a	2.2	11		SW	Oak	2.06	b	1.41	11
		Spruce	8.9	a	1.5	12			Spruce	5.59	a	2.80	12
		Sasa	7.5	a	1.9	12			*Sasa*	0.89	c	0.40	12
S_R	Rain		1.27		–	1	C2	Rain		0.14		–	1
	TF	Oak	0.84	a	0.05	4	(Raman unit)	TF	Oak	1.63	b	1.03	4
		Spruce	0.89	a	0.08	4			Spruce	4.78	a	0.98	4
		Sasa	0.86	a	0.08	4			*Sasa*	0.39	c	0.16	4
	LL	Oak	0.71	a	0.04	12		LL	Oak	3.01	b	2.22	12
		Spruce	0.71	a	0.03	12			Spruce	7.22	a	2.62	12
		Sasa	0.69	a	0.03	12			*Sasa*	1.68	b	0.50	12
	SW	Oak	0.75	a	0.05	11		SW	Oak	1.60	b	0.98	11
		Spruce	0.73	a	0.06	12			Spruce	4.60	a	2.14	12
		Sasa	0.76	a	0.07	12			*Sasa*	0.89	b	0.33	12
HIX	Rain		1.00		–	1	C3	Rain		0.35		–	1
	TF	Oak	5.18	a	1.17	4	(Raman unit)	TF	Oak	0.68	b	0.29	4
		Spruce	3.51	ab	0.73	4			Spruce	4.78	a	3.10	4
		Sasa	2.32	b	0.76	4			*Sasa*	0.40	b	0.28	4
	LL	Oak	8.68	a	1.80	12		LL	Oak	0.36	b	0.18	12
		Spruce	9.15	a	1.56	12			Spruce	0.77	a	0.48	12
		Sasa	6.70	b	1.57	12			*Sasa*	0.50	b	0.36	12
	SW	Oak	8.02	a	1.96	11		SW	Oak	0.40	b	0.37	11
		Spruce	7.46	a	1.68	12			Spruce	0.86	a	0.39	12
		Sasa	6.62	a	1.66	12			*Sasa*	0.22	b	0.15	12
FI	Rain		1.82		–	1	C4	Rain		0.15		–	1
	TF	Oak	1.44	a	0.01	4	(Raman unit)	TF	Oak	0.86	a	0.50	4
		Spruce	1.35	b	0.01	4			Spruce	1.58	a	0.38	4
		Sasa	1.51	a	0.06	4			*Sasa*	0.16	b	0.08	4
	LL	Oak	1.41	a	0.09	12		LL	Oak	1.78	b	1.18	12
		Spruce	1.41	a	0.04	12			Spruce	3.62	a	1.23	12
		Sasa	1.43	a	0.05	12			*Sasa*	0.91	b	0.26	12
	SW	Oak	1.53	ab	0.06	11		SW	Oak	1.03	b	0.60	11
		Spruce	1.50	b	0.06	12			Spruce	2.56	a	1.10	12
		Sasa	1.57	a	0.04	12			*Sasa*	0.54	b	0.19	12

Appendix table 1. (Continued)

Variable	Sample	Vegetation	Mean		sd	n
%C1	Rain		3.7		–	1
(%)	TF	Oak	34.5	a	3.9	4
		Spruce	29.1	a	4.8	4
		Sasa	16.5	b	5.2	4
	LL	Oak	44.0	a	5.5	12
		Spruce	45.0	a	3.2	12
		Sasa	38.1	b	4.4	12
	SW	Oak	39.8	a	3.8	11
		Spruce	40.0	a	3.4	12
		Sasa	34.4	b	4.8	12
%C2	Rain		21.0		–	1
(%)	TF	Oak	32.4	a	2.0	4
		Spruce	31.4	a	4.5	4
		Sasa	35.2	a	2.1	4
	LL	Oak	31.7	b	2.2	12
		Spruce	33.8	a	1.9	12
		Sasa	34.4	a	2.2	12
	SW	Oak	32.1	c	2.3	11
		Spruce	33.6	b	1.3	12
		Sasa	35.6	a	1.9	12
%C3	Rain		52.4		–	1
(%)	TF	Oak	16.5	a	6.1	4
		Spruce	29.0	a	11.1	4
		Sasa	30.0	a	8.0	4
	LL	Oak	4.9	b	2.4	12
		Spruce	3.9	b	2.3	12
		Sasa	9.1	a	4.5	12
	SW	Oak	6.9	a	4.7	11
		Spruce	7.2	a	3.7	12
		Sasa	8.2	a	4.5	12
%C4	Rain		23.0		–	1
(%)	TF	Oak	16.6	a	1.0	4
		Spruce	10.5	b	1.8	4
		Sasa	18.3	a	4.9	4
	LL	Oak	19.4	a	3.6	12
		Spruce	17.2	b	1.4	12
		Sasa	18.5	ab	1.9	12
	SW	Oak	21.2	ab	2.2	11
		Spruce	19.2	b	2.1	12
		Sasa	21.8	a	1.5	12

Appendix table 2. Fluxes of water, dissolved nitrogen, and dissolved organic carbon in rain, throughfall(TF), litter leachate(LL), and soil water(SW)

Variable	Sample	Vegetation	Mean		sd	n	Variable	Sample	Vegetation	Mean		sd	n
Water volume	Rain		6.9		–	1	DON	Rain		0.7		–	1
(mm rain day^{-1})	TF	Oak	5.9	a	0.5	4	(mg m^{-2} day^{-1})	TF	Oak	4.1	a	1.8	4
		Spruce	2.8	b	1.6	4			Spruce	2.8	a	1.1	4
		Sasa	6.5	a	0.9	4			*Sasa*	1.8	a	0.2	4
	LL	Oak	4.3	ab	2.8	12		LL	Oak	4.2	a	2.7	12
		Spruce	2.9	b	3.1	12			Spruce	6.0	a	7.4	12
		Sasa	5.2	a	1.2	12			*Sasa*	3.7	a	1.0	12
	SW	Oak	3.6	a	2.4	12		SW	Oak	1.8	a	1.5	12
		Spruce	4.3	a	3.6	12			Spruce	6.7	a	6.7	12
		Sasa	5.1	a	4.2	12			*Sasa*	1.8	a	1.4	12
NH_4^+	Rain		1.31		–	1	DOC	Rain		13.7		–	1
(mg m^{-2} day^{-1})	TF	Oak	0.70	a	0.73	4	(mg m^{-2} day^{-1})	TF	Oak	95.3	ab	51.7	4
		Spruce	0.13	a	0.07	4			Spruce	130.2	a	53.8	4
		Sasa	0.34	a	0.06	4			*Sasa*	21.2	b	9.5	4
	LL	Oak	3.52	a	2.99	12		LL	Oak	107.7	a	65.6	12
		Spruce	2.05	a	2.73	12			Spruce	208.0	a	211.8	12
		Sasa	3.75	a	2.08	12			*Sasa*	74.9	a	21.7	12
	SW	Oak	0.90	a	0.83	12		SW	Oak	52.7	ab	33.5	12
		Spruce	2.39	a	3.00	12			Spruce	268.7	a	267.5	12
		Sasa	2.18	a	1.59	12			*Sasa*	43.5	b	36.8	12
NO_3^-	Rain		0.84		–	1	TN	Rain		2.87		–	1
(mg m^{-2} day^{-1})	TF	Oak	0.08	b	0.02	4	(mg m^{-2} day^{-1})	TF	Oak	4.95	a	2.49	4
		Spruce	0.03	b	0.04	4			Spruce	2.92	a	1.11	4
		Sasa	0.43	a	0.14	4			*Sasa*	2.55	a	0.17	4
	LL	Oak	2.31	b	1.94	12		LL	Oak	10.18	a	6.55	12
		Spruce	0.53	b	0.59	12			Spruce	8.61	a	9.75	12
		Sasa	4.26	a	3.12	12			*Sasa*	11.80	a	5.05	12
	SW	Oak	2.51	ab	2.24	12		SW	Oak	5.33	a	3.97	12
		Spruce	1.08	b	1.00	12			Spruce	10.33	a	9.24	12
		Sasa	4.55	a	3.33	12			*Sasa*	8.68	a	5.15	12
DIN	Rain		2.16		–	1							
(mg m^{-2} day^{-1})	TF	Oak	0.81	a	0.79	4							
		Spruce	0.17	a	0.08	4							
		Sasa	0.79	a	0.14	4							
	LL	Oak	5.94	ab	4.37	12							
		Spruce	2.65	b	2.84	12							
		Sasa	8.13	a	4.62	12							
	SW	Oak	3.49	a	2.97	12							
		Spruce	3.63	a	3.58	12							
		Sasa	6.88	a	4.12	12							

Note: different letters indicate significant differences ($P < 0.05$) among vegetation types within each sample type

Chapter 4. General discussion

4.1 How do trees and understory vegetation affect the soil nitrogen dynamics in a cool-temperate mixed forest?

The main objective of this dissertation was to understand the effects of tree species and understory species grown in a cool-temperate mixed forest on soil N dynamics. In this chapter, I will discuss on the influence of trees and understory vegetation on soil N dynamics in the studied mixed forest based on the findings of Chapter 2 and 3 and previous studies conducted in northern Hokkaido, on relationship of forest dynamics and environmental change to soil N dynamics, and on limitations of this study and emerging questions.

In Chapter 2, I tried to understand the spatial variation of soil N dynamics and the effects of plant distribution on the variation. Therefore, I examined the spatial pattern of litterfall, soil water content, thickness of O horizon, and soil inorganic N contents, and analyzed the relationship with plant distribution in a relatively small (800 m^2) and flat area. The spatial variation in soil N dynamics, especially the soil NO_3^- content, was found to be controlled by the spatial distribution of coniferous and broadleaved trees and the canopy gaps that is dominated by *Sasa* through their effects on litter decomposition and hydrology in the mixed conifer-broadleaved forest stand (Fig.2.3). The soil NO_3^- content was relatively high near the broadleaved trees and in the canopy gap, while it was low near the coniferous trees (Fig. 2.2). The spatial variation in litter composition was related to the adjacent plant composition (Table 2.3 and 2.4). The coniferous litter showed higher C/N ratio than the broadleaved and *Sasa* litter (Table 2.7). The O horizon became thicker as the relative abundance of coniferous litter increased (Table 2.4). These results suggested that the plant distribution creates the spatial variation in the thickness of O horizon via the difference in the litter quality. The spatial variations of the O horizon thickness and the abundance of coniferous trees were the controlling factors of soil moisture (Table 2.5). The soils under thick O horizon and near coniferous trees exhibited low soil water content, while those under thin O horizon and near broadleaved trees and in the canopy gap showed high soil water content (Fig. 2.2). The soil NO_3^- content increased with increasing soil water content, probably through the positive influence of soil moisture on nitrifier activity (Tables 2.5 and 2.8).

In Chapter 3, the effects of DOM on soil N dynamics, especially NO_3^- leaching from the mineral soil, was examined to understand how litter decomposition is related to soil N dynamics. I collected throughfall, litter leachate, and soil water under oak,

spruce and *Sasa* in canopy gaps, and examined the proportion of atmospheric NO_3^- to total NO_3^- and the differences in the DOM quality of water sample among these plants. Then, the influence of DOM quality on NO_3^- leaching from the forest floor and surface mineral soil were analyzed. The proportion of atmospheric NO_3^- to total NO_3^- identified using the $\Delta^{17}O$ value of NO_3^- indicated that most of the NO_3^- in the litter leachate and soil water was not direct input of atmospheric NO_3^-, but was NO_3^- produced by soil microbes (Table 3.4). The biodegradability and relative N content to C in the litter leachate, which are described by the suite of optical indices of DOM and DOC/DON ratio, was in descending order of *Sasa,* oak, and spruce (Figs. 3.4, 3.8 and 3.9). Thick O horizon produced DOM with higher proportion of plant-derived humic-like DOM and higher degree of humification, while thin O horizon produced DOM with higher proportion of tyrosine-like DOM (Fig. 3.10). The more recalcitrant characteristics of DOM in litter leachate of oak compared with those of *Sasa* was probably due to the more recalcitrant DOM in the throughfall beneath oak than *Sasa* (Figs. 3.8, 3.9). These results suggested that the differences in the degree of litter decomposition and in the throughfall DOM properties create the differences in the quality of DOM that leaches to the soil. The NO_3^- flux and the proportion of NO_3^- to DIN in the soil water was higher in the canopy gap than spruce (Fig. 3.5). The variation in the proportion of NO_3^- to DIN in the soil water was explained by the DOM quality in the litter leachate. Litter leachate DOM with higher proportion of tyrosine-like and microbially derived DOM and less humified, and low DOC/DON ratio was related to higher NO_3^-/DIN in the soil water (Table 3.6 and Fig. 3.10B). Chapter 3 showed that differences in litter decomposition and DOM quality in throughfall among vegetation types shapes DOM quality that is supplied to mineral soil, then lead to differences in NO_3^- leaching.

Therefore, it can be concluded that the plant distribution controls the availability and leaching of soil NO_3^- through the interacting effect of litter decomposition, hydrology, and quality of organic matter (Fig. 4). As a result, the availability and leaching of soil NO_3^- are relatively high in canopy gaps that are dominated by *Sasa* and near broadleaved trees, while those are relatively low near coniferous trees in the mixed conifer-broadleaved forest of northern Japan (Fig. 4).

Although many studies have suggested that litter quality, litter decomposition, soil moisture, and DOM quality affect soil N dynamics, few studies have examined these factors simultaneously in mixed forests. The results of this study suggest that spatial variations of these factors are primarily controlled by plant distribution, thereby relating to the spatial variation of soil NO_3^-. The lower soil NO_3^- availability and net nitrification around coniferous trees than broadleaved trees were consistent with the

following report. Augusto et al. (2015) reviewed the influence of evergreen coniferous and deciduous broadleaved tree species on nutrient cycling of temperate and boreal forests and concluded that N mineralization and nitrification are generally similar or lower under evergreen coniferous stands than under deciduous broadleaved stands.

The relatively thin O horizon and high availability and leaching of NO_3^- in the canopy gaps were unexpected as Tripathi et al. (2006) and Watanabe et al. (2013) reported that the initial decomposition of *Sasa* litter was slower than those of tree leaf litter. Temperature and moisture generally influence litter decomposition (Prescott 2010). Soil moisture was higher in the canopy gaps than under closed canopy in this study, therefore, moister conditions in the canopy gap may be suitable for the decomposition of *Sasa* litter in the canopy gaps. Recently, Ni et al. (2016) found that the thicker snow cover in canopy gap, which provides thermal resistance, can enhance litter decomposition during winter by suppressing humification of litter in an alpine forest. Additionally, larger snowpack has been suggested to related to higher soil moisture during early growing seasons (Maurer and Bowling 2014), which could also enhance litter decomposition. Therefore, these mechanisms might be responsible for the observed thinner O horizon in the canopy gaps in the cool-temperate mixed forest examined in this study, where snow depth reaches up to 200 cm. However, further investigations of the temperature and moisture conditions in the forest floor, snowpack, and the timing of snowmelt are needed.

Fukuzawa et al. (2006 and 2015) found that *Sasa* prevents N leaching for at least three years after single-tree cutting and for at least one year after clear-cutting by increasing its leaf and fine root biomass and N uptake. They concluded that *Sasa* plays significant roles in mitigating the loss of N from the soil following tree cuttings. However, this study found that canopy gaps, with their ages at least seven years, exhibit high level of soil NO_3^- leaching compared with the adjacent coniferous and broadleaved trees. These findings imply that *Sasa* acts as a short-term sink of inorganic N when disturbance such as tree cutting increases its availability, while once *Sasa* reaches their maximum biomass, their uptake cannot keep up the high production of inorganic N in the soil, then nitrification and NO_3^- leaching will increase in the canopy gap in the longer term. It should be noted, however, that the age of canopy gap examined in this study is uncertain, therefore, long-term response of canopy gap need to be examined in the future study.

4.2 Relationship of forest dynamics and environmental change to soil N dynamics

It has been suggested that positive feedback between tree species and soil determines the spatial distribution of tree species in some previous studies. For example, a mosaic of hemlock and sugar maple patches formed on uniform parent material and landform in the Sylvania Woods of Upper Michigan has been stable for millennia (Davis et al. 1992). This spatial pattern of tree species has been suggested to be a result of positive feedback of these two species: sugar maple regeneration was inhibited by low soil fertility beneath hemlock while hemlock regeneration is inhibited by the physical barrier of maple leaf litter (Frelich et al. 1993). In a study conducted in the same forest, Ferrari (1999) has suggested that difference in litter quality that affect soil N availability feeds back to tree fitness through difference in preference of N form between hemlock and sugar maple, which creates and maintains the canopy mosaic.

In the mixed conifer-broadleaved forest examined in this study, soil NO_3^- contents, net production, and NO_3^- leaching were different beneath spruce, oak, and *Sasa* in canopy gaps. However, it is questionable whether the difference in soil NO_3^- availability for plants benefits the fitness of their seedlings and saplings and create the persistent pattern of coniferous and broadleaved trees and *Sasa* understory in this type of forest. Persistent distribution of coniferous and broadleaved trees has not been reported in cool-temperate mixed forests in Hokkaido. Hiura and Fujiwara (1999) suggested that the coexistence of multiple tree species in these forests is maintained by reciprocal replacement of conifers and broadleaved trees. They suggested that pathogen and herbivory are the mechanisms for causing the reciprocal replacement. Noguchi and Yoshida (2004) reported that regeneration density of canopy species was higher under dense conifer canopy than canopy gap. They attributed this to the stronger negative effect of *Sasa* than shading effect of canopy species on tree regeneration. Also, simultaneous death of *Sasa*, which occurs at intervals of several decades, has been considered to induce synchronization of tree regeneration (Nakashizuka and Numata 1982). These studies suggest that forest dynamics in cool-temperate mixed forests of Hokkaido is strongly affected by pathogen, herbivory, the presence of *Sasa* and that spatial pattern of soil N availability may not be a strong factor that determines the plant distribution. However, the finding of this study that soil NO_3^- content is relatively low near coniferous trees and is relatively high near broadleaved trees and in canopy gaps may be important for the growth of successfully established seedlings and saplings of canopy species if the nitrogen form affect their growth. Additionally, such knowledge is valuable for forestry practice since site preparation and supplemental planting to ensure

regeneration has been suggested in locations where natural regeneration is difficult (Noguchi and Yoshida 2004).

Given that long-term positive feedback between plant species and soil is less likely, and the plant distribution continuously changes as a result of reciprocal replacement and/or because of the influence of *Sasa* in the cool-temperate mixed forests, the relationship between the current plant distribution and spatial pattern of soil N dynamics observed in this study implies that spatial pattern of soil N dynamics will respond rapidly to the future environmental change through a shift in plant distribution. Studies that examined the demography of major tree species in mixed forests of northern Hokkaido implied decreasing dominance of coniferous species in the future because the survival rate, life expectancy and regeneration of coniferous species were lower than those of broadleaved species (Hiura and Fujiwara 1999; Yoshida et al. 2006; Noguchi & Yoshida 2007). Additionally, it is predicted that the relative abundance of coniferous species will decrease and that of broadleaved species will increase in Hokkaido as global warming proceeds (Tanaka et al. 2009). Global warming is also expected to increase the frequency of strong typhoons (Emanuel 2005; Webster et al. 2005), which is a major factor that creates canopy gaps (Yoshida and Noguchi 2009). Coniferous trees have been found to be more vulnerable to strong winds than broadleaved trees (Yoshida and Noguchi 2009). Therefore, an increase in the frequency and magnitude of typhoons might result in a decrease in coniferous trees and an increase in canopy gap area in cool-temperate mixed forests of Hokkaido. This study found that soils near broadleaved trees and those in canopy gaps exhibit higher contents, production, and leaching of NO_3^- than those near coniferous trees. Therefore, if natural succession or global warming decreases coniferous trees and increases broadleaved trees and/or canopy gaps, it could increase NO_3^- leaching, which may affect stream water quality.

4.3 Limitation and emerging questions

This study found the relatively high NO_3^- availability and NO_3^- leaching in the canopy gaps where *Sasa* dominates the forest floor and some broadleaved trees are grown. Because this study was conducted in a single watershed, it is necessary to examine whether same trend can be obtained in other cool-temperate mixed forest where *Sasa* is dominant in the forest floor to generalize the findings. In addition, it is not clear whether the relatively thin O horizon, high soil moisture, and high NO_3^- availability and NO_3^- leaching observed in this study are caused by the specific

characteristics of *Sasa* litter, or by the environmental conditions such as throughfall flux, temperature, and snowpack, which are specific to canopy gaps, or by the interaction of these factors. Hence, the influence of canopy gap creation and subsequent dominance by understory vegetation on soil N dynamics should be examined in other forest ecosystems with dense understory vegetation.

This study focused on the influences of vegetation on soil N dynamics at a relatively small scale. The understandings at small scale would contribute to evaluate and predict the impacts of small-scale disturbance such as windfall and selection cutting on ecosystem processes. However, in order to understand the impacts of disturbance at larger scale, it is necessary to examine how the small-scale heterogeneity in soil N dynamics is integrated at watershed scale or landscape scale. This would involve understanding of not only vegetation-soil N dynamics relationships but also the effects of hydrology and geology. As for N leaching from forest soils, this study examined only leaching at the depth of 10 cm in the mineral soil. As N in the leaching water is consumed by root- and microbial- uptake, and by denitrification in the lower soil horizons and ground water, changes in plant composition may not be directly reflected in the N concentrations in stream water. Future study should examine whether tree species composition and proportion of canopy gap in watersheds are related to NO_3^- concentration in stream water.

In order to understand how forest dynamics is related to soil N dynamics and to predict the impact of vegetation change caused by environmental change on soil N dynamics and related ecosystem services, it is crucial to know what stages of forest succession the study is examining. As this study captured a snapshot of plant-soil relationship in a dynamic natural forest stand, it is still not clear that how fast soil N dynamics changes after canopy gap is formed and how long the observed pattern of soil N dynamics would last. These insights would be very important to predict the impacts of vegetation change in the future.

4.5 General conclusion

This study examined the influence of trees and understory vegetation on soil N dynamics in a cool-temperate mixed forest of northern Japan. Fig. 4 describes the summary of the findings in this study. The NO_3^- contents and net nitrification rates in soil were relatively high around broadleaved trees and in the canopy gap dominated by *Sasa*, while they were relatively low around coniferous trees. Intensive survey of litterfall, O horizon thickness, soil moisture revealed that these spatial pattern of soil

NO_3^- was created by the plant distribution through the interacting effects of litterfall and hydrological processes in the canopy-litter-soil continuum. NO_3^- flux and NO_3^-/DIN ratio in the litter leachate and soil water were higher beneath *Sasa* dominated canopy gap than beneath spruce. Most of the leaching NO_3^- was derived from nitrification in the soil rather than the direct inputs of atmospheric NO_3^- deposition. The DOM properties of the litter leachate was influenced by litter decomposition (i.e., the thickness of O horizon) and the DOM properties of throughfall. The DOM property of the litter leachate beneath spruce was characterized as low biodegradability and low relative N content (i.e, high proportion of plant-derived humic-like DOM and high DOC/DON ratio), while that beneath *Sasa* in the canopy gaps was characterized as high biodegradability and high relative N content (i.e, high proportion of tyrosine-like DOM and low DOC/DON ratio). The DOM property of oak litter leachate showed intermediate characteristics in terms of biodegradability compared to *Sasa* and spruce. The NO_3^-/DIN ratio in the soil water increased with increasing proportion of tyrosine-like and microbially-derived DOM, and decreasing degree of humification and DOC/DON ratio in the litter leachate, suggesting that higher biodegradability of the DOM leached from forest floor enhances nitrification in the soil. Overall, coniferous and broadleaved trees and *Sasa*-dominated canopy gap influence the availability and leaching of NO_3^- in the soil through their effects on litter chemistry, soil moisture, and DOM quality. The strong influence of *Sasa* understory on the tree regeneration suggested that the spatial pattern of soil NO_3^- availability is not the cause of plant distribution, but a result of plant distribution which is affected by natural disturbances (such as typhoon). Relatively high availability and leaching of NO_3^- imply that an increase in stream water NO_3^- concentration may occur if environmental change reduces the abundance of coniferous trees and increase that of broadleaved trees and canopy gap.

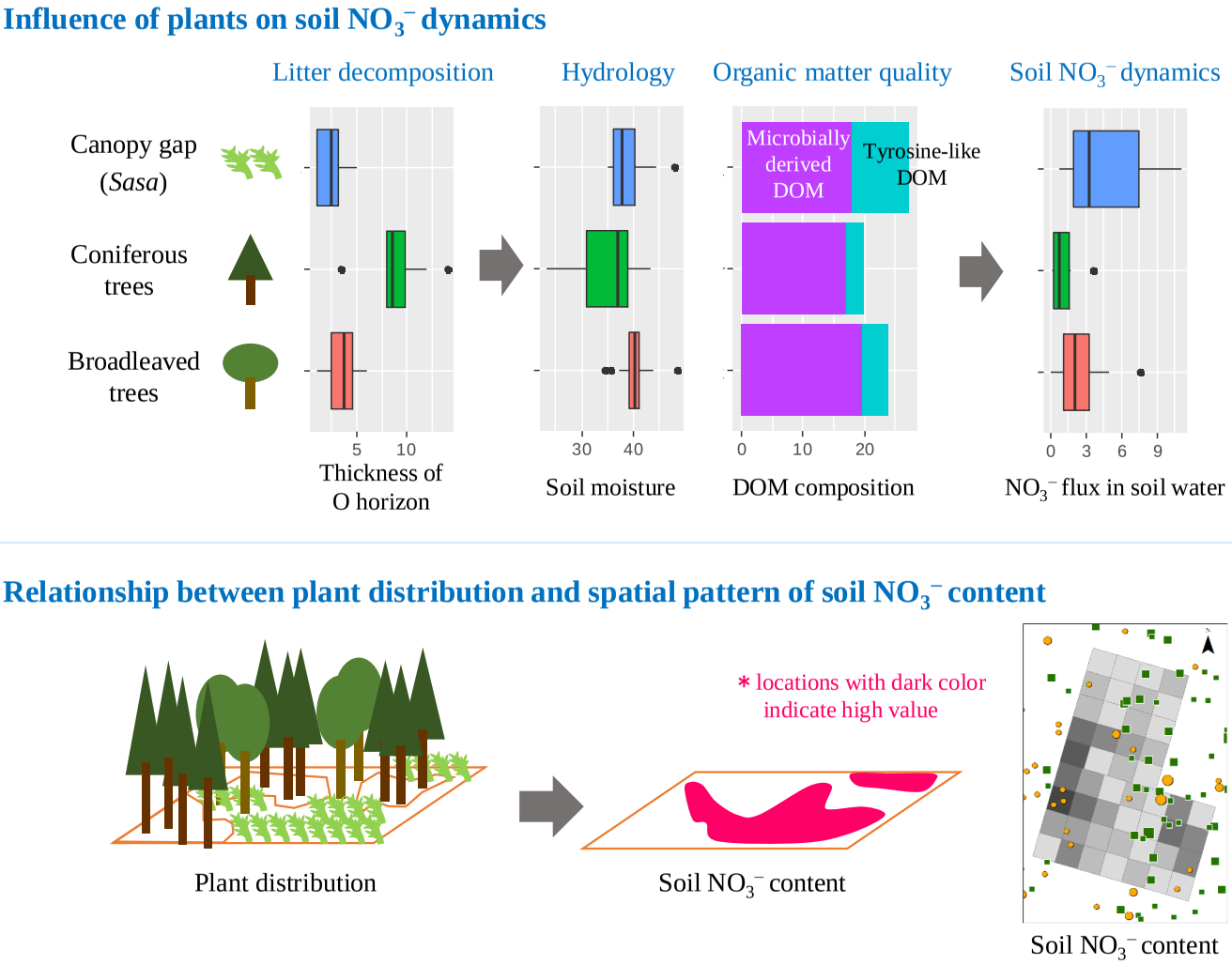

Fig. 4 Schematic diagram of the effects of trees and understory vegetation on soil N dynamics in a cool-temperate mixed forest examined in this study.

5. Acknowledgements

I am deeply thankful to my supervisor, Dr. Hideaki Shibata, for his kind and insightful teaching throughout my Ph.D study. He was always available and spent a lot of time for answering my questions, reviewing my writings, and gave me insightful comments. He funded me for sampling, laboratory works, and attending conferences and other programs. I would also like to thank Dr. Karibu Fukuzawa for teaching laboratory work. He spent so much time for me when I had problems with the analytical tools. He also gave me valuable comments on my research. I would like to thank Dr. Toshiya Yoshida for arranging my fieldwork in the Uryu Experimental Forest, for giving me information on the forest dynamics of the study site, and for reviewing my writings. I would like to thank Dr. Tsunehiro Watanabe for helping my laboratory works, for discussing about my research, and giving me valuable comments. I would like to thank Dr. Fuyuki Sato for reviewing my writings and giving me critical comments on my study.

I would like to thank Dr. Youhei Yamashita for kindly letting me use his spectrophotometer and spectrofluorometer and for teaching me everything I needed to measure and understand the optical properties of DOM in my water samples. He was always available for answering my questions, reviewing my writings, and helped me understand the data.

I would like to thank Dr. Fumiko Nakagawa and Dr. Urumu Tsunogai for kindly measuring the natural stable isotopic composition of NO_3^- in my water sample. They also gave me opportunities to join the internship program funded by Nagoya University and gave me valuable comments on my research.

I would like to thank Dr. Junichi Kashiwagi for teaching me spatial analysis and kindly let me use his software for spatial analysis. I would also like to Dr. Masae Ishihara for her grate help with my statistical analysis using R software. I would like to thank the teaching staff of Field Science Center of Northern Biosphere, Hokkaido University for giving me critical comments on my research. I would also like to thank the technical staff of Uryu Experimental Forest for arranging transport and helping my fieldwork. They sometimes even provided me meals. I would also like to thank the students in Dr. Shibata's laboratory for giving me critical comments on my research. I would also like to thank other students and postdoctoral researchers in the Field Science Center of Northern Biosphere, Sapporo for making my study enjoyable. I would like to thank the students in Field Science Center of Northern Biosphere, Nayoro for their great support during my stay in Nayoro for the field and laboratory works.

Finally, I would like to thank my family and friends for their great support during my Ph.D works.

6. References

Asbjornsen H et al. (2011) Ecohydrological advances and applications in plant-water relations research: a review. J Plant Ecol 4:3-22 doi:10.1093/jpe/rtr005

Attiwill PM (1994) The disturbance of forest ecosystems - the ecological basis for conservative management. Forest Ecol Manag 63:247-300 doi:10.1016/0378-1127(94)90114-7

Augusto L, De Schrijver A, Vesterdal L, Smolander A, Prescott C, Ranger J (2015) Influences of evergreen gymnosperm and deciduous angiosperm tree species on the functioning of temperate and boreal forests. Biol Rev 90:444-466 doi:10.1111/brv.12119

Baldrian P, Merhautova V, Petrankova M, Cajthaml T, Snajdr J (2010) Distribution of microbial biomass and activity of extracellular enzymes in a hardwood forest soil reflect soil moisture content. Appl Soil Ecol 46:177-182 doi:10.1016/j.apsoil.2010.08.013

Balisky AC, Burton PJ (1993) Distinction of soil thermal regimes under various experimental vegetation covers. Can J Soil Sci 73:411-420 doi:10.4141/cjss93-043

Barbier S, Balandier P, Gosselin F (2009) Influence of several tree traits on rainfall partitioning in temperate and boreal forests: a review. Ann For Sci 66:602 doi:10.1051/forest/2009041

Beer C et al. (2010) Terrestrial Gross Carbon Dioxide Uptake: Global Distribution and Covariation with Climate. Science 329:834-838 doi:10.1126/science.1184984

Bengtson P, Falkengren-Grerup U, Bengtsson G (2005) Relieving substrate limitation-soil moisture and temperature determine gross N transformation rates. Oikos 111:81-90 doi:10.1111/j.0030-1299.2005.13800.x

Bengtson P, Falkengren-Grerup U, Bengtsson G (2006) Spatial distributions of plants and gross N transformation rates in a forest soil. J Ecol 94:754-764 doi:10.1111/j.1365-2745.2006.01143.x

Binkley D, Giardina C (1998) Why do tree species affect soils? The Warp and Woof of tree-soil interactions. Biogeochemistry 42:89-106 doi:10.1023/a:1005948126251

Booth MS, Stark JM, Rastetter E (2005) Controls on nitrogen cycling in terrestrial ecosystems: A synthetic analysis of literature data. Ecol Monogr 75

doi:10.1890/04-0988

Bormann FH and Likens GE (1979) Pattern and Process in a Forested Ecosystem. Springer-Verlag, New York

Boyden S, Montgomery R, Reich PB, Palik B (2012) Seeing the forest for the heterogeneous trees: stand-scale resource distributions emerge from tree-scale structure. Ecol Appl 22:1578-1588 doi:10.1890/11-1469.1

Burgess SSO, Adams MA, Turner NC, Ong CK (1998) The redistribution of soil water by tree root systems. Oecologia 115:306-311 doi:10.1007/s004420050521

Bustamante M, Verdejo V, Zúñiga C, Espinosa F, Orlando J, Carú M (2012) Comparison of water availability effect on ammonia-oxidizing bacteria and archaea in microcosms of a Chilean semiarid soil. Front Microbiol 3:282 doi:10.3389/fmicb.2012.00282

Chapin FS III, Matson PA, Vitousek PM (2011) Principles of Terrestrial Ecosystem Ecology. 2nd edn. Springer, New York

Chapman SK, Langley JA, Hart SC, Koch GW (2006) Plants actively control nitrogen cycling: uncorking the microbial bottleneck. New Phytologist 169:27-34 doi:10.1111/j.1469-8137.2005.01571.x

Collins SL et al. (2011) An integrated conceptual framework for long-term social-ecological research. Front Ecol Environ 9:351-357 doi:10.1890/100068

Compton JE et al. (2011) Ecosystem services altered by human changes in the nitrogen cycle: a new perspective for US decision making. Ecol Lett 14:804-815 doi:10.1111/j.1461-0248.2011.01631.x

Cory RM, Kaplan LA (2012) Biological lability of streamwater fluorescent dissolved organic matter. Limnol Oceanogr 57:1347-1360 doi:10.4319/lo.2012.57.5.1347

Cory RM, McKnight DM (2005) Fluorescence spectroscopy reveals ubiquitous presence of oxidized and reduced quinones in dissolved organic matter. Environ Sci Technol 39:8142-8149 doi:10.1021/es0506962

Costa AW, Michalski G, Schauer AJ, Alexander B, Steig EJ, Shepson PB (2011) Analysis of atmospheric inputs of nitrate to a temperate forest ecosystem from $\Delta^{17}O$ isotope ratio measurements. Geophys Res Lett 38 doi:10.1029/2011gl047539

Davis MB, Sugita S, Calcote RR, Frelich LE (1992) Effects of invasion by *Tsuga canadensis* on a North American forest ecosystem. In Teller AJ, Mathy P, Jeffers JNR (eds) Responses of forest ecosystems to environmental changes, Elsevier, London, pp 34-44

De Schrijver A et al. (2007) The effect of forest type on throughfall deposition and seepage flux: a review. Oecologia 153:663-674 doi:10.1007/s00442-007-0776-1

Doerr SH, Shakesby RA, Walsh RPD (2000) Soil water repellency: its causes, characteristics and hydro-geomorphological significance. Earth-Science Reviews 51:33-65 doi:10.1016/s0012-8252(00)00011-8

Don A, Kalbitz K (2005) Amounts and degradability of dissolved organic carbon from foliar litter at different decomposition stages. Soil Biol Biochem 37:2171-2179 doi:10.1016/j.soilbio.2005.03.019

Dormann CF (2007) Effects of incorporating spatial autocorrelation into the analysis of species distribution data. Global Ecol Biogeogr 16:129-138 doi:10.1111/j.1466-8238.2006.00279.x

Emanuel K (2005) Increasing destructiveness of tropical cyclones over the past 30 years Nature 436:686-688 doi:10.1038/nature03906

Enriquez S, Duarte CM, Sandjensen K (1993) Patterns in decomposition rates among photosynthetic organisms - The importance of detritus C-N-P content. Oecologia 94:457-471 doi:10.1007/bf00566960

FAO 2016 Global Forest Resource Assessment. How are the world's forests changing? Second edition, Rome. http://www.fao.org/3/a-i4793e.pdf. Accessed 15 December 2016

Fenn ME et al. (1998) Nitrogen excess in North American ecosystems: Predisposing factors, ecosystem responses, and management strategies. Ecol Appl 8:706-733 doi:10.2307/2641261

Ferrari JB (1999) Fine-scale patterns of leaf litterfall and nitrogen cycling in an old-growth forest. Can J Forest Res 29:291-302 doi:10.1139/cjfr-29-3-291

Ferrari JB, Sugita S (1996) A spatially explicit model of leaf litter fall in hemlock-hardwood forests. Can J Forest Res 26:1905-1913 doi:10.1139/x26-215

Finzi AC, Van Breemen N, Canham CD (1998) Canopy tree soil interactions within

temperate forests: Species effects on soil carbon and nitrogen. Ecol Appl 8:440-446 doi:10.2307/2641083

Franklin JF (1993) Preserving biodiversity - species, ecosystems, or landscapes. Ecol Appl 3:202-205 doi:10.2307/1941820

Frelich LE, Calcote RR, Davis MB, Pastor J (1993) Patch formation and maintenance in an old-growth hemlock-hardwood forest. Ecology 74:513-527 doi:10.2307/1939312

Froberg M, Kleja DB, Hagedorn F (2007) The contribution of fresh litter to dissolved organic carbon leached from a coniferous forest floor. Eur J Soil Sci 58:108-114 doi:10.1111/j.1365-2389.2006.00812.x

Fukuzawa K et al. (2006) Effects of clear-cutting on nitrogen leaching and fine root dynamics in a cool-temperate forested watershed in northern Japan. Forest Ecol Manag 225:257–261 doi:10.1016/j.foreco.2006.01.001

Fukuzawa K, Shibata H, Takagi K, Satoh F, Koike T, Sasa K (2015) Roles of dominant understory Sasa bamboo in carbon and nitrogen dynamics following canopy tree removal in a cool-temperate forest in northern Japan. Plant Spec Biol 30:104-115 doi:10.1111/1442-1984.12086

Gross KL, Pregitzer KS, Burton AJ (1995) Spatial variation in nitrogen availability in three successional plant communities. J Ecol 83:357-367 doi:10.2307/2261590

Guckland A, Jacob M, Flessa H, Thomas FM, Leuschner C (2009) Acidity, nutrient stocks, and organic-matter content in soils of a temperate deciduous forest with different abundance of European beech (*Fagus sylvatica* L.). J Plant Nutr Soil Sc 172:500-511 doi:10.1002/jpln.200800072

Guggenberger G, Zech W, Schulten HR (1994) Formation and mobilization pathways of dissolved organic matter: evidence from chemical structural studies of organic matter fractions in acid forest floor solutions. Org Geochem 21:51-66 doi:10.1016/0146-6380(94)90087-6

Harpold AA, Molotch NP, Musselman KN, Bales RC, Kirchner PB, Litvak M, Brooks PD (2015) Soil moisture response to snowmelt timing in mixed-conifer subalpine forests. Hydrol Process 29:2782-2798 doi:10.1002/hyp.10400

Helms JR, Stubbins A, Ritchie JD, Minor EC, Kieber DJ, Mopper K (2008) Absorption spectral slopes and slope ratios as indicators of molecular weight, source, and photobleaching of chromophoric dissolved organic matter. Limnol Oceanogr 53:955-969 doi:10.4319/lo.2008.53.3.0955

Hirobe M, Tokuchi N, Iwatsubo G (1998) Spatial variability of soil nitrogen transformation patterns along a forest slope in a *Cryptomeria japonica* D. Don plantation. Eur J Soil Biol 34:123-131 doi:10.1016/S1164-5563(00)88649-5

Hirobe M, Koba K, Tokuchi N (2003) Dynamics of the internal soil nitrogen cycles under moder and mull forest floor types on a slope in a *Cryptomeria japonica* D. Don plantation. Ecol Res 18:53-64 doi:10.1046/j.1440-1703.2003.00532.x

Hiura T, Fujiwara K (1999) Density-dependence and co-existence of conifer and broad-leaved trees in a Japanese northern mixed forest. J Veg Sci 10:843-850 doi:10.2307/3237309

Hiura T, Sano J, Konno Y (1996) Age structure and response to fine scale disturbances of *Abies sachalinensis*, *Picea jezoensis*, *Picea glehnii*, and *Betula ermanii* growing under the influence of a dwarf bamboo understory in northern Japan. Can J Forest Res 26:289-297 doi:10.1139/x26-032

Hobbie SE (1992) Effects of plant-species on nutrient cycling. Trends Ecol Evol 7:336-339 doi:10.1016/0169-5347(92)90126-v

Isobe K et al. (2015) Microbial regulation of nitrogen dynamics along the hillslope of a natural forest. Front Environ Sci 2:63 doi:10.3389/fenvs.2014.00063

IUSS Working group. WRB (2006) World reference base for soil resources 2006. A framework for international classification, correlation and communication. World Soil Resources Reports 103, FAO, Rome

John R et al. (2007) Soil nutrients influence spatial distributions of tropical tree species. P Natl Acad Sci USA 104:864-869 doi:10.1073/pnas.0604666104

Kaiser J, Hastings MG, Houlton BZ, Rockmann T, Sigman DM (2007) Triple oxygen isotope analysis of nitrate using the denitrifier method and thermal decomposition of N_2O. Anal Chem 79:599-607 doi:10.1021/ac061022s

Kalbitz K, Meyer A, Yang R, Gerstberger P (2007) Response of dissolved organic matter in the forest floor to long-term manipulation of litter and throughfall inputs. Biogeochemistry 86:301-318 doi:10.1007/s10533-007-9161-8

Kalbitz K, Schmerwitz J, Schwesig D, Matzner E (2003) Biodegradation of soil-derived dissolved organic matter as related to its properties. Geoderma 113:273-291 doi:10.1016/s0016-7061(02)00365-8

Kendall, C., Elliott, E. M. and Wankel, S. D.(2007) Tracing anthropogenic inputs of nitrogen to ecosystems, in “Stable isotopes in ecology and environmental sciences” (Eds Michener, R. and Lajtha, K), pp . 375-449, Blackwell Publishing Ltd, Oxford, UK

Kiikkila O, Kitunen V, Smolander A (2006) Dissolved soil organic matter from surface organic horizons under birch and conifers: Degradation in relation to chemical characteristics. Soil Biol Biochem 38:737-746 doi:10.1016/j.soilbio.2005.06.024

Kiikkila O, Kitunen V, Smolander A (2011) Properties of dissolved organic matter derived from silver birch and Norway spruce stands: Degradability combined with chemical characteristics. Soil Biol Biochem 43:421-430 doi:10.1016/j.soilbio.2010.11.011

Kiikkila O, Smolander A, Kitunen V (2013) Degradability, molecular weight and adsorption properties of dissolved organic carbon and nitrogen leached from different types of decomposing litter. Plant Soil 373:787-798 doi:10.1007/s11104-013-1837-3

Knops JMH, Bradley KL, Wedin DA (2002) Mechanisms of plant species impacts on ecosystem nitrogen cycling. Ecol Lett 5:454-466 doi:10.1046/j.1461-0248.2002.00332.x

Lawaetz AJ, Stedmon CA (2009) Fluorescence intensity calibration using the Raman scatter peak of water. Appl Spectrosc 63:936-940

Legendre P (1993) Spatial autocorrelation - trouble or new paradigm. Ecology 74:1659-1673 doi:10.2307/1939924

Le Mellec A, Meesenburg H, Michalzik B (2010) The importance of canopy-derived dissolved and particulate organic matter (DOM and POM) - comparing throughfall solution from broadleaved and coniferous forests. Ann For Sci 67 doi:10.1051/forest/2009130

Lovett GM, Weathers KC, Arthur MA, Schultz JC (2004) Nitrogen cycling in a northern hardwood forest: Do species matter? Biogeochemistry 67 doi:10.1023/B:BIOG.0000015786.65466.f5

Maurer GE, Bowling DR (2014) Seasonal snowpack characteristics influence soil temperature and water content at multiple scales in interior western US mountain ecosystems. Water Resour Res 50:5216-5234 doi:10.1002/2013wr014452

McDowell WH (2003) Dissolved organic matter in soils - future directions and unanswered questions. Geoderma 113:179-186 doi:10.1016/s0016-7061(02)00360-9

McKinley DC et al. (2011) A synthesis of current knowledge on forests and carbon storage in the United States. Ecol Appl 21:1902-1924 doi:10.1890/10-0697.1

McKnight DM, Boyer EW, Westerhoff PK, Doran PT, Kulbe T, Andersen DT (2001) Spectrofluorometric characterization of dissolved organic matter for indication of precursor organic material and aromaticity. Limnol Oceanogr 46:38-48

Melillo JM, Aber JD, Muratore JF (1982) Nitrogen and lignin control of hardwood leaf litter decomposition dynamics. Ecology 63:621-626 doi:10.2307/1936780

Michalski G, Meixner T, Fenn M, Hernandez L, Sirulnik A, Allen E, Thiemens M (2004) Tracing atmospheric nitrate deposition in a complex semiarid ecosystem using $\Delta^{17}O$. Environ Sci Technol 38:2175-2181 doi:10.1021/es034980+

Michalzik B, Kalbitz K, Park JH, Solinger S, Matzner E (2001) Fluxes and concentrations of dissolved organic carbon and nitrogen - a synthesis for temperate forests. Biogeochemistry 52:173-205 doi:10.1023/a:1006441620810

Murphy KR, Stedmon CA, Wenig P, Bro R (2014) OpenFluor - A spectral database of auto-fluorescence by organic compounds in the environment. Anal. Methods, 6, 658-661. DOI:10.1039/C3AY41935E

Muscolo A, Sidari M, Mercurio R (2007) Influence of gap size on organic matter decomposition, microbial biomass and nutrient cycle in Calabrian pine (*Pinus laricio,* Poiret) stands. Forest Ecol Manag 242:412-418 doi:10.1016/j.foreco.2007.01.058

Naithani KJ, Baldwin DC, Gaines KP, Lin H, Eissenstat DM (2013) Spatial distribution of tree species governs the spatio-temporal interaction of leaf area index and soil moisture across a forested landscape. Plos One 8 doi:10.1371/journal.pone.0058704

Nakagawa F, Suzuki A, Daita S, Ohyama T, Komatsu DD, Tsunogai U (2013) Tracing atmospheric nitrate in groundwater using triple oxygen isotopes: evaluation based on bottled drinking water. Biogeosciences 10:3547-3558 doi:10.5194/bg-10-3547-2013

Nakashizuka T and Numata M (1982) Regeneration process of climax beech forests I. Structure of a beech forest with the undergrowth of *Sasa*. Jap J Ecol 32:57–67

Ni XY, Yang WQ, Tan B, Li H, He J, Xu LY, Wu FZ (2016) Forest gaps slow the sequestration of soil organic matter: a humification experiment with six foliar litters in an alpine forest. Sci Rep 6 doi:10.1038/srep19744

Nilsson MC, Wardle DA (2005) Understory vegetation as a forest ecosystem driver: evidence from the northern Swedish boreal forest. Front Ecol Environ 3:421–428 doi:10.1890/1540-9295(2005)003[0421:uvaafe]2.0.co;2

Nishimura S, Maie N, Baba M, Sudo T, Sugiura T, Shima E (2012) Changes in the quality of chromophoric dissolved organic matter leached from senescent leaf litter during the early decomposition. J Environ Qual 41:823-833 doi:10.2134/jeq2011.0342

Noguchi M, Yoshida T (2004) Tree regeneration in partially cut conifer-hardwood mixed forests in northern Japan: roles of establishment substrate and dwarf bamboo. Forest Ecol Manag 190:335-344 doi:10.1016/j.foreco.2003.10.024

Noguchi M, Yoshida T (2005) Factors influencing the distribution of two co-occurring dwarf bamboo species (*Sasa kurilensis* and *S.senanensis*) in a conifer-broad leaved mixed stand in northern Hokkaido. Ecol Res 20:25-30 doi:10.1007/s11284-004-0009-6

Noguchi M, Yoshida T (2007) Regeneration responses influenced by single-tree selection harvesting in a mixed-species tree community in northern Japan. Can J Forest Res 37:1554-1562 doi:10.1139/x07-103

Ogawa A, Shibata H, Suzuki K, Mitchell MJ, Ikegami Y (2006) Relationship of topography to surface water chemistry with particular focus on nitrogen and

organic carbon solutes within a forested watershed in Hokkaido, Japan. Hydrol Process 20:251-265 doi:10.1002/hyp.5901

Ohno T (2002) Fluorescence inner-filtering correction for determining the humification index of dissolved organic matter. Environ Sci Technol 36:742-746 doi:10.1021/es0155276

Oren R, Ewers BE, Todd P, Phillips N, Katul G (1998) Water balance delineates the soil layer in which moisture affects canopy conductance. Ecol Appl 8:990-1002 doi:10.2307/2640956

Osaka K et al. (2010) Hydrological influences on spatiotemporal variations of delta ^{15}N and ^{18}O of nitrate in a forested headwater catchment in central Japan: Denitrification plays a critical role in groundwater. J Geophys Res-Biogeo 115 doi:10.1029/2009jg000977

Ozawa M, Shibata H, Satoh F, Sasa K (2001) Effects of surface soil removal on dynamics of dissolved inorganic nitrogen in a snow-dominated forest. ScientificWorldJournal. 1(S2):527-33 doi:10.1100/tsw.2001.311

Plant RE (2012). Spatial data analysis in ecology and agriculture using R. CRC Press, Boca Raton, FL

Prescott CE (2005) Do rates of litter decomposition tell us anything we really need to know? Forest Ecol Manag 220:66-74 doi:10.1016/j.foreco.2005.08.005

Prescott CE (2010) Litter decomposition: what controls it and how can we alter it to sequester more carbon in forest soils? Biogeochemistry 101:133-149 doi:10.1007/s10533-010-9439-0

Qualls RG, Haines BL (1992) Biodegradability of dissolved organic matter in forest throughfall, soil solution, and stream water. Soil Sci Soc Am J 56:578-586

Qualls RG, Haines BL, SwankSource WT (1991) Fluxes of dissolved organic nutrients and humic substances in a deciduous forest. Ecology 72:254-266 doi:10.2307/1938919

Reich PB et al. (2005) Linking litter calcium, earthworms and soil properties: a common garden test with 14 tree species. Ecol Lett 8 doi:10.1111/j.1461-0248.2005.00779.x

Robertson GP, Huston MA, Evans FC, Tiedje JM (1988) Spatial variability in a successional plant community - patterns of nitrogen availability Ecology 69:1517-1524 doi:10.2307/1941649

Rose LA, Sebestyen SD, Elliott EM, Koba K (2015) Drivers of atmospheric nitrate processing and export in forested catchments. Water Resour Res 51:1333-1352 doi:10.1002/2014wr015716

Rothe A, Huber C, Kreutzer K, Weis W (2002a) Deposition and soil leaching in stands of Norway spruce and European Beech: Results from the Hoglwald research in comparison with other European case studies. Plant Soil 240:33-45 doi:10.1023/a:1015846906956

Rothe A, Kreutzer K, Kuchenhoff H (2002b) Influence of tree species composition on soil and soil solution properties in two mixed spruce-beech stands with contrasting history in Southern Germany. Plant Soil 240:47-56 doi:10.1023/a:1015822620431

Royo AA, Carson WP (2006) On the formation of dense understory layers in forests worldwide: consequences and implications for forest dynamics, biodiversity, and succession. Can J Forest Res 36:1345-1362 doi:10.1139/x06-025

Scott NA, Binkley D (1997) Foliage litter quality and annual net N mineralization: Comparison across North American forest sites. Oecologia 111:151-159 doi:10.1007/s004420050219

Stedmon CA, Markager S, Bro R (2003) Tracing dissolved organic matter in aquatic environments using a new approach to fluorescence spectroscopy. Mar Chem 82:239-254 doi:10.1016/s0304-4203(03)00072-0

Stedmon CA, Bro R (2008) Characterizing dissolved organic matter fluorescence with parallel factor analysis: a tutorial. Limnol Oceanogr -Meth 6:572-579

Tanaka N, Nakazono E, Tsuyama I, Matsui T (2009) Assessing impact of climate warming on potential habitats of ten conifer species in Japan. Chikyu Kankyo 14: 153-164 (In Japanese)

Tietema A, Warmerdam B, Lenting E, Riemer L (1992) Abiotic factors regulating nitrogen transformations in the organic layer of acid forest soils: Moisture and pH. Plant Soil 147:69-78 doi:10.1007/bf00009372

Toyooka K (1983) Biomass of *Sasa* dwarf bamboo in Hokkaido. Bamboo J 1:22–24 (In

Japanese)

Tripathi SK, Sumida A, Shibata H, Ono K, Uemura S, Kodama Y, Hara T (2006) Leaf litterfall and decomposition of different above- and belowground parts of birch (*Betula ermanii*) trees and dwarf bamboo (*Sasa kurilensis*) shrubs in a young secondary forest in Northern Japan. Biol Fert Soils 43:237-246 doi:10.1007/s00374-006-0100-y

Tsunogai U et al. (2014) Quantifying the effects of clear-cutting and strip-cutting on nitrate dynamics in a forested watershed using triple oxygen isotopes as tracers. Biogeosciences 11:5411-5424 doi:10.5194/bg-11-5411-2014

Tsunogai U et al. (2016) Accurate and precise quantification of atmospheric nitrate in streams draining land of various uses by using triple oxygen isotopes as tracers. Biogeosciences 13:3441-3459 doi:10.5194/bg-13-3441-2016

Vitousek PM et al. (1997) Human alteration of the global nitrogen cycle: Sources and consequences. Ecol Appl 7:737-750 doi:10.2307/2269431

Vitousek PM, Howarth RW (1991) Nitrogen limitation on land and in the sea: How can it occur? Biogeochemistry 13:87–115 doi:10.1007/BF00002772

Vitousek PM, Matson PA (1988) Nitrogen transformations in a range of tropical forest soils Soil Biol Biochem 20:361-367 doi:10.1016/0038-0717(88)90017-x

Vodde F et al. (2011) The influence of storm-induced microsites to tree regeneration patterns in boreal and hemiboreal forest. J For Res-Jpn 16:155-167 doi:10.1007/s10310-011-0273-6

Wardle DA, Bardgett RD, Klironomos JN, Setala H, van der Putten WH, Wall DH (2004) Ecological linkages between aboveground and belowground biota. Science 304:1629-1633 doi:10.1126/science.1094875

Watanabe T, Fukuzawa K, Shibata H (2013) Temporal changes in litterfall, litter decomposition and their chemical composition in Sasa dwarf bamboo in a natural forest ecosystem of northern Japan. J For Res-Jpn 18:129-138 doi:10.1007/s10310-011-0330-1

Webster PJ, Holland GJ, Curry JA, Chang HR (2005) Changes in tropical cyclone number, duration, and intensity in a warming environment. Science 309:1844-1846 doi:10.1126/science.1116448

Weishaar JL, Aiken GR, Bergamaschi BA, Fram MS, Fujii R, Mopper K (2003) Evaluation of specific ultraviolet absorbance as an indicator of the chemical composition and reactivity of dissolved organic carbon. Environ Sci Technol 37:4702-4708 doi:10.1021/es030360x

Yamashita Y, Kloeppel BD, Knoepp J, Zausen GL, Jaffe R (2011) Effects of watershed history on dissolved organic matter characteristics in headwater streams. Ecosystems 14:1110-1122 doi:10.1007/s10021-011-9469-z

Yoshida T, Noguchi M (2009) Vulnerability to strong winds for major tree species in a northern Japanese mixed forest: analyses of historical data. Ecol Res 24:909-919 doi:10.1007/s11284-008-0566-1

Yoshida T, Noguchi M, Akibayashi Y, Noda M, Kadomatsu M, Sasa K (2006) Twenty years of community dynamics in a mixed conifer - broad-leaved forest under a selection system in northern Japan. Can J Forest Res 36:1363-1375 doi:10.1139/x06-041

Zech W et al. (1997) Factors controlling humification and mineralization of soil organic matter in the tropics. Geoderma 79:117-161 doi:10.1016/s0016-7061(97)00040-2

Zsolnay A, Baigar E, Jimenez M, Steinweg B, Saccomandi F (1999) Differentiating with fluorescence spectroscopy the sources of dissolved organic matter in soils subjected to drying. Chemosphere 38:45-50 doi:10.1016/s0045-6535(98)00166-0

7. Summary

Soil N dynamics is an important process that affect various ecosystem functions and services in forest ecosystems. Vegetation is a major factor that controls soil N dynamics through the supply of litterfall and absorption of N, and tree species differ their influence on soil N dynamics. Disturbances are inevitable process in natural forests and it affects soil N dynamics through the shift in the abundance and composition of vegetation. However, our understanding of plant species effects on soil N dynamics in forest ecosystem is largely derived from studies that focused on tree species grown in monoculture. Therefore, how soil N dynamics are influenced by plants in natural forests where small-scale disturbances occasionary changes composition and configuration of both trees and understory vegetation is not fully understood.

Cool-temperate mixed conifer-broadleaved forest is a major forest type in Hokkaido. Dwarf bamboo, which dominates the forest floor, strongly affects tree regeneration by retarding their natural regeneration in canopy gaps. Therefore, plant distribution is largely influenced by small-scale disturbance, such as windfall, in this forest ecosystems. I studied how trees and understory vegetation in a natural mixed forest influence soil N dynamics in a natural mixed conifer-broadleaved forest of Uryu Experimental Forest of Hokkaido University, northern Japan. Specifically, I conducted two studies; the objective of the first study was to understand the spatial pattern of soil N availability and the relation to the forest structure. The objective of the second study was to understand the difference in the dynamics of DOM and DIN from forest canopy to surface soil among vegetation types, and whether DOM properties influence DIN dynamics.

In the first study (Chapter 2), I examined the spatial pattern of inorganic N pools in surface soil by intensive grid samplings of soils at a relatively small scale with flat topography, and analyzed the relationship with the distributions of coniferous and broadleaved trees as well as *Sasa* in the understory. I also examined litterfall properties and composition, thickness of O horizon, soil properties to understand how plants influence the spatial pattern of soil N pool. The distributions of overstory and understory vegetation were found to create spatial patterns of nitrification potential and soil NO_3^- content in a conifer-broadleaved mixed forest with a dense *Sasa* undergrowth. The plants affected these spatial patterns of nitrification potential and soil NO_3^- content through their effects on litter decomposition and soil moisture regime. The dominance of recalcitrant coniferous litter resulted in a thick O horizon, while the dominance of fast-decomposing broadleaved and *Sasa* litters led to a thin O horizon. Differences in

the canopy interception of precipitation between the conifer-dominated area and the canopy gap could also contributed to the spatial pattern of O horizon thickness through its influence on the moisture conditions of the forest floor. Locations around coniferous trees where the O horizon is thick had dry soils, whereas locations beneath broadleaved trees and in the canopy gap where the O horizon was thin exhibited high soil water contents. High soil water content was related to high nitrification rates and, hence, high soil NO_3^- contents.

In Chapter 3, I examined the differences in DOM and DIN dynamics from forest canopy to surface mineral soil between oak, spruce, and *Sasa* grown in canopy gaps. Then, whether DOM properties affect NO_3^- leaching was analyzed. The concentrations and fluxes of DOC, DOC, NH_4^+ and NO_3^-, the spectrofluorometric indices of DOM, and stable isotopic composition of NO_3^- in throughfall, litter leachate, and soil water were measured for the three vegetation types. The relative contribution of atmospheric NO_3^- to the total NO_3^- in the litter leachate and soil water was about 14 % and 7%, respectively, indicating that NO_3^- productions in the forest floor and soil are the major source of leaching NO_3^-. DOM in throughfall, litter leachate, and soil water beneath *Sasa* was characterized as low concentrations and fluxes of DON and DOC, low DOC/DON ratio, low contents of recalcitrant fraction, while these variables were high beneath spruce. NO_3^- concentrations and fluxes and the proportion of NO_3^- to DIN were also different among the vegetation types with the litter leachate and soil water beneath *Sasa* showing higher value than those beneath spruce. Characteristics of DOM and DIN beneath oak often showed intermediate values. The lack of significant increase in DOC and DON from throughfall to litter leachate, as well as significant decrease in the tyrosine-like fraction of DOM suggested tree canopy is an important source of DOM, especially biodegradable fraction. The differences in the DOM properties of litter leachate was considered to be caused by the difference in organic matter storage in Oe/Oa horizon and DOM quality of throughfall. The high NO_3^-/DIN ratio in the litter leachate and the soil water were related to low DOC/DON ratio of DOM in the throughfall and the litter leachate. In addition, the NO_3^- concentration and NO_3^-/DIN ratio in the litter leachate and the soil water was positively related to the relative proportion of microbially-derived DOM and negatively related to the relative proportion of humic-like DOM from forest floor and soil. These results suggest that differences in DOM quality among vegetation types strongly affect NO_3^- leaching from forest floor and surface mineral soil.

From the two studies, I found that spatial distributions of coniferous and broadleaved trees, and canopy gaps with *Sasa* influences soil N dynamics, especially

soil NO_3^- contents, net nitrification rates, and NO_3^- leaching, through differences in litterfall chemistry, soil moisture, and DOM quality in the cool-temperate mixed forest stand. Locations beneath *Sasa* in canopy gaps show higher levels of soil NO_3^- contents, net nitrification rates, and NO_3^- leaching compared to locations beneath and around coniferous trees. As future change in global climate is expected to increase the intensity and frequency of natural disturbances such as typhoon, the findings of this study will contribute to evaluate and predict the impact of the environmental changes on soil N dynamics through vegetation change.

学 位 論 文 内 容 の 要 旨

森林生態系において土壌中での窒素動態は森林の純一次生産や生態系機能・サービスをコントロールするプロセスであり、植生はリターの供給や養分吸収を介して土壌窒素動態に影響する重要な要因である。林床にササが密生する針広混交林は北海道の代表的な森林タイプであり、そのような森林では台風などの撹乱により林冠ギャップが形成されると、急速にササが林床を覆うため樹木の天然更新が起こりにくい。その結果、林冠ギャップが長期的に維持されるため、針葉樹、広葉樹、ササが密生する林冠ギャップがモザイク状に分布する特徴をもつ。土壌の窒素無機化・硝化速度は植生や土壌タイプによって異なることが知られているが、局所的な林冠ギャップの存在を通じて樹木と下層植生が不均一に分布する冷温帯針広混交林において、植生の空間分布による水、有機物、養分フローの空間パターンが土壌窒素の動態にどのように影響しているのかは十分に理解されていない。そこで本研究は、冷温帯針広混交林において植生による林床リター、溶存有機物の質、土壌水分の違いが土壌中の窒素動態にどのように影響するのかを明らかにすることを目的とした。

研究は北海道北部に位置する北海道大学雨龍研究林の冷温帯針広混交林で行った。第二章では土壌中の窒素無機化速度に影響する要因として、植生によるリターの質と土壌水分の違いに着目し、針広混交林内におけるリターフォール、土壌水分、林床リター、土壌窒素プールの空間分布を詳細に分析し、それらと植生分布との関係性を解析した。林内 48 ヶ所におけるグリッド調査（約 800m^2）では、表層土壌に含まれる無機態窒素、土壌水分および林床リター層の厚さを測定した。また、下層植生（ササ）の被度に基づいた 3 種類のコドラート調査（各 5 反復）では、リターフォールの量・組成、表層土壌の理化学性、室内培養による正味無機化・硝化速度などを測定した。その結果、リターフォールの種組成（針葉樹、広葉樹、ササの相対割合）には、周囲の針葉樹・広葉樹本数、ササバイオマスと有意な正の相関関係が認められた。また、針葉樹のリターフォールは広葉樹やササと比べて炭素／窒素比が有意に高かった。林床のリター層は針葉樹リターの割合が多い場所ほど厚くなる一方、ササが優占して広葉樹が混じっている場所では薄くなる傾向があった。これらの結果から、林内における針葉樹と広葉樹、ササの不均一分布により、土壌へ供給されるリターフォールの組成が場所により異なることが示された。また、針葉樹リターは広葉樹やササよりも分解速度が遅いことから、リターの分解性の違いによって林床リター層の厚さの空間パターンが形成されていることが示唆された。さらに、周囲に針葉樹が多く、林床リター層が厚い場所ほど土壌水分は低い傾向にあったことから、針葉樹の林冠による高い降雨遮断や、針葉樹下での厚いリター層の

存在が土壌水分の分布に影響していることが示唆された。そして、土壌水分と土壌の硝酸態窒素（NO_3^-）現存量には有意な正の相関関係が認められ、土壌のNO_3^-現存量は室内培養実験による正味硝化速度と有意な正の相関関係を示した。これらのことから、森林内における不均一な植生分布に影響されている土壌水分の違いは、土壌微生物による硝化活性への影響を介して土壌 NO_3^-現存量の空間パターンを形成していることが示唆された。つまり、リター分解と土壌水分、微生物活性への影響を介して、針葉樹周辺では NO_3^-現存量が小さく、逆にササが密生する林冠ギャップと広葉樹の周辺では土壌 NO_3^-現存量が大きくなることが明らかとなった。

第三章では、土壌微生物により無機化、硝化される窒素の基質として、また土壌微生物活性のエネルギー源としての溶存有機物（DOM）に着目した。DOMは様々な特徴をもつ画分の集合であり、植生によって溶存有機態炭素／窒素比（DOC／DON 比）や分解性、分子量などの特徴が変動する可能性がある。ここでは、針葉樹と広葉樹、ササにおける DOC、DON の濃度やフラックス、DOMの質の違いが土壌中の窒素動態に及ぼす影響について、特に土壌における NO_3^-生成や溶脱に着目して研究した。第二章の調査地を含む約 3ha の集水域において、アカエゾマツ、ミズナラ、林冠ギャップ（ササ優占）が優占する場所で林内雨、リター層浸透水、鉱質土壌浸透水（深度 10 cm）を採取し、DOC、DONの濃度とフラックスを分析するとともに、吸光光度法・蛍光光度法を用いてDOM の質的評価を行った。また、それぞれの水サンプルに含まれる NO_3^-の三酸素同位体異常（$\Delta^{17}O$）を分析し、大気由来 NO_3^-と土壌微生物由来 NO_3^-の相対的な寄与率を求めた。そして、土壌に供給される DOM の量や質が硝化プロセスに与える影響を調べるため、主成分分析および重回帰分析により DOM の量や質と溶存 NO_3^-濃度や溶存無機態窒素（DIN）に占める NO_3^-の割合（NO_3^-/DIN 比）との関係を解析した。浸透水に含まれる NO_3^-に占める大気由来 NO_3^-の割合は、リター層浸透水で平均 16%、土壌水で平均 7%であり、リター層や土壌から溶脱する NO_3^-は大気沈着を直接的に由来するよりも、土壌微生物による窒素無機化・硝化のプロセスを経由するものが主体であることが明らかとなった。ササの下を浸透する DOM は、アカエゾマツやミズナラと比べて DOC、DON 濃度、DOC/DON 比が低く、難分解性を示す腐植様物質の割合も低かった。一方、これらの値はアカエゾマツの下を浸透する DOM が最も高い値を示した。また、リター層および鉱質土壌の浸透水による NO_3^-フラックスと NO_3^-/DIN 比はアカエゾマツよりもササが有意に高かった。さらに、林内雨やリター層浸透水として供給される DOC/DON 比が低いほど、リター層と鉱質土壌浸透水の NO_3^-/DIN 比が高くなることが示された。また、リター層や土壌の DOM に占める微生物由来の割合が高く、腐植様物質の割合が低いほど、溶脱する NO_3^-濃度や NO_3^-/DIN 比

が高い傾向が認められた。このことから、植生により土壌の DOM の質（DOC／DON 比、DOM の由来）が異なり、それが土壌からの NO_3^-溶脱に強く影響していることが明らかとなった。

本研究から、林冠ギャップを含む冷温帯針広混交林の針葉樹、広葉樹、ササの不均一分布は、リターフォールの質と土壌水分率、溶存有機物の質の違いを介して土壌 NO_3^-の現存量、正味硝化速度、溶脱 NO_3^-濃度やフラックスの空間変動に影響していることが明らかとなった。そして、ササが優占する林冠ギャップでは針葉樹周辺と比べて土壌中の NO_3^-濃度やフラックスが高いことが明らかとなった。本研究の成果は、台風撹乱等で形成された林冠ギャップによる植生の不均一分布と土壌窒素動態の空間的な関係性を示したものであり、将来の気候変動による植生変化が生態系の窒素循環に与える影響を予測するうえでも非常に有意義なものである。